Environmentally-benign and Practical Synthesis of Biodegradable and Biocompatible Aliphatic Polyesters

A Dissertation for the Degree of Doctor of Philosophy

Tatsuya Saito

Hokkaido University

March, 2019

Acknowledgments

The study presented in this dissertation has been performed under the direction of Professor Toshifumi Satoh, Division of Biotechnology and Macromolecular Chemistry, Faculty of Engineering, Hokkaido University, from 2013 to 2019. The author wishes to express his sincere gratitude to Professor Toshifumi Satoh for his kind instruction, helpful advice, and unstinting encouragement throughout the course of this work.

The author is also deeply grateful to Associate Professor Kenji Tajima, Associate Professor Takuya Yamamoto, and Assistant Professor Takuya Isono, Division of Biotechnology and Macromolecular Chemistry, Faculty of Engineering, Hokkaido University, for their helpful and valuable suggestion with continuous encouragement throughout this work.

The author is further indebted to Drs. Kosuke Makiguchi, Naoya Sakai, Kenji Takada, Seiya Kikuchi, and Yusuke Satoh for their patient teaching and fruitful daily discussion. The author wants to express his special thanks for Messrs. Yusuke Aizawa, Takafumi Oyama, and Kaoru Takojima for their contribution to this dissertation work. The author thanks all of the member of Professor Satoh's group, especially Messrs. Kodai Watanabe, Brian J. Ree, Ryoto Tanaka, Li-Che Hsu, Nao Kawakami, Kohei Honda, Reina Murano, Yoshinobu Mato, Yusuke Kajita, Saburo Kobayashi, Tomoki Shingu, Saki Nakahira, Ko Ishii, Satoshi Katsuhara, Yasuko Takagi, Shunma, Tanaka, Ryoya Komaki, Masato Uenishi, Bono Aoshima, Noya Kaizawa, Hiroko Ninoyu, Kaiyu Fujiwara, Hiroshi Makino with their friendship.

The author is very grateful to the Research Fellowships of the Japan Society for the Promotion of Science (JSPS) for Young Scientists during 2017-2019.

Finally, the author would like to express his utmost gratitude to family for their understanding, support, and continuous encouragement throughout his research and daily life.

March, 2019

Tatsuya Saito

Contents

Chapter 1

General Introduction

1.1 Introduction to Aliphatic Polyesters

Polymeric materials have significantly improved the quality of human life over the last half-century, and they are now indispensable to our modern society. The global production of plastics reached approximately 300 million tons in 2014 and the demand for polymeric materials is still increasing. [1] On the other hand, the majority of the produced plastics eventually end up as waste, which has a serious impact on our environment. The amount of plastic waste generated in 2010 was estimated to be more than 300 million tons [2], and they are buried or incinerated, and if not, permanently stay on the land or in the ocean. Indeed, 4.8 ~ 12.7 million tons of plastic waste was released into the ocean in 2014 [2], and it is said that the weight of plastic waste in the ocean will be greater than that of fish in 2050. Therefore, the environmental pollution caused by polymeric materials has been considered as one of the most serious issues in the world over the last several decades.

Along with the increasing concerns for environmental pollution by plastic wastes, aliphatic polyesters (APEs) have been gaining much attention as biodegradable polymeric materials.[3,4] APE is a category of polymers composed of an aliphatic main chain with ester linkages, and they undergo decomposition into non-toxic compounds, such as carbon dioxide, methane, and water, via an enzymatic reaction by microorganisms and/or simple chemical hydrolysis in aqueous media. Therefore, the replacement of the conventional non-degradable polymers, such as polyethylene and polystyrene, by APEs has been recognized as one of the reasonable solutions to the plastic waste issue.

APEs are classified into two categories: natural origin APEs and chemical origin APEs.[5] Poly(hydoroxyalkanoate)s (PHAs) are representative natural origin APEs produced by microorganisms through the bacterial fermentation of carbohydrates or lipids (Figure 1.1). Such a sustainable character of PHA is highly attractive from the green chemistry point of view, though the industrial production of PHA is still challenging due to the high production cost and

limited scalability. On the other hand, chemical origin APEs, such as poly(L-lactide) (PLLA), poly(ε-caprolactone) (PCL), poly(trimethylene carbonate) (PTMC), and poly(butylene succinate) (PBS), are commercially produced. The APE materials are used not only for environmental purposes, such as compostable packaging containers, plasticulture, and environmental remediation films, but also for biomedical applications including medical implants, surgical sutures, and medical devices due to their good biocompatibility with the human body.[6]

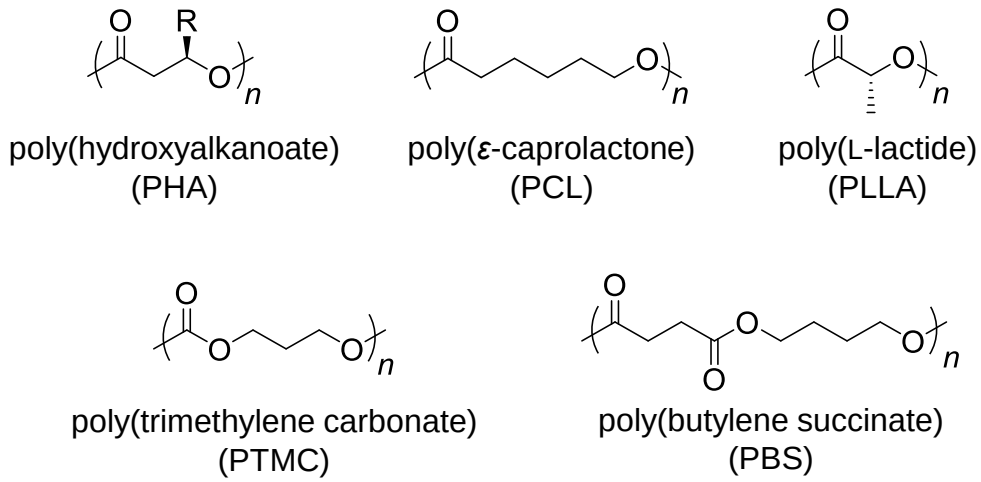

Figure 1.1. Chemical structure of representative aliphatic polyesters.

From a mechanistic point of view, the synthetic strategy for aliphatic polyesters can be classified into two different types.[5] One is the polycondensation of dicarboxylic acids and diols (Scheme 1.1). The polycondensation method can produce various types of aliphatic polyesters depending on the choice of the dicarboxylic acids and diols. In addition, the self-polycondensation of hydroxyacids also yields APEs. For example, PLLA can be synthesized by the self-polycondensation of L-lactic acid. However, the polycondensation follows a step-growth mechanism, therefore, a high reaction temperature, reduced pressure, and long reaction

time are required to obtain a high molecular weight product, and their dispersity converges to 2. Another method is the ring-opening polymerization (ROP) of cyclic esters, where the repeated transesterification between the cyclic ester and hydroxyl group of the propagating chain-end increases the molecular weight of the product by following the chain-growth mechanism (Scheme 1.2). In contrast to the polycondensation method, the ROP method offers good control over the molecular weight and dispersity of the products. Due to this great advantage, the ROP method is more preferably used for the production of APEs.

Scheme 1.1. Polycondensation of dicarboxylic acid and diol and self-polycondensation of hydroxyacid

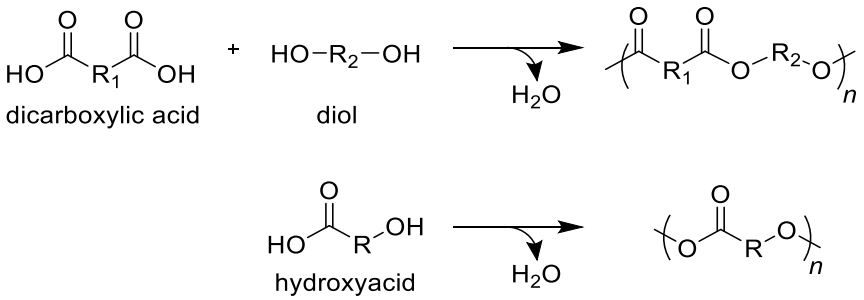

Scheme 1.2. Ring-opening polymerization of cyclic esters and cyclic carbonate

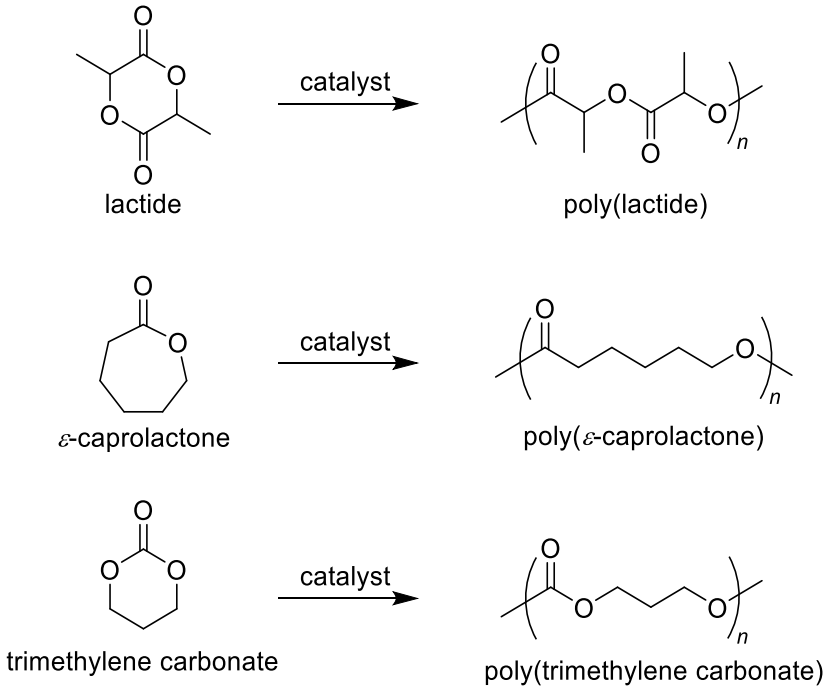

1.2 Synthesis of Aliphatic Polyesters via Ring-opening Polymerization

For the ROP of the cyclic esters, several classes of metal-based initiators/catalysts, such as metal alkoxides and carboxylates, have been employed.[7-9] The mechanisms of the metal-catalyzed polymerization are classified as either (1) anionic polymerization or (2) coordination-insertion polymerization. The anionic polymerization mechanism is observed in the ROP using alkali metal alkoxides. For the anionic polymerization mechanism, the ROP proceeds via transesterification between the monomer and anionic initiator/alkoxide propagating chain end (Scheme 1.3(a)). However, the high nucleophilicity and/or strong basicity of the alkoxide lead to undesired side reactions, such as inter- and intramolecular transesterifications.

A coordination-insertion mechanism is observed in the ROP using the metal alkoxides or carboxylates, *e.g.,* $Al(O\textit{i}Pr)_3$ and $Sn(Oct)_2$.[9] In this case, the ROP proceeds through the insertion of the monomer into the metal-oxygen bond (Scheme 1.3(b)). Metal carboxylates are used in the presence of active hydrogen compounds, such as alcohols, as the initiator because of their weaker nucleophilic character in comparison to alkoxides (Scheme 1.4). Due to the milder character of the coordination-insertion catalysts than that of the alkali metal alkoxides, the ROP proceeds in a controlled manner to give APEs possessing a predictable molecular weight and narrow dispersity with a good chain end fidelity even under bulk conditions, which offers many advantages for industrial scale production. In addition, $Sn(Oct)_2$ is commercially available, easy to handle and soluble in the common organic solvents, which are great advantages for both the industrial and laboratory-scale productions of the APEs. Therefore, many APEs are now commercially produced by using $Sn(Oct)_2$. However, the potential toxicity of the contaminated metal catalyst residues in the resulting APEs is a concern when it comes to their environmental and biomedical applications. Therefore, an alternative approach to produce APEs free from metal contamination has been highly desired.

Scheme 1.3. Ring-opening polymerization of cyclic esters using metal-based catalyst via (a) anionic polymerization mechanism and (b) coordination-insertion mechanism

(a) Anionic polymerization mechanism

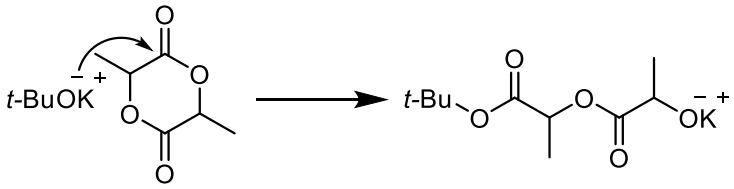

(b) Coordination-insertion polymerization mechanism

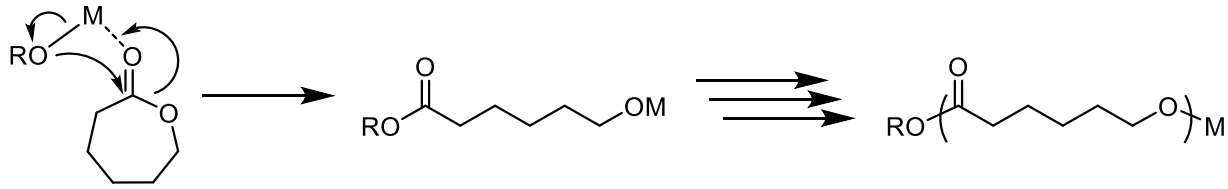

ROM: Al $(OR)_3$, Bu_2Sn $(OR)_2$, etc.

Scheme 1.4. Coordination-insertion polymerization of cyclic esters using metal carboxylate catalyst with alcohol initiator

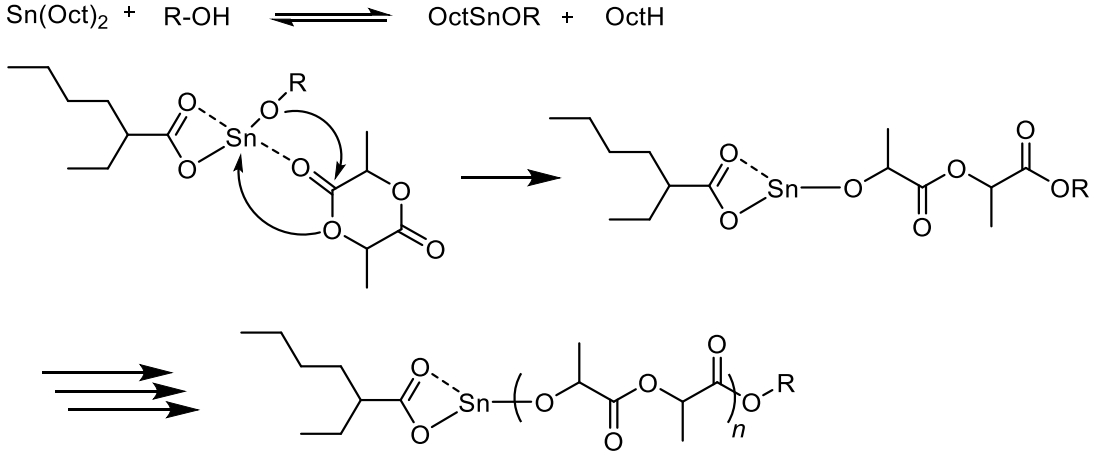

1.3 Organocatalytic Ring-opening Polymerization

An "organocatalyst" can be defined as a catalyst composed only of nonmetal elements, such as carbon, oxygen, hydrogen, nitrogen, etc. [10,11] Since the concept of an organocatalyst was first proposed by MacMillan in 2000, organocatalysts have attracted great attention as a powerful tool for metal-free organic syntheses along with the increasing attention to green chemistry. [12,13]

In the polymer chemistry field, the first example of the polymerization using an organocatalyst was reported by Hedrick in 2001, in which *N*,*N*'-dimethyl-4-aminopyridine (DMAP) was used for the ROP of lactide (LA). [14] Following this report, many organocatalytic polymerization systems for heterocyclic monomers [14-71] and vinyl monomers [19,20,72-84] were developed. Remarkable effort has been directed toward the ROP of cyclic esters during the last decade because the metal-free process is highly attractive for the production of biodegradable and biocompatible APEs.

Organocatalysts used for the ROP can be roughly classified as either nucleophilic catalysts or hydrogen-bonding catalysts.[18] In the ROP using the nucleophilic catalyst, such as *N*-heterocyclic carbenes and phosphine,[21-25] the catalyst directly attacks the monomer to generate a more reactive zwitterionic intermediate, which is subsequently protonated by the initiating/propagating alcohol followed by acylation to form a ring-opened alcohol. This reaction repeatedly occurs to the give the linear APEs (Scheme 1.5).

Scheme 1.5. Proposed mechanism of the ROP using nucleophilic catalyst

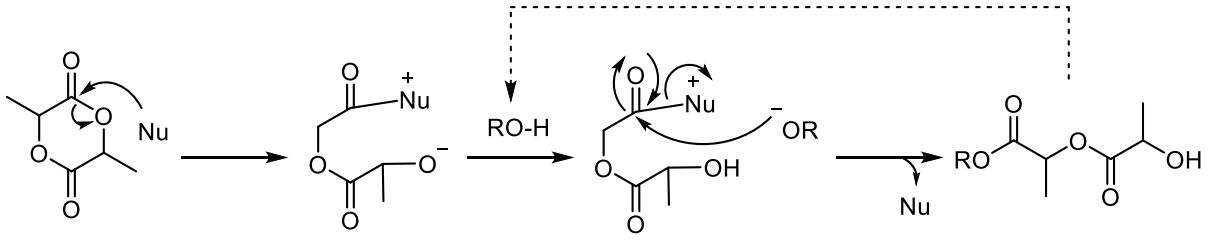

The hydrogen-bonding catalysts are categorized into monofunctional catalysts and bifunctional catalysts (catalytic system) according to their activation mode. As for the monofunctional catalysts, strong organic bases, such as 1,8-diazabicyclo[5,4,0]undec-7-ene (DBU),[26] *N*-methyl-1,5,7-triazabicyclo[4,4,0]dec-5-ene (MTBD),[26] 2-*tert*-butylimino-2-diethylamino-1,3-dimethylperhydro-1,3,2-diazaphosphorine (BEMP),[27] and 1-*tert*-butyl-2,2,4,4,4-pentakis(dimethylamino)-2Λ^5,4Λ^5-catenadi(phosphazene) (*t*-Bu-P$_2$),[28] have been used in the ROP of cyclic esters as a hydrogen bond acceptor to activate the propagating chain end (Scheme 1.6(a) and Figure 1.2). In addition, strong organic acids, such as methane sulfonic acid (MSA), trifluoromethane sulfonic acid (TfOH), and triflimide (Tf$_2$NH), also act as monofunctional catalysts (Figure 1.2).[30-34] These strong organic acids work as hydrogen bond donors to activate the carbonyl group of the monomer (Scheme 1.6(b)). Due to the strong basicity/acidity of the monofunctional catalyst, the ROP proceeds even via the single activation of the chain end or monomer.

Scheme 1.6. Activation modes of the hydrogen bonding catalyst

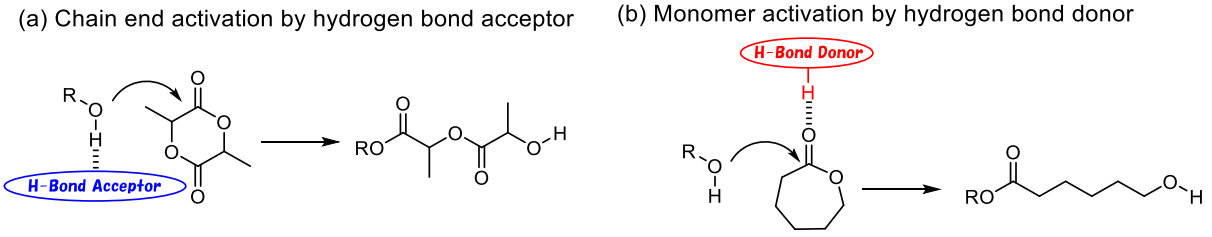

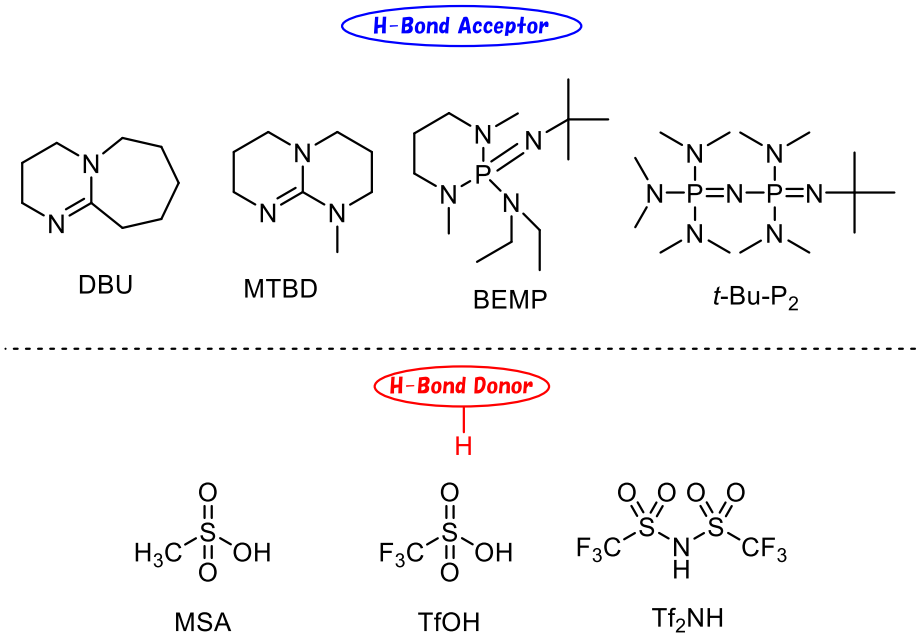

Figure 1.2. Representative monofunctional catalysts.

In contrast to the monofunctional catalysts, bifunctional catalysts/catalytic systems simultaneously activate the monomer and chain end (Figure 1.3).[31-43] The term bifunctional catalyst refers to a catalyst possessing both the hydrogen bond donor and acceptor sites in a molecule. Takemoto's catalyst,[35] 1,5,7-triazabicyclo[4,4,0]dec-5-ene (TBD),[26,36] and organophosphates [39-42] are representative bifunctional catalysts. Meanwhile, the bifunctional catalytic system is a mixture of the hydrogen bond donor and hydrogen bond acceptor molecules, and various combinations have been revealed to be effective for the ROP of cyclic esters. In addition, several organic salts have also been reported to exhibit the bi-activation property. [50-56]

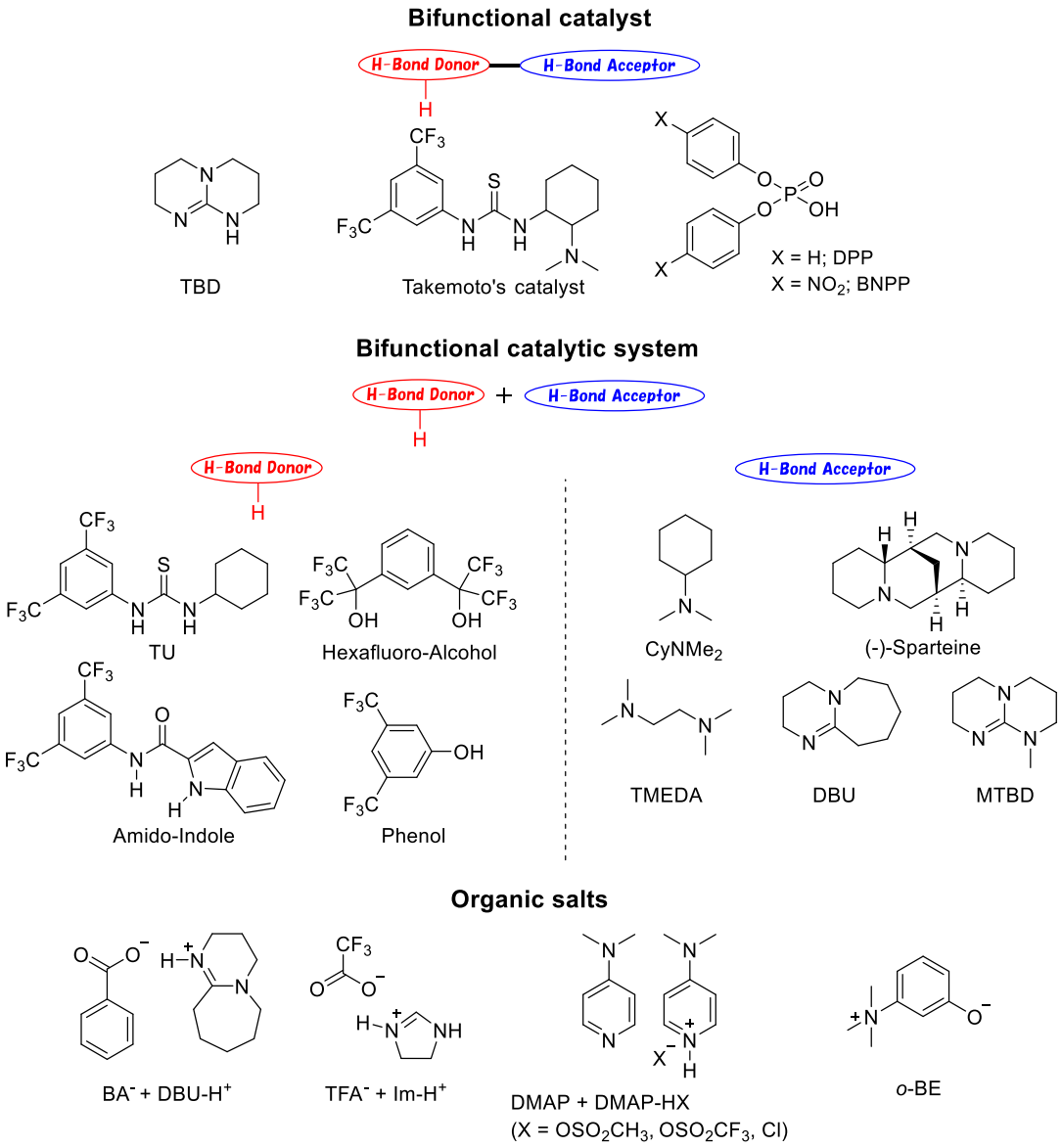

Figure 1.3. Representative bifunctional catalysts and bifunctional catalytic systems for the ROP of cyclic esters.

Due to the bi-activation property, the bifunctional catalysts/catalytic systems exhibit outstanding catalytic activities while each activation site alone is less active (Figure 1.4). For instance, organophosphates, such as diphenyl phosphate (DPP; pK_a = 3.7) and bis(4-nitrophenyl) phosphate (BNPP; pK_a = 1.7),[41]catalyze the ROP of ε-caprolactone (CL), δ-valerolactone (VL), and β-butyrolactone (BL),[39-42] while the ROPs of these lactones generally require a strong acidic catalyst, such as MSA (pK_a = −2.6) and TfOH (pK_a = −14).[89] This experimental observation was explained by density functional theory (DFT) calculations; the binding free energy of DPP with methanol (−7.3 kcal mol^{-1}) was lower than that of TfOH (−2.6 kcal mol^{-1}) as well as MSA (−2.7 kcal mol^{-1}), which suggested that the phosphoryl oxygen more efficiently acted as a hydrogen bonding acceptor than the sulfonate oxygen to activate the propagating chain-end.[34] Similarly, the thiourea + dimethylcyclohexylamine catalytic system catalyzes the ROP of L-lactide (L-LA), while both thiourea and dimethylcyclohexylamine have an insufficient activation ability in their single use.[35] Therefore, a bifunctional catalyst/catalytic system enables us to operate the ROP without using strong acids/bases, which can be a great advantage in the APE synthesis.[18] In general, the bifunctional catalyst/catalytic system exhibits a high selectivity for the ring-opening of the monomer relative to the intra- and inter molecular transesterifications to give APEs possessing controlled molecular weights and narrow dispersities with a high chain-end fidelity, while strong acids/bases lead to such undesirable side reactions. Therefore, the bifunctional catalyst/catalytic system is now recognized as a facile strategy to access biodegradable and biocompatible APE materials.

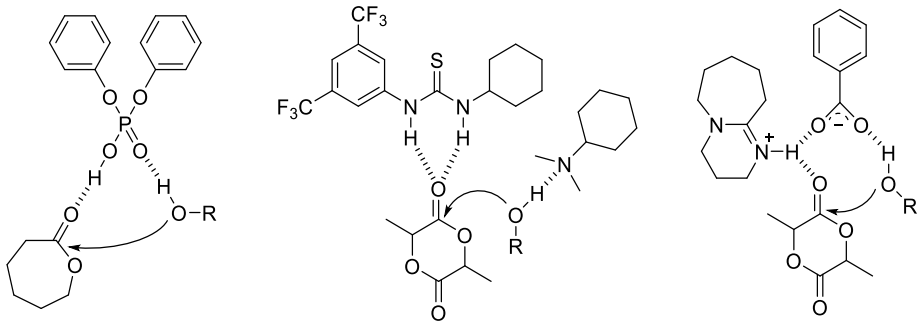

Figure 1.4. Bifunctional activation mechanism for the ROP of cyclic esters

As already described, the organocatalytic ROP has been significantly developed in order to achieve an environmentally-benign APE production. However, the organocatalysts have not replaced metal-based catalysts for the industrial production of aliphatic polyesters due to the unavoidable difficulties of organocatalysts, including high production costs, an extremely strong acidity/basicity, and/or low activity. Even for bifunctional catalysts, there are still many drawbacks, such as the use of a solvent and their low availability. Therefore, the development of an ROP system considering industrial requirements needs to be free from the dependence of a conventional metal-based catalyst.

1.4 Objective and Outline of the Thesis

As already described, the importance of biodegradable and biocompatible APE materials is now significantly increasing for environmental and biomedical purposes. The APE materials are usually synthesized using metal-based catalysts, like the Sn-containing catalyst. However, taking into account that they decompose in the soil, ocean, and human body, the use of metal-based catalysts is not preferred due to their potential toxicity. Therefore, the organocatalytic ROP has been developed over the last decade to establish clean and environmentally-benign synthesis methods to produce clean APEs without contamination by a toxic compound.

Organocatalysts are now employed in place of the conventional metal-based catalysts for laboratory scale APE synthesis due to the good accessibility to the well-defined APEs. However, despite the numerous efforts to achieve an environmentally-benign APE synthesis, the industrial application of the organocatalytic ROP system is still challenging. For example, the majority of organocatalytic ROPs is conducted in organic solvents, such as dichloromethane and toluene, which leads to a higher production cost and poor sustainability. To achieve the practical production of APEs, the bulk condition is highly preferred. In addition, organocatalysts used for the ROP are still more expensive than the conventional metal-based counterparts, otherwise, they need several synthesis steps from commercially-available reagents, which also lead to higher production costs. Furthermore, some of the organocatalysts show a cytotoxicity, and thus, "metal-free" does not necessarily mean biocompatible.[90] To make the organocatalytic ROP be more versatile, clean, and practical, the author developed three concepts to realize the goal of the environmentally-benign production of APE materials; (1) no use of toxic compounds, (2) low production cost (bulk process using readily available catalyst), and (3) easy operation without a complicated procedure. Therefore, the objective of this thesis is to establish a novel ROP system to produce a more versatile, practical, and environmentally-

benign approach beyond conventional systems using metal-based catalysts as well as organocatalysts.

To this end, the author first addressed the improvement of the conventional organocatalytic ROP by applying the bulk polymerization condition to overcome the use of a solvent. An organophosphate was chosen as the catalyst because of the low acidity, low toxicity, low corrosivity, and sufficient chemical stability of the organophosphates definitely suited for an industrial application. The author next focused on trimethyl glycine (TMG), which is a zwitterionic compound found in plants as well as in humans, as an appropriate candidate for the ROP catalyst to achieve the environmentally-benign production of APE materials. Furthermore, the author tried establishing an alkali metal carboxylate catalytic system as an innovative ROP system substituting for conventional systems using metal-based catalysts and organocatalysts.

An outline of the thesis is described in the following pages:

Chapter 2 describes the bulk ROP of cyclic esters using organophosphates, as shown in Scheme 1.7. By applying the bulk polymerization condition to the organophosphate-catalyzed ROP, the amount of loaded catalyst and reaction time were successfully reduced while maintaining both a sufficient polymerization ability and controlled/living nature. DPP could promote the ROP of various cyclic monomers, such as CL, δ-valerolactone (VL), 1,5-dioxepan-2-one (DXO), and TMC, leading to a well-defined APE including an aliphatic polycarbonate (APC) and aliphatic polyester-ether (APEE). A kinetic study revealed the controlled/living nature of the present bulk ROP system, which allowed us to produce the block copolymers composed of APEs, APEE, and APC in one-pot. The syntheses of the end-functionalized PCLs and PTMCs were successfully demonstrated using alcohol initiators possessing highly reactive functional groups. The broad utility of the organophosphate-catalyzed bulk ROP system was verified by the synthesis of the end-functionalized polyesters including the PCL-diol and star-shaped PCL-polyols. For further application, the author demonstrated the one-pot synthesis of polyurethanes via the ROP of CL and subsequent urethane formation reaction.

Scheme 1.7. Bulk ring-opening polymerization of cyclic esters using organophosphate catalyst

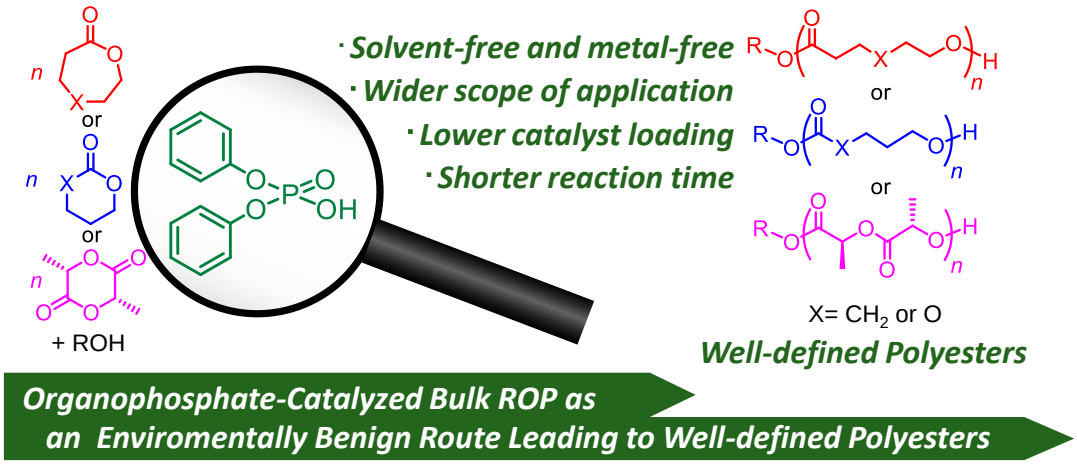

Chapter 3 describes the bulk ROP of cyclic carbonates leading to a biodegradable and biocompatible APC using TMG, as shown in Scheme 1.8. The ROP of TMC using TMG achieved the precise control over the molecular weight (~4,000) and dispersity (~1.22) to form well-defined PTMCs. The results of a matrix-assisted laser desorption/ionization time-of flight mass spectral analysis and a post polymerization experiment confirmed the controlled/living nature of the present ROP system. The screening of TMG analogues for the catalyst of the ROP revealed that the combination of carboxylate anions and quaternary ammonium cations in the TMG is an essential structural requirement. The FT-IR analysis of the TMC and alcohol initiator in the presence/absence of TMG confirmed the bi-activation ability of the TMG. End-functionalized APCs were successfully obtained using alcohol initiators bearing clickable functionalities, such as azido and ethynyl groups. Furthermore, the author demonstrated the synthesis of the APC-diol and -triol, which can be used as the soft segment of the APC-based polyurethane.

Scheme 1.8. Bulk ring-opening polymerization of cyclic carbonate using trimethyl glycine as a catalyst

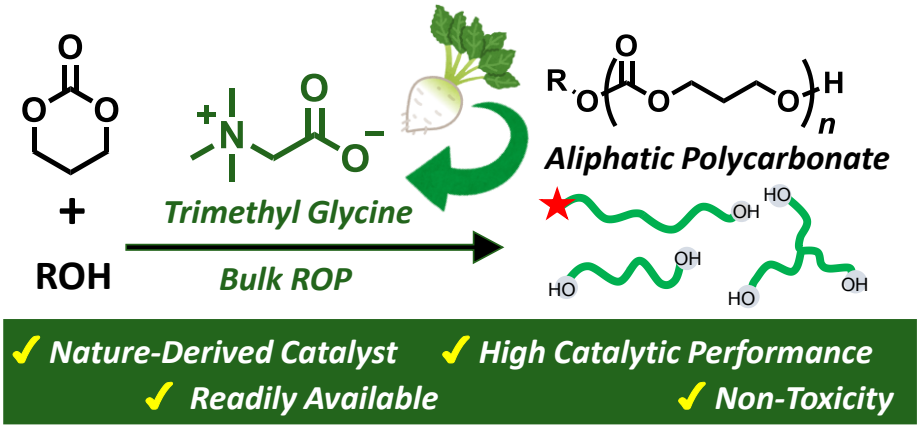

Chapter 4 describes the alkali-metal carboxylate-catalyzed ROP of cyclic esters, as shown in Scheme 1.9. Sodium acetate, which is used in industry as a food additive, catalyzed the ROP of L-LA in a controlled manner to give PLLAs possessing predictive molecular weights ranging from 3,500 to 22,600 and narrow dispersities. A kinetic experiment for the ROP of L-LA confirmed the controlled/living nature. By combining with functional initiators, end-functionalized polyesters, and multi-hydroxyl-containing polyesters, including PLLA-diol and star-shaped PLLA, were obtained. Furthermore, a block copolymer containing the PLLA segment was successfully synthesized using a macroinitiator possessing a hydroxyl group at the chain end. Sodium acetate could promote the ROP of the racemic DL-lactide (DL-LA) and TMC to give well-defined poly(DL-lactide) and PTMC. Furthermore, the tunability of the alkali metal carboxylates by the appropriate choice of the alkyl moiety and counter cation enables not only control of the polymerization behavior, but also expands the scope of the applicable monomers to CL and VL. Finally, the FT-IR measurement revealed the bifunctional character of the alkali metal carboxylate, in which the capability of activating the propagating chain end and monomer can be tuned by choosing the alkyl chain and counter cation of the catalyst.

Scheme 1.9. Alkali metal carboxylate-catalyzed ring-opening polymerization of cyclic esters and cyclic carbonate

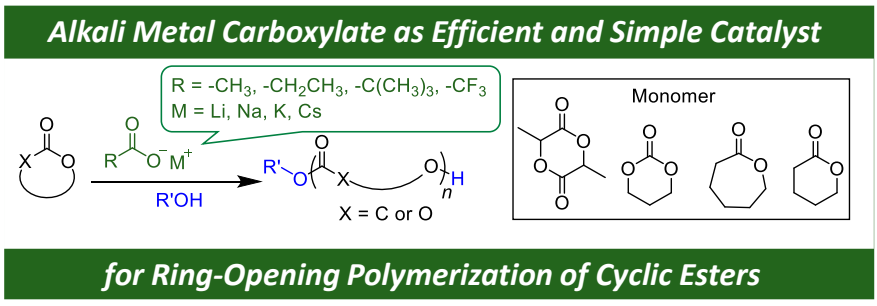

Chapter 5 summarizes the environmentally-benign and practical synthesis of aliphatic polyesters as the overall conclusions of this thesis.

1.5 References

1. Zhu, Y.; Romain, C.; Williams, C. K. *Nature* **2016**, *540*, 354−362.
2. Jambeck, J. R.; Gayer, R.; Wilcox, C.; Siegler, T. R.; Perryman, M.; Andrady, A.; Narayan, R.; Law, K. L. *Science* **2015**, *347*, 768−771.
3. Gross, R. A.; Lalra, B. *Science* **2002**, *297*, 803−807.
4. Rabnawaz, M.; Wyman, I.; Auras, R.; Cheng, S. *Green Chem*. **2017**, *19*, 4737-4753.
5. Okuda, M. *Prog. Polym. Sci.* **2002**, *27*, 87−133.
6. Aguirre E.C.; Franco F. I.; Samsudin, H.; Fang, X.; Auras, R. *Adv. Drug. Deliv. Rev.* **2016**, 107, 333−366.
7. Labet, M.; Thielemans, W. *Chem. Soc. Rev.* **2009**, *38*, 3484−3504.
8. Dechy-Cabaret, O.; Martin-Vaca, B.; Bourissou, D. *Chem. Rev.* **2004**, *104*, 6147−6176.
9. Albertson, A.-C.; Varma, I. K. *Biomacromolecules* **2003**, *4*, 1466−1486
10. Ahrendt, K. A.; Borths, C. J.; MacMallin, D. W. C. *J. Am. Chem. Soc.* **2000**, *122*, 4243−4244.
11. List, B.; Lerner, R. A.; Barbas III, C. F. *J. Am. Chem. Soc.* **2000**, *122*, 2395−2396.
12. Dalko, P. I.; Moisan, L. *Angew. Chem. Int. Ed.* **2004**, *43*, 5138−5175.
13. MacMillan, D. W. C *Nature*, **2008**, *445*, 304−308.
14. Nederberg, F.; Connor, E. F.; Möller, M.; Glauser, T.; Hedrick, J. L. *Angew. Chem. Int. Ed.* **2001**, *40*, 2712−2715.
15. Kamber, N. E.; Jeong, W.; Waymouth, R. M.; Pratt, R. C.; Lohemeijer B. G. G.; Hedrick, J. L. *Chem. Rev.* **2007**, *107*, 5813−5840.
16. Kiesewetter, M. K.; Shin, E. J.; Hedrick, J. L.; Waymouth, R. M. *Macromolecules* **2010**, *43*, 2093−2107.
17. Dove, A. P. ACS Macro Lett. **2012**, *1*, 1409−1412.
18. Thomas, C.; Bibal, B. *Green Chem*. **2014**, *16*, 1684−1699.
19. Ottou, W. N.; Sardon, H.; Mecerreyes, D.; Vignolle, J.; Taton, D. *Prog. Polym. Sci.* **2016**, *56*, 64−115.
20. Hu, S.; Zhao, J.; Zhang, G.; Schlaad, H. *Prog. Polym. Sci.* **2017**, *74*, 34−77.
21. Myers, M.; Connor, E. F.; Glauser, T.; Mock, A.; Nyce, G.; Hedrick, J. L. *J. Polym. Sci., Part A: Polym. Chem.* **2002**, *40*, 844−851.
22. Connor, E. F.; Nyce, G. W.; Myers, M.; Mock, A.; Hedrick, J. L. *J. Am. Chem. Soc.* **2002**, *124*, 914−915.
23. Nyce, G. W.; Glauser, T.; Connor, E. F.; Mock, A.; Waymouth, R. M.; Hedrick, J. L. *J. Am.*

Chem. Soc. **2003**, *125*, 3046−3056.

24. Dove, A. P.; Pratt, R. C.; Lohmeijer, B. G. G.; Culkin, D. A.; Hagberg, E. C.; Nyce, G. W.; Waymouth, R. M.; Hedrick, J. L. *Polymer* **2006**, *47*, 4018−4025.
25. Kamber, N. E.; Jeong, W.; Gonzalez, S.; Hedrick, J. L.; Waymouth, R. M. *Macromolecules* **2009**, *42*, 1634−1639.
26. Lohmeijer, B. G. G.; Pratt, R. C.; Leibfarth, F.; Logan, J. W.; Long, D. A.; Dove, A. P.; Nederberg, F.; Choi, J.; Wade, C.; Waymouth, R. M.; Hedrick, J. L. *Macromolecules* **2006**, *39*, 8574–8583.
27. Zhang, L.; Nederberg, F.; Pratt, R. C.; Waymouth, R. M.; Hedrick J. L.; Wade, C. G. *Macromolecules 2007*, **40**, 4154–4158.
28. Zhang, L.; Nederberg, F.; Messman, J. M.; Pratt, R. C.; Hedrick, J. L.; Wade, C. G. *J. Am. Chem. Soc.* **2007**, *129*, 12610–12611.
29. Nederberg, F.; Lohmeijer, B. G. G.; Leibfarth, F.; Pratt, R. C.; Choi, J.; Dove, A. P.; Waymouth R. M.; Hedrick, J. L. *Biomacromolecules* **2007**, *8*, 153–160.
30. Bourissou, D.; Martin-Vaca, B.; Dumitrescu, A.; Graullier, M.; Lacombe, F. *Macromolecules* **2005**, *38*, 9993–9998.
31. Gazeau-Bureau, S.; Martin-Vaca, B.; Bourissou, D.; Navarro C.; Magnet, S. *Macromolecules* **2008**, *41*, 3782–3784.
32. Delcroix, D.; Martin-Vaca, B.; Bourissou D.; Navarro, C. *Macromolecules* **2010**, *43*, 8828–8835.
33. Makiguchi, K.; Kikuchi, S.; Satoh, T.; Kakuchi, T. *J. Polym. Sci., Part A: Polym. Chem.* **2013**, *51*, 2455−2463.
34. Susperregui, N.; Delcroix, D.; Martin-Vaca, B.; Bourissou D.; Maron, L. *J. Org. Chem.* **2010**, *75*, 6581–6587.
35. Dove, A. P.; Pratt, R. C.; Lohmeijer, B. G. G.; Waymouth R. M.; and Hedrick, J. L. *J. Am. Chem. Soc.* **2005**, *127*, 13798–13799.
36. Pratt, R. C.; Lohmeijer, B. G. G.; Long, D. A.; Waymouth, R. M.; Hedrick, J. L. *J. Am. Chem. Soc.* **2006**, *128*, 4556–4557.
37. Bouyahyi, M.; Pepels, M. P. F.; Heise A.; Duchateau, R. *Macromolecules* **2012**, *45*, 3356–3666.
38. Silvers, A. L.; Chang, C.-C.; Emrick, T. *J. Pol. Sci., Part A: Polym. Chem.* **2012**, *50*, 3517–3529.

39. Makiguchi, K.; Satoh, T.; Kakuchi, T. *Macromolecules* **2011**, *44*, 1999−2005.
40. Makiguchi, K.; Ogasawara, Y.; Kikuchi, S.; Satoh, T.; Kakuchi, T. *Macromolecules* **2013**, *46*, 1772−1782.
41. Makiguchi, K.; Satio, T.; Satoh, T.; Kakuchi, T. *J. Polym. Sci., Part A: Polym. Chem.* **2014**, *52*, 2032−2039.
42. Makiguchi, K.; Yamanaka, T.; Kakuchi, T.; Terada, M.; Satoh, T. *Chem. Commun.* **2014**, *50*, 2883−2885.
43. Miyake, G. M.; Chen, E. Y. X. *Macromolecules* **2011**, *44*, 4116−4124.
44. Pratt, R. C.; Lohmeijer, B. G. G.; Long, D. A.; Pontus Lundberg, P. N.; Dove, A. P.; Li, H.; Wade, C.; Waymouth, R. M.; Hedrick, J. L. *Macromolecules* **2006**, *39*, 7863–7871.
45. Thomas, C.; Peruch F.; Bibal, B. *RSC Adv.* **2012**, *2*, 12851–12856.
46. Koeller, S.; Kadota, J.; Deffieux, A.; Peruch, F.; Massip, S.; Léger, J.-M.; Desvergne, J.-P.; Bibal, B. *J. Am. Chem. Soc.* **2009**, *131*, 15088–15089.
47. Koeller, S.; Kadota, J.; Peruch, F.; Deffieux, A.; Pinaud, N.; Pianet, I.; Massip, S.; Leger, J.-M.; Desvergne J.-P.; Bibal, B. *Chem.–Eur. J.* **2010**, *16*, 4196–4205.
48. Xu, S.; Sun, H.; Liu, J.; Xu, J.; Pan, X.; Dong, H.; Liu, Y.; Li, Z.; Guo, K. *Polym. Chem.* **2016**, *7*, 6843–6853.
49. Dhamaratne, N. U.; Pothupitiya, J. U.; Bannin, T. J.; Kazakov, O. I.; Liesewetter, M. K. *ACS Macro Lett.* **2017**, *6*, 421–425.
50. Kadota, J.; Pavlovic, D.; Desvergne, J.-P.; Bibal, B.; Peruch, F. Deffieux, A. *Macromolecules* **2010**, *43*, 8874–8879.
51. Coady, D. J.; Fukushima, K.; Horn, H. W.; Rice, J. E.; Hedrick, J. L. *Chem. Commun.* **2011**, *47*, 3105–3107.
52. Coulembier, O.; Josse, T.; Guillerm, B.; Gerbaux, P.; Dubois, P. *Chem. Commun.* **2012**, *48*, 11695–11697.
53. Guillerm, B.; Lemaur, V.; Cornil, J.; Lazzaroni, R.; Dubois, P.; Coulembier, O. *Chem. Commun.* **2014**, *50*, 10098–10101.
54. Chesterman, J. P.; Amsden, B. G. *Polym. Chem.* **2016**, *7*, 6946–6953.
55. Liu. J.; Xu, J.; Li, Z.; Xu, S.; Wang, X.; Wang, H.; Guo, T.; Gao, Y.; Zhang, L.; Guo, K. *Polym. Chem.* **2017**, *8*, 7054–7068
56. Xu, J.; Liu, J.; Li, Z.; Wang, H.; Xu, S.; Guo, T.; Zhu, H.; Wei, F.; Zhu, Y.; Guo, K. *Polymer* **2018**, *154*, 17–26.

57. Esswein, B.; Möller, M. *Angew. Chem. Int. Ed.* **1996**, *35*, 623–625.
58. Esswein, B.; Steidl, N. M.; Möller, M. *Macromol. Rapid Commun.* **1996**, *17*, 143–148.
59. Esswein, B.; Molenberg, A.; Möller, M. *Macromol. Symp.* **1996**, *107*, 331–340.
60. Rexin, O.; Mülhaupt, R. *J. Polym. Sci., Polym. Chem.* **2002**, *40*, 864–873.
61. Hans, M.; Keul, H.; Möller, M. *Polymer* **2009**, *50*, 1103–1108.
62. Schmalz, H.; Lanzerdörfer, M. G.; Abetz, V.; Müller, A. H. E. *Macromol. Chem. Phys.* **2003**, *204*, 1056–1071.
63. Misaka, H.; Sakai, R.; Satoh, T.; Kakuchi, T. *Macromolecules* **2011**, *44*, 9099–9107.
64. Misaka, H.; Tamura, E.; Makiguchi, K.; Kamoshida, K.; Sakai, R.; Satoh, T.; Kakuchi, T. *J. Polym. Sci., Part A, Polym. Chem.* **2012**, *50*, 1941–1952.
65. Memenger, Jr. W.; Campbell, G. C.; Davidson, F. *Macromolecules* **1996**, *29*, 6475-6480.
66. Rodriguez, M.; Marrot, S.; Kato, T.; Sterin, S.; Fleury, E.; Baceiredo, A. J. *Organomet. Chem.* **2007**, *692*, 705–708.
67. Lohmeijer, B. G.; Dubois, G.; Leibfarth, F.; Pratt, R. C.; Nederberg, F.; Nelson, A.; Waymouth, R. M.; Wade, C.; Hedrick, J. L. *Org. Lett.* **2006**, *8*, 4683–4686.
68. Iwasaki, Y.; Yamaguchi, E. *Macromolecules* **2010**, *43*, 2664–2666.
69. Zhang, S.; Li, A.; Zou, J.; Lin, L. Y.; Wooley, K. L. *ACS Macro Lett.* **2012**, *1*, 328−333.
70. Clément, B.; Grignard, B.; Koole, L.; Jérôme, C.; Lecomte, P. *Macromolecules* **2012**, *45*, 4476−4486.
71. Steinbach, T.; Schröder, R.; Ritzc, S.; Wurm, F. R. *Polym. Chem.* **2013**, *4*, 4469–4479.
72. Zhang, S.; Wang, H.; Shen, Y.; Zhang, F.; Seetho, K.; Zou, J.; Taylor, J.-S. A.; Dove, A. P.; Wooley, K. L. *Macromolecules* **2013**, *46*, 5141–5149.
73. du Boullay, O. T.; Marchal, E.; Martin-Vaca, B.; Cossio, F. P.; Bourissou, D. *J. Am. Chem. Soc.* **2006**, *128*, 16442–16443.
74. Illy, N.; Boileau, S.; Buchmann, W.; Penelle, J.; Barbier, V. *Macromolecules* **2010**, *43*, 8782–8789.
75. Illy, N.; Boileau, S.; Penelle, J.; Barbier, V. *Macromol. Rapid Commun.* **2009**, *30*, 1731–1735.
76. Scholten, M. D.; Hedrick, J. L.; Waymouth, J. L. *Macromolecules* **2008**, *41*, 7399–7404.
77. Kakuchi, T.; Chen, Y.; Kitakado, J.; Mori, K.; Fuchise, K; Satoh, T. *Macromolecules* **2011**, *44*, 4611–4647.
78. Fuchise, K.; Sakai, R.; Satoh, T.; Sato, S.-i.; Narumi, A. Kawaguchi, S.; Kakuchi, T.

Macromolecules **2010**, *43*, 5589–5594.

79. Takada, K.; Fuchise, K. Chen, Y.; Satoh, T.; Kakuchi, T. *J. Polym. Sci., Part A: Polym. Chem.* **2012**, *50*, 3560–3566.
80. Kikuchi, S.; Chen, Y.; Kitano, K.; Takada, K.; Satoh, T.; Kakuchi, T. *Polym. Chem.* **2015**, 6, 6845–6856.
81. Treat, N. J.; Sprafke, H.; Kramer, J. W.; Clark, P. G.; Barton, B. E.; Read de Alaniz, J.; Fors, B. P.; Hawker, C. J. *J. Am. Chem. Soc.* **2014**. *136*, 16096–16101.
82. Discekici, E. H.; Anastasaki, A. Read de Alaniz, J.; Hawker, C. J. *Macromolecules* **2018**, *51*, 7421–7434.
83. Huang, Z.; Gu, Y.; Liu, X.; Zhang, L.; Cheng, Z. Zhu, X. *Macromol. Rapid Commun. 38*, 1600461–160046.
84. Pan, X; Fang, C.; Fantin, M.; Malhotra, N.; So, W. Y.; Peteanu, L. A.; Isse, A. A.; Gennaro, Liu, P.; Mathjaszewski, K. *J. Am. Chem. Soc.* **2016**, *138*, 2411–2425.
85. Utiyama, M.; Satoh, K.; Kamigaito, M. *Angew. Chem. Int. Ed.* **2014**, *54*, 1924–1928.
86. Ogawa, K. A.; Goetz, A. E.; Boydston, A. J. *J. Am. Chem. Soc.* **2016**, *137*, 1400–1403.
87. Goetz, A. E.; Boydston, A. J. *J. Am. Chem. Soc.* **2015**, *137*, 7572–7575.
88. Denmark, S. E.; Kalyani, D.; Collins, W. R. *J. Am. Chem. Soc.* **2010**, *132*, 12752–12765.
89. Christ, P.; Lindsay A. G., Vormittag, S. S.; Neudörfl, J.M.; Berkessel, A.; O'Donoghue, A. C. *Chem. Eur. J.* **2011**, *17*, 8524–8528.
90. Nachtergael, A.; Coulembier, O.; Dubois, P.; Helvenstein, M.; Duez, P.; Blankert, B.; Mespouille, L. *Biomacromolecules* **2015**, *16*, 507–514.

Chapter 2

Bulk Ring-opening Polymerization of Cyclic Esters Using Organophosphate Catalyst

2.1 Introduction

In the last decade, organocatalytic polymerization has been developed as a clean and precise synthesis method leading to no metal-contaminating polymeric materials.[1-6] For the synthesis of aliphatic polyesters (APEs), the organocatalytic strategy provides a significant advantage because the contamination of the metal-based catalyst residues could become a concern for their biomedical and environmental applications. To date, various types of organic acid/base catalysts have been developed as efficient catalysts for the ring-opening polymerization (ROP) of cyclic esters. In general, organic Brønsted acids, *e.g.*, methane sulfonic acid (MSA) and triflimide, were found to be suitable for the polymerization of lactones,[7-18] whereas organic bases, *e.g.*, 1,8-diazadicyclo[5.4.0]undec-7-ene (DBU) and *N*-methyl-1,5,7-triazabicyclo[4,4,0]dec-5-ene (MTBD), were effective for the ROP of the lactide (LA).[19-25] In addition, the bifunctional catalyst/catalytic system possessing two activation sites for the monomer and propagating chain end also turned out to be effective for the ROP of ε-caprolactone (CL) and LA.[26-35]

Despite such considerable efforts, there are still many problems to be overcome for the industrial scale production of APE using an organocatalytic system. In general, a strong acidity or basicity is required to catalyze the ROP of cyclic esters, which is often accompanied by undesirable side reactions, such as inter- and intra-transesterifications, resulting in less control over the molecular weight and dispersity ($Đ$). Furthermore, Bourissou *et al*. reported that the high acidity of a catalyst caused deactivation of the propagating chain end, resulting in interruption of the high molecular weight polymer production.[8] In addition, (super) strong acids/bases seriously damage the reaction vessel as well as the human body, and some of them are unstable in moisture and/or air. These properties make it difficult to operate the polymerization process on an industrial scale.

In contrast, organophosphates, such as diphenyl phosphate (DPP; pK_a = 3.7) and bis(4-

nitrophenyl)phosphate (BNPP; pK_a = 1.7),[15] were reported as efficient weak Brønsted acids catalysts for the ROP of cyclic esters and carbonates to produce the corresponding well-defined APEs including aliphatic polycarbonates (APCs).[14,15,36] Therefore, the organophosphates have many significant advantages over the above-mentioned strong organic acids. As described in chapter 1, organophosphates simultaneously activate the monomer and propagating chain end by the phosphoric acid moiety and phosphoryl oxygen, respectively, which enables them to effectively catalyze the ROPs under mild reaction conditions in spite of their low acidity. In addition to the low acidity, the low toxicity, low corrosivity, and sufficient chemical stability of the organophosphates are highly attractive for application in an industrial scale process.[37] However, some problems still remained for the organophosphate-catalyzed ROP, *e.g.*, the amount of the loaded catalyst and the use of a solvent. In a previous procedure, an equimolar amount of the catalyst is required with respect to the initiator, and the monomer concentration is typically 1.0 mol L^{-1}, which lead to a higher production cost and environmental pollution. To make the organophosphate-catalyzed ROP be more versatile, facile, and environmentally-benign, of particular interest is to establish a solvent-free ROP process with a reduced catalyst loading.

In this chapter, the author describes the organophosphate-catalyzed bulk ROP of various cyclic esters, such as CL, δ-valerolactone (VL), L-lactide (L-LA), 1,5-dioxepan-2-one (DXO), and trimethylene carbonate (TMC), as an environmentally-benign way to produce the APEs including APC and aliphatic polyester-ether (APEE) (Scheme 2.1). In this study, the amount of the loaded catalyst and reaction time could be significantly reduced due to the bulk polymerization condition while maintaining both the sufficient polymerization ability and controlled/living nature. The broad utility of the organophosphate-catalyzed bulk ROP system was verified through the synthesis of the block copolyesters as well as the functionalized polyesters, such as the end-clickable poly(ε-caprolactone)s (PCLs) and PCL-polyols. It is

worthy to note that the synthesis of the PCL-polyols, which are the industrially important prepolymers for polyurethanes, was accomplished by applying the bulk conditions, whereas it was difficult by the conventional procedure in solution. For further application in industrial processes, the author demonstrated the one-pot synthesis of polyurethanes via the ROP of CL and subsequent urethane formation reaction, in which both reactions were catalyzed solely by the organophosphate.

Scheme 2.1. Organophosphate-catalyzed bulk ROP leading to block copolyesters, end-functionalized polyesters, and PCL-based polyurethane

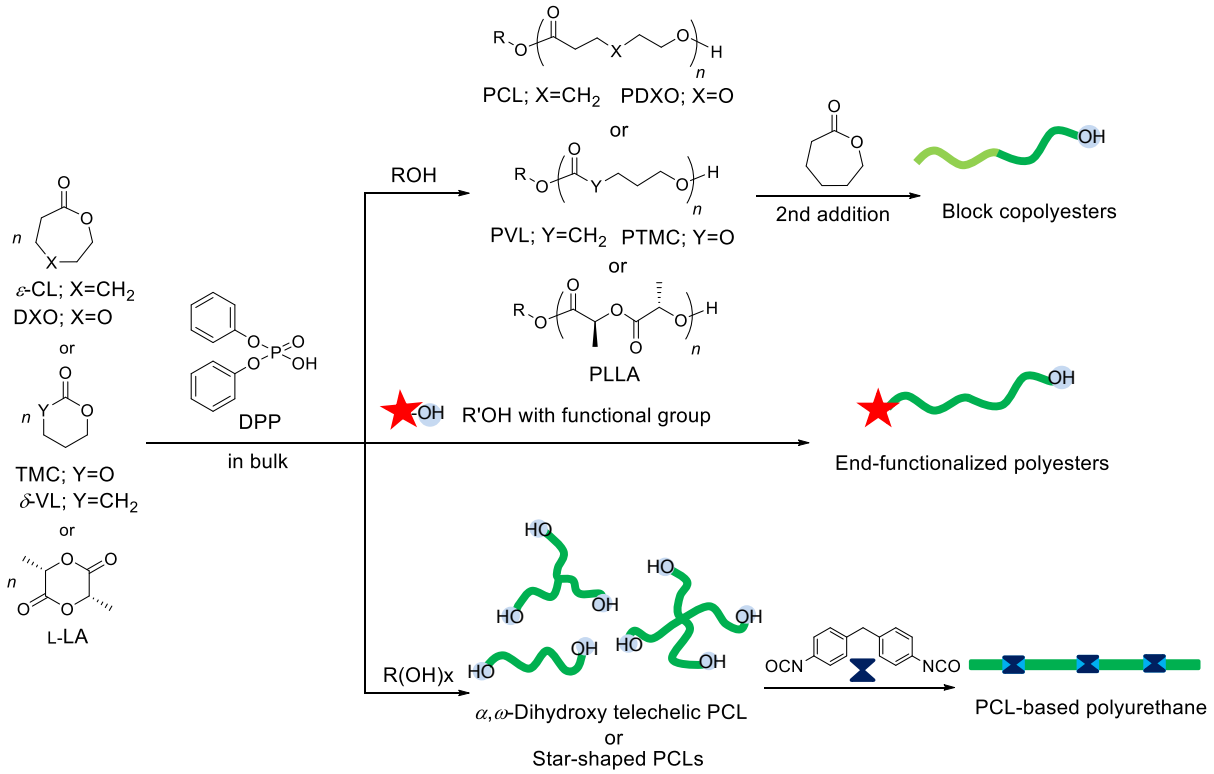

All the processes were performed in one-pot synthesis in the bulk

2.2 Results and Discussion

2.2.1 Ring-opening Polymerization of Cyclic Esters Catalyzed by Organophosphates in the Bulk

To clarify the advantage of the bulk polymerization condition for the DPP-catalyzed ROP over the solution polymerization procedure, the author first attempted the bulk polymerization of CL at the $[CL]_0/[initiator]_0/[DPP]$ ratio of 50/1/0.05 at 80 °C, where 3-phenyl-1-propanol (PPA) was used as the initiator (run 1 in Table 2.1). The polymerization homogeneously proceeded while the viscosity of the reaction mixture increased with the reaction time. The monomer conversion reached 92.4% within 250 min to give the PCL, indicating the high catalytic performance of DPP under the bulk polymerization condition. The ^{1}H NMR spectrum of the obtained PCL exhibited minor signals due to the 3-phenyl-1-propoxy group along with the signals due to the PCL main chain (Figure 2.1(a)). The number-average molecular weight ($M_{n,NMR}$) was determined to be 5,500 from the ^{1}H NMR measurement, which was in good agreement with the theoretical value ($M_{n,th.}$ = 5,400). The size exclusion chromatography (SEC) trace of the obtained PCL was monodispersed with the $Đ$ value of 1.08 (Figure 2.1(b)) implying the well-controlled nature of the bulk polymerization system. Furthermore, the matrix-assisted laser desorption/ionization time-of-flight mass spectrum (MALDI-TOF MS) of the obtained PCL displayed only one series of peaks corresponding to the PCL possessing a PPA residue at the α-chain end (Figure 2.2), which confirmed the absence of cyclic byproduct derived from intramolecular transesterification. These data demonstrated that the DPP-catalyzed ROP in the bulk offers a high degree of control over the molecular weight and dispersity as well as the polymer structure, which is comparable to that observed for the conventional DPP-catalyzed ROP in solution. Thus, the present bulk polymerization procedure has the greater advantage of being able to produce the well-defined PCLs without any solvents at a lower catalyst loading.

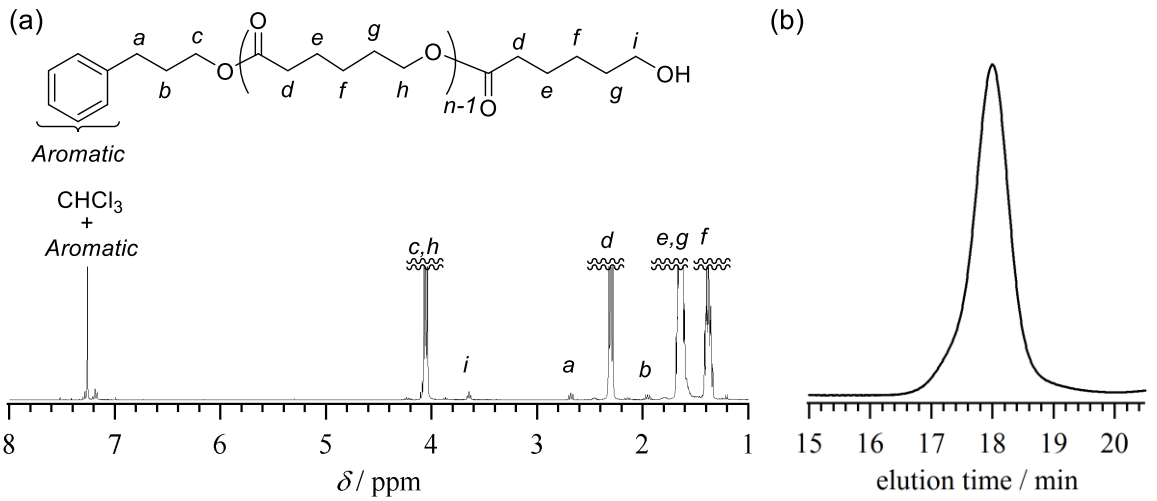

Figure 2.1. (a) ^{1}H NMR spectrum in $CDCl_3$, and (b) SEC trace (eluent, $CHCl_3$; flow rate, 1.0 mL min^{-1}) of the PCL obtained from run 1 in Table 2.1.

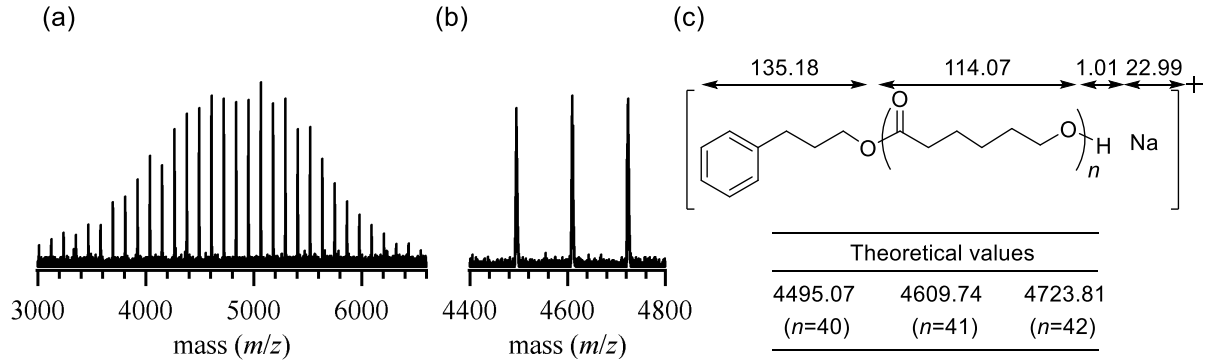

Figure 2.2. (a) MALDI-TOF MS spectrum of PCL (run 1 in Table 2.1), (b) expanded spectrum (ranging from 4,400 to 4,800), and (c) theoretical molecular weights.

To explore the full potential of the organophosphate as the catalyst, the author examined BNPP and di(2,6-xylyl)phosphate (DXP), which are analogues of DPP having electron-withdrawing and electron-donating substituents, respectively, as the catalyst for the bulk ROP of CL (runs 2 and 3 in Table 2.1). Each organophosphate catalyzed the ROP of CL at the $[CL]_0/[PPA]_0/[BNPP \text{ or } DXP]$ ratio of 50/1/0.05 at 80 °C to produce well-defined PCLs with predicted molecular weight values and narrow $Đ$ values. The quality of the PCLs obtained with the different organophosphates is virtually the same. However, the kinetics of the ROP

was significantly varied depending on the substituent of the organophosphates. The turnover frequency (TOF) values were calculated to be 222 h^{-1}, 306 h^{-1}, and 155 h^{-1} for the ROPs at the $[CL]_0/[PPA]_0/[organophosphate]$ ratio of 50/1/0.05 using DPP, BNPP, and DXP, respectively. These results revealed that the electron withdrawing substituents on the organophosphate increase the polymerization kinetics. Thus, the appropriate choice of the substituents on the organophosphates allows the precise tuning of the polymerization conditions, such as the reaction time and temperature as well as the catalyst loading.

Table 2.1. Bulk ring-opening polymerization of CL catalyzed by organophosphates [a]

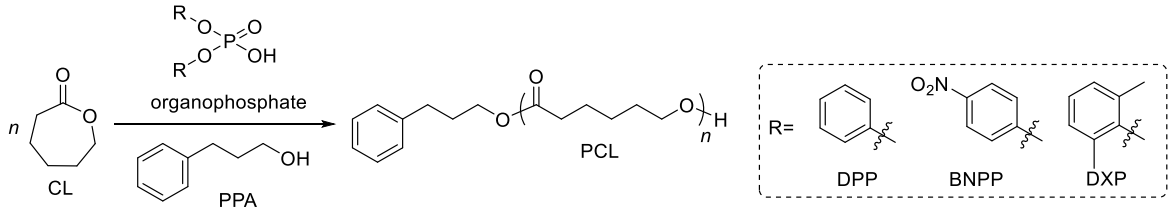

run	cat.	$[M]_0/[PPA]_0$ /[cat.]	time (min)	conv. (%) [b]	$M_{n,th.}$ [c]	$M_{n,NMR}$ [b]	$M_{n,SEC}$ [d]	$Đ$ [d]	TOF (h^{-1})
1	DPP	50/1/0.05	250	92.4	5,400	5,500	11,100	1.08	222
2	BNPP	50/1/0.05	180	91.8	5,400	5,400	11,000	1.09	306
3	DXP	50/1/0.05	360	93.1	5,500	5,500	11,900	1.11	155

[a] Polymerization conditions: atmosphere, Ar; temperature, 80 °C. [b] Determined by ^{1}H NMR spectrum of the obtained polymer in $CDCl_3$. [c] Calculated from $[CL]_0/[PPA]_0 \times$ conv. × (M.W. of CL) + (M.W. of PPA). [d] Determined by SEC measurement of the obtained polymer in $CHCl_3$ using polystyrene standards.

The author next investigated the effect of the catalyst loading on the polymerization behavior. The DPP-catalyzed bulk ROP of CL with varying $[PPA]_0/[DPP]$ ratios from 1/1.00 to 1/0.01 were conducted (runs 1, 4 – 7 in Table 2.2) at 80 °C. In case of the bulk ROP at the $[CL]_0/[PPA]_0/[DPP]$ ratio of 50/1/1, the monomer conversion reached 86.3% within 12 min. This is in sharp contrast to the ROP in toluene at the $[CL]_0/[PPA]_0/[DPP]$ ratio of 50/1/1 (run 8

in Table 2.2), which required 300 min to reach an 83.6% monomer conversion. These results clearly demonstrated the advantage of the DPP-catalyzed bulk ROP over the solution polymerization conditions. Surprisingly, the DPP-catalyzed bulk ROP proceeded in a well-controlled manner with sufficient TOF values even at the $[PPA]_0/[DPP]$ ratio of 1/0.01, leading to the well-defined PCLs. In contrast, the DPP-catalyzed ROP of CL in solution did not proceed even at the $[PPA]_0/[DPP]$ of 1/0.1 (run 9 in Table 2.2), meaning that the amount of loaded catalyst was successfully reduced to 1/100 of the DPP-catalyzed ROP of cyclic esters, due to bulk conditions. Therefore, the bulk condition allowed the full potentials of the catalytic ability of the organophosphate, resulting in remarkably higher TOF values and a lower catalyst loading than that required for the conventional solution polymerization while keeping the well-controlled manner of the polymerization.

Table 2.2. Ring-opening polymerization of CL with varying the amount of loaded DPP [a]

run	$[M]_0/[PPA]_0$ /[DPP]	time (min)	conv. (%) [b]	$M_{n,th.}$ [c]	$M_{n,NMR}$ [b]	$M_{n,SEC}$ [d]	$Đ$ [d]	TOF (h^{-1})
1	50/1/0.05	250	92.4	5,400	5,500	11,100	1.08	222
4	50/1/1.00	12	86.2	5,100	5,200	9,900	1.27	215
5	50/1/0.10	120	84.5	5,000	5,100	9,100	1.14	211
6	50/1/0.03	420	78.4	4,600	4,800	9,700	1.07	186
7	50/1/0.01	1,560	84.7	5,000	5,200	11,300	1.09	163
8 [e]	50/1/1.00	300	83.6	4,900	5,100	10,000	1.08	8
9 [e]	50/1/0.10	300	4.8	400	800	800	1.16	4

[a] Polymerization conditions: atmosphere, Ar; temperature, 80 °C. [b] Determined by ^{1}H NMR spectrum of the obtained polymer in $CDCl_3$. [c] Calculated from $[CL]_0/[PPA]_0 \times$ conv. × (M.W. of CL) + (M.W. of PPA). [d] Determined by SEC measurement of the obtained polymer in $CHCl_3$ using polystyrene standards.

2.2.2 DPP-Catalyzed Bulk ROP of Cyclic Esters, Cyclic Ester-ether, and Cyclic Carbonate

To expand the scope of monomer, the author performed the DPP-catalyzed ROP of VL, DXO, TMC, and L-LA to produce the corresponding polymers, *i.e.*, poly(*δ*-valerolactone) (PVL), poly(1,5-dioxepan-2-one) (PDXO), poly(trimethylene carbonate) (PTMC), and poly(L-lactide) (PLLA), respectively. The bulk ROP of *δ*-VL, an analog of CL having a six-membered ring, was first examined at the $[\delta\text{-VL}]_0/[\text{PPA}]_0/[\text{DPP}]$ ratio of 25/1/0.05 at 80 °C. The monomer conversion reached 94.9% within 15 min to give a narrowly dispersed PVL with the $M_{n,NMR}$ value of 2,400 that was in good agreement with the $M_{n,th}$ value (2,500), as listed in Table 2.3. The PVLs with the desirable molecular weight were produced by varying the $[\delta\text{-VL}]_0/[\text{PPA}]_0$ ratios (runs 12 – 14 in Table 2.3). The optimized bulk ROP procedure was applied to DXO with the varying $[\text{DXO}]_0/[\text{PPA}]_0$ of 25 – 100, which gave the PDXOs with the $M_{n,NMR}$ and $Đ$ values of 2,900 – 10,900 and 1.13 – 1.23, respectively (runs 15 – 17 in Table 2.3). The bulk ROP of TMC at the $[\text{TMC}]_0/[\text{PPA}]_0/[\text{DPP}]$ ratios of 25/1/0.05, 50/1/0.05, and 100/1/0.05 also smoothly proceeded at 80 °C to give the corresponding PTMCs with the $M_{n,NMR}$s and $Đ$s of 2,500 – 7,900 and 1.07 – 1.09, respectively (runs 18 – 20 in Table 2.3). The ^{1}H NMR spectra of all the obtained polymers showed signals corresponding to a 3-phenyl-1-propoxy group at the *α*-chain end, suggesting that PPA was incorporated as the initiator in all cases. In addition, the MALDI-TOF MS spectral analysis provided further evidence that the DPP-catalyzed bulk ROPs led to well-defined polymers without any undesirable reactions (Figures 2.4, 2.5, and 2.6). Notably, there was no evidence of a decarboxylation reaction during the bulk ROP of TMC. In the MALDI-TOF MS spectrum of the obtained PTMC, only one series of peaks was observed, which corresponded to the expected chemical structure of the PTMC. For example, the measured molecular weight of 4343.65 matched well with the theoretical one ($[\text{M+Na}]^+ = 4343.38$) for the 41-mer of the PTMC possessing a 3-phenyl-1-propoxy group at the *α*-chain end. This is in contrast with the ROP system for TMC catalyzed by super Bronsted acids such as TfOH, which

usually suffers from decarboxylation resulting in partial incorporation of ether bonds in the PTMC backbone.[40] Therefore, the author achieved the highly efficient solvent-free production of various APEs, APEE, and APC using organophosphates with a remarkably small catalyst loading. Indeed, the DPP-catalyzed bulk ROPs of CL, VL, DXO, and TMC could be operated with 0.05 – 0.20 mol% catalyst loadings, which correspond to 1/20 of catalyst loading required for a conventional solution polymerization procedure.

Table 2.3. Bulk ring-opening polymerization of cyclic esters, cyclic ester-ether, and cyclic carbonate catalyzed by DPP [a]

run	monomer (M)	$[M]_0/[PPA]_0$ /[DPP]	time (h)	conv. (%) [b]	$M_{n,th.}$ [c]	$M_{n,NMR}$ [b]	$M_{n,SEC}$ [d]	$Đ$ [d]
10	CL	25/1/0.05	1.7	94.2	2,800	2,700	5,900	1.16
1	CL	50/1/0.05	4.2	92.4	5,400	5,500	11,100	1.08
11	CL	100/1/0.05	17	77.0	8,900	9,200	17,100	1.12
12	VL	25/1/0.05	0.25	94.9	2,500	2,400	5,800	1.08
13	VL	50/1/0.05	0.67	90.4	4,700	5,000	9,400	1.08
14	VL	100/1/0.05	3.0	80.6	8,200	8,600	17,900	1.07
15	DXO	25/1/0.05	3.2	96.8	3,000	2,900	2,900	1.14
16	DXO	50/1/0.05	7.5	88.3	5,300	5,300	4,400	1.13
17	DXO	100/1/0.05	24	90.1	10,600	10,900	7,200	1.23
18	TMC	25/1/0.05	9.5	93.0	2,500	2,500	4,100	1.09
19	TMC	50/1/0.05	17	91.8	4,800	4,700	6,800	1.07
20	TMC	100/1/0.05	54	75.0	7,800	7,900	9,000	1.08
21 [e]	L-LA	50/1/0.50	22	85.7	6,300	6,800	9,700	1.23

[a] Polymerization conditions: atmosphere, Ar; temperature, 80 °C. [b] Determined by ^{1}H NMR spectrum of the obtained polymer in $CDCl_3$. [c] Calculated from $[M]_0/[PPA]_0 \times$ conv. × (M.W. of M) + (M.W. of PPA). [d] Determined by SEC measurement of the obtained polymer in $CHCl_3$ using polystyrene standards. [e] The polymerization was conducted at 130 °C.

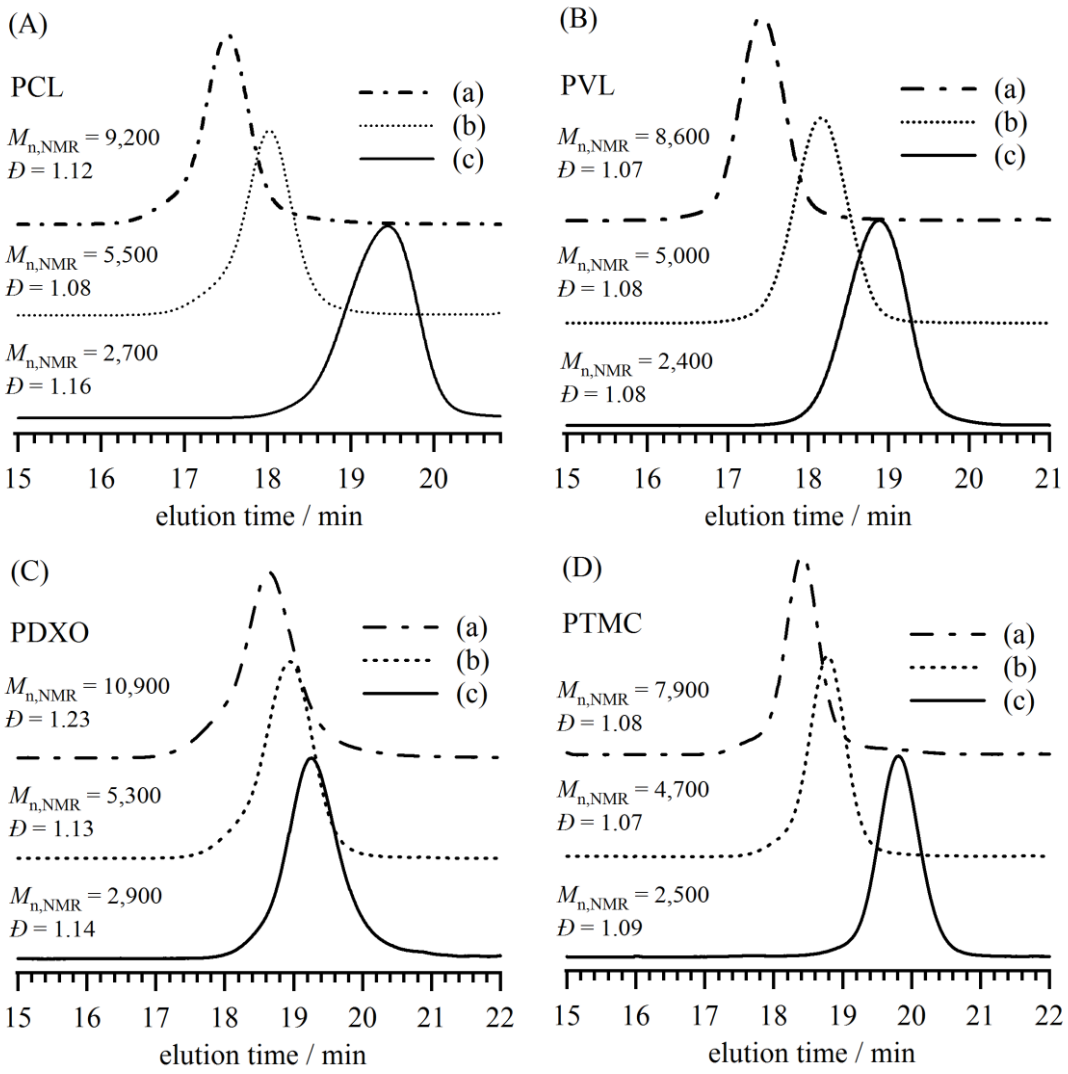

Figure 2.3. SEC traces of (A) the obtained PCLs, (B) PVLs, (C) PDXOs, and (D) PTMCs with the $[M]_0/[PPA]_0$ ratios of (a) 100/1, (b) 50/1, and (c) 25/1 (eluent, $CHCl_3$; flow rate, 1.0 mL min^{-1}).

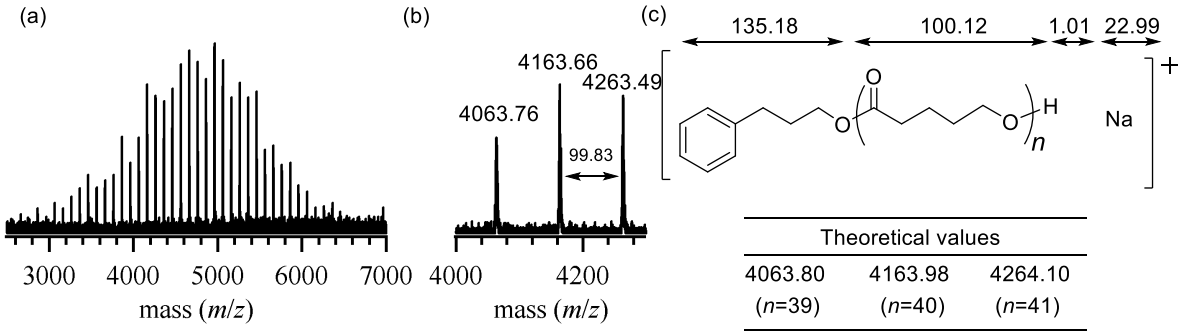

Figure 2.4. (a) MALDI-TOF MS spectrum of PVL (run 13 in Table 2.3), (b) expanded spectrum (ranging from 4,000 to 4,300), and (c) theoretical molecular weight values.

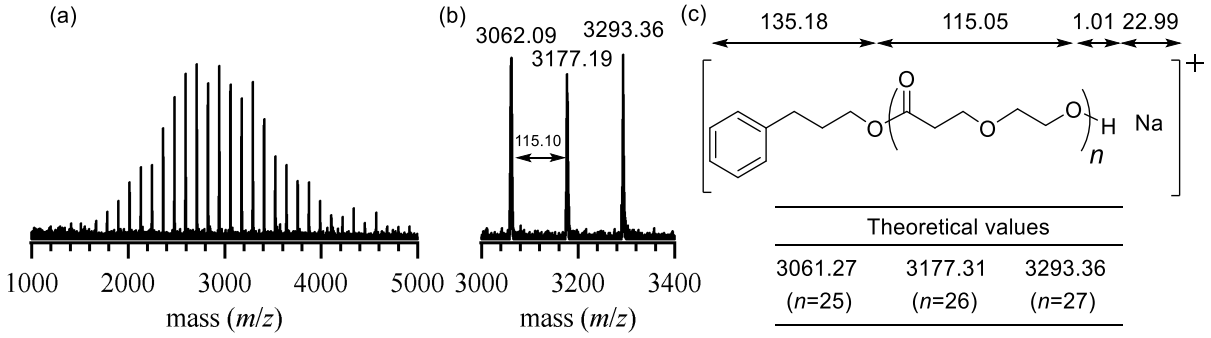

Figure 2.5. (a) MALDI-TOF MS spectrum of PDXO (run 16 in Table 2.3), (b) expanded spectrum (ranging from 3,000 to 3,400), and (c) theoretical molecular weight values.

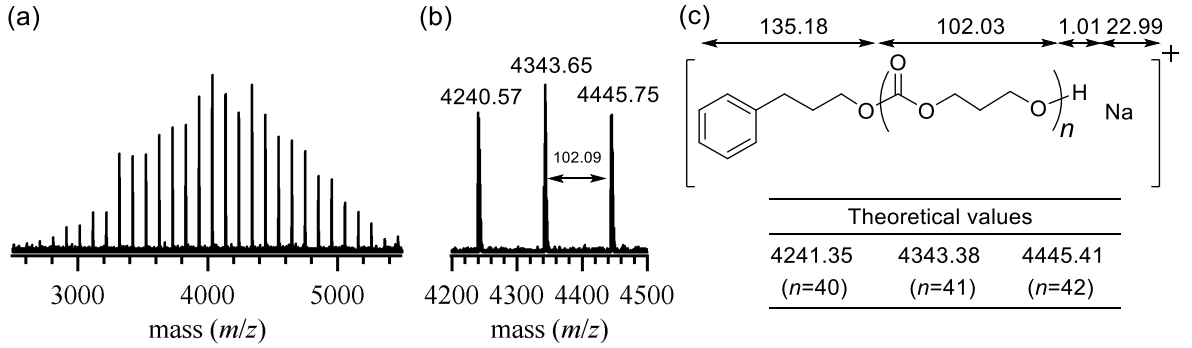

Figure 2.6. (a) MALDI-TOF MS spectrum of PTMC (run 19 in Table 2.3), (b) expanded spectrum (ranging from 4,200 to 4,500), and (c) theoretical molecular weight values.

Previous work reported that the DPP-catalyzed ROP of L-LA hardly proceeded under the conventional solution polymerization conditions.[34] Thus, a challenge still exists in the synthesis of polylactides using the DPP catalyst. Therefore, the author attempted the DPP-catalyzed ROP of L-LA at the $[\text{L-LA}]_0/[\text{PPA}]_0/[\text{DPP}]$ ratio of 50/1/0.50 using the bulk conditions. Considering the higher melting and crystallization temperatures of the resulting PLLA, the bulk polymerization was conducted at 130 °C (run 21 in Table 2.3). Surprisingly, the monomer conversion reached 85.7% within 24 h, giving a PLLA with the $M_{\text{n,NMR}}$ and $Đ$ values of 6,800 and 1.23, respectively (Figures 2.7). In addition, the homonuclear decoupled ^{1}H NMR spectrum of the resulting PLLA displayed a singlet signal due to the methine group derived from an exclusive *iii* tetrad stereosequence, suggesting that stereoinversion of the monomer and PLLA main chain did not occur during the polymerization (Figure 2.7(b)). This result is in contrast to the organobase-catalyzed ROP of L-LA, which often suffer from stereoinversion leading to the PLLAs with an imperfect isotacticity.[24] Although the MALDI-TOF MS spectrum detected evidence of side reactions, such as intramolecular and intermolecular transesterifications (Figure 2.8), the above-described results clearly demonstrated the broad monomer scope of the present polymerization procedure.

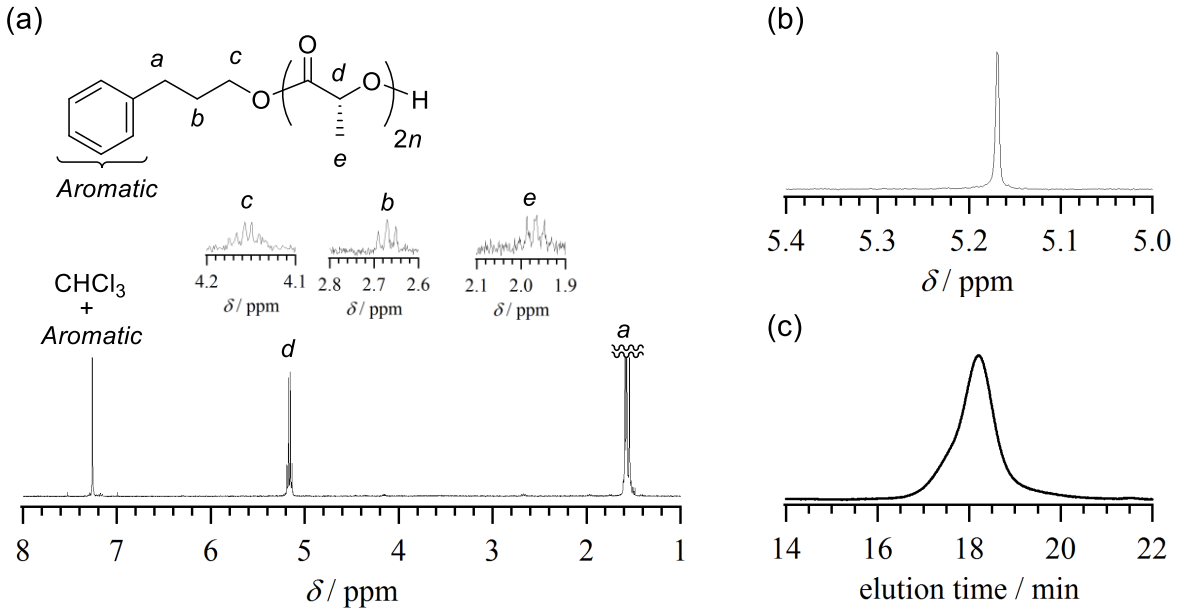

Figure 2.7. (a) ^{1}H NMR spectrum of PLLA in $CDCl_3$ (run 21 in Table 2.3), (b) ^{1}H NMR spectrum of PLLA methine resonances with selective decoupling of PLLA methyl resonances, and (c) SEC trace of the PLLA (eluent, $CHCl_3$; flow rate, 1.0 mL min^{-1}).

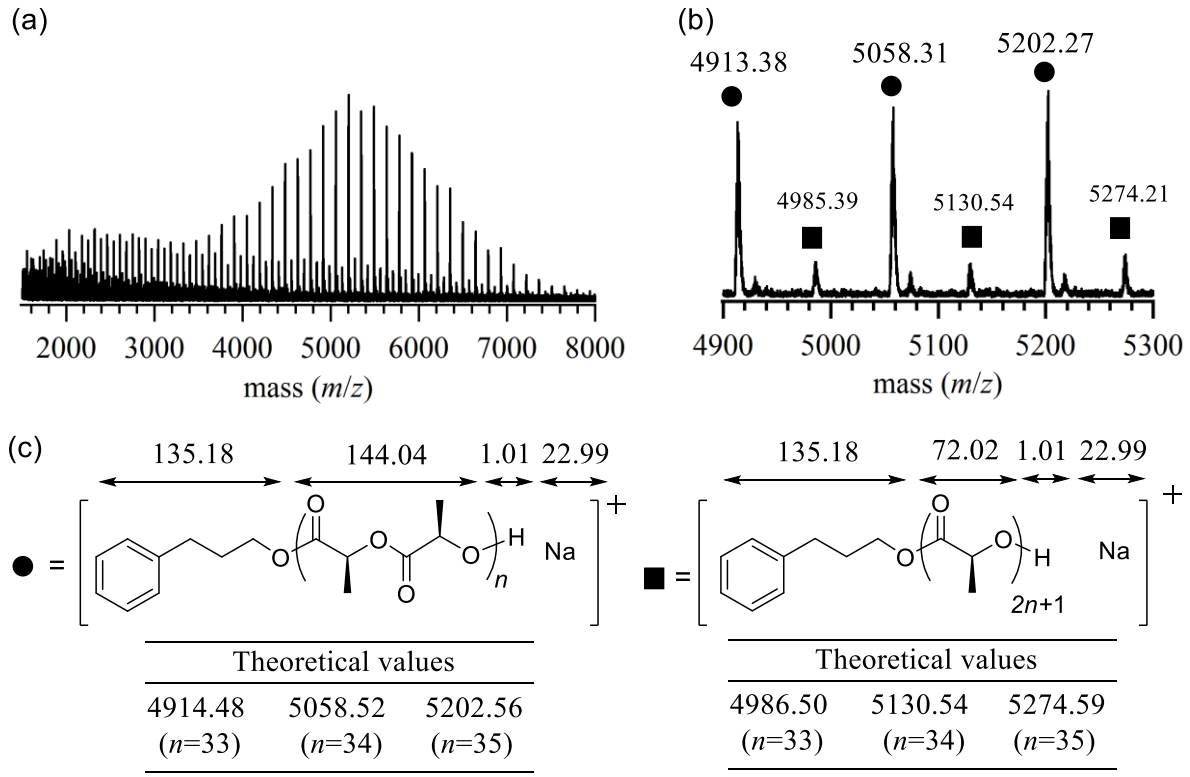

Theoretical values		
4914.48	5058.52	5202.56
(*n*=33)	(*n*=34)	(*n*=35)

Theoretical values		
4986.50	5130.54	5274.59
(*n*=33)	(*n*=34)	(*n*=35)

Figure 2.8. (a) MALDI-TOF MS spectrum of PLLA (run 21 in Table 2.3), (b) expanded spectrum (ranging from 4,900 to 5,300), and (c) theoretical molecular weight values.

2.2.3 Controlled/Living Nature of DPP-catalyzed ROP in the Bulk

To clarify the controlled/living nature of the present polymerization system, kinetic studies for the DPP-catalyzed bulk ROP of CL and TMC were carried out at the [CL or TMC]$_0$/[PPA]$_0$/[DPP] ratio of 50/1/0.05 at 80 °C (Figures 2.9 and 2.10). In both cases, the kinetic plots showed a linear increase in the monomer conversion with the reaction time. In addition, the $M_{n,NMR}$s values of the resulting PCLs and PTMCs were in good agreement with the $M_{n,th.}$ values, and the $Đ$s were maintained in relativity low values ranging from 1.07 to 1.16 for the PCL and from 1.05 to 1.11 for the PTMC, respectively. These results obviously represent distinctive features of the typical controlled/living polymerization.

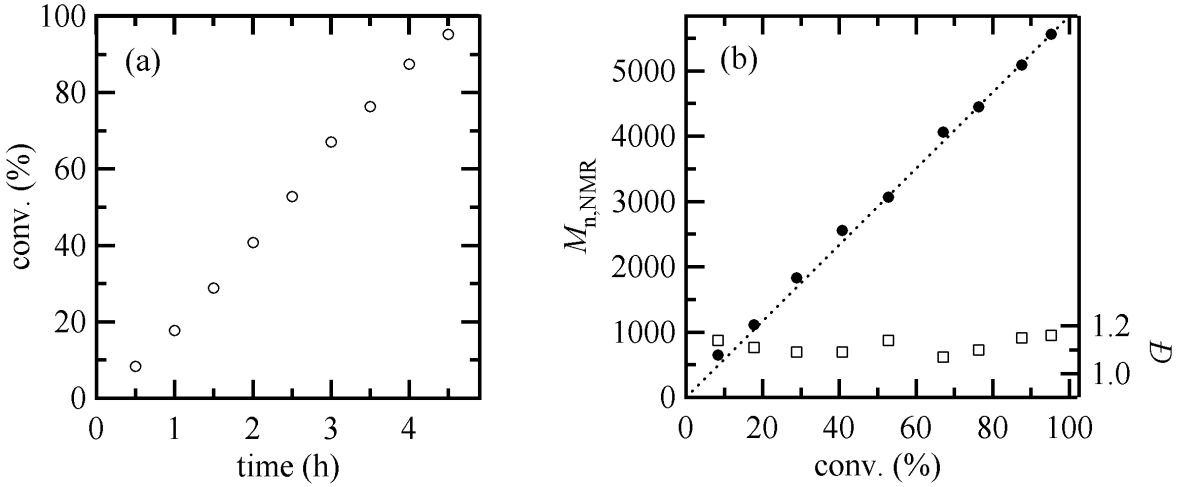

Figure 2.9. (a) Kinetic plots for the DPP-catalyzed bulk ROP of CL with [CL]$_0$/[PPA]$_0$/[DPP] = 50/1/0.05, and (b) dependence of $M_{n,NMR}$ (●), $Đ$ (□) and $M_{n,th.}$ (dotted line) on monomer conversion (conv.).

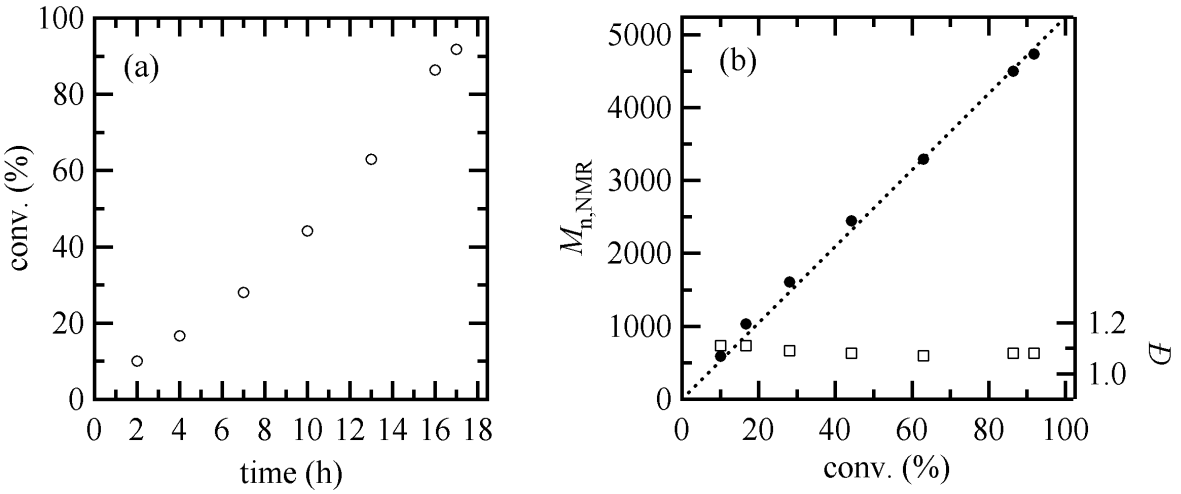

Figure 2.10. (a); Kinetic plots for the DPP-catalyzed bulk ROP of TMC with $[TMC]_0/[PPA]_0/[DPP] = 50/1/0.05$, and (b); dependence of $M_{n,NMR}$ (●), $Đ$ (□) and $M_{n,th.}$ (dotted line) on monomer conversion (conv.).

To further confirm the living character of the growing chain end, we performed the block copolymerization by the sequential monomer addition procedure in the bulk; the CL or TMC are polymerized as the first monomer (M_1) at the $[CL \text{ or } TMC]_0/[PPA]_0/[DPP]$ ratio of 25/1/0.05 to reach almost complete conversion, and an equimolar amount of VL with respect to the M_1 was then added to the reaction mixture as second monomer (M_2) to afford PCL-*b*-PVL and PTMC-*b*-PVL (Table 2.4). The monomodal SEC traces of the polymers obtained from the first polymerization clearly shifted to the higher molecular weight region while maintaining low *Đ*s after the second polymerization, indicating that the second polymerization of VL was efficiently initiated from the *ω*-chain end hydroxyl group of PCL or PTMC (Figures 2.11). In the ^{1}H NMR spectra, the signals due to the PCL or PTMC as well as the PVL backbones were observed along with the minor signals due to the PPA residue (Figures 2.12). These results obviously represent the success of the block copolymerization to afford the well-defined PCL-*b*-PVL and PTMC-*b*-PVL, which confirmed that the growing chain end had a living character even in the bulk condition. In addition, PVL-*b*-PCL and PDXO-*b*-PCL were also obtained using

the same procedure, which suggests the versatility of the present bulk ROP system for various block copolymers production regardless of the monomer addition sequence.

Table 2.4. Block copolymerization of CL, VL, DXO, and TMC catalyzed by DPP in bulk [a]

run		monomer (M)	$[M]_0/[PPA]_0$	time (min)	conv. (%) [b]	$M_{n,th.}$ [c]	$M_{n,NMR}$ [b]	$Đ$ [d]
22	M_1	CL	25/1	90	94.7	2,800	2,800	1.11
	M_2	VL	25/1	20	78.6	4,800 [e]	5,000	1.13
23	M_1	TMC	25/1	560	96.0	2,600	2,500	1.17
	M_2	VL	25/1	20	78.4	4,500 [e]	4,800	1.13
24	M_1	VL	25/1	15	97.1	2,700	2,600	1.15
	M_2	CL	25/1	125	88.0	5,100 [e]	5,200	1.15
25	M_1	DXO	25/1	210	97.2	3,000	3,100	1.20
	M_2	CL	25/1	130	90.1	5,500 [e]	6,000	1.16

[a] Polymerization conditions: atmosphere, Ar; temperature, 80 °C. [b] Determined by ^{1}H NMR spectrum of the obtained polymer in $CDCl_3$. [c] Calculated from $[M_1]_0/[PPA]_0$ × conv. × (M.W. of M_1) + (M.W. of PPA). [d] Determined by SEC measurement of the obtained polymer in $CHCl_3$. [e] Calculated from $[M_2]_0/[PPA]_0$ × conv. × (M.W. of M_2) + ($M_{n,NMR}$ of the polymer obtained from first polymerization).

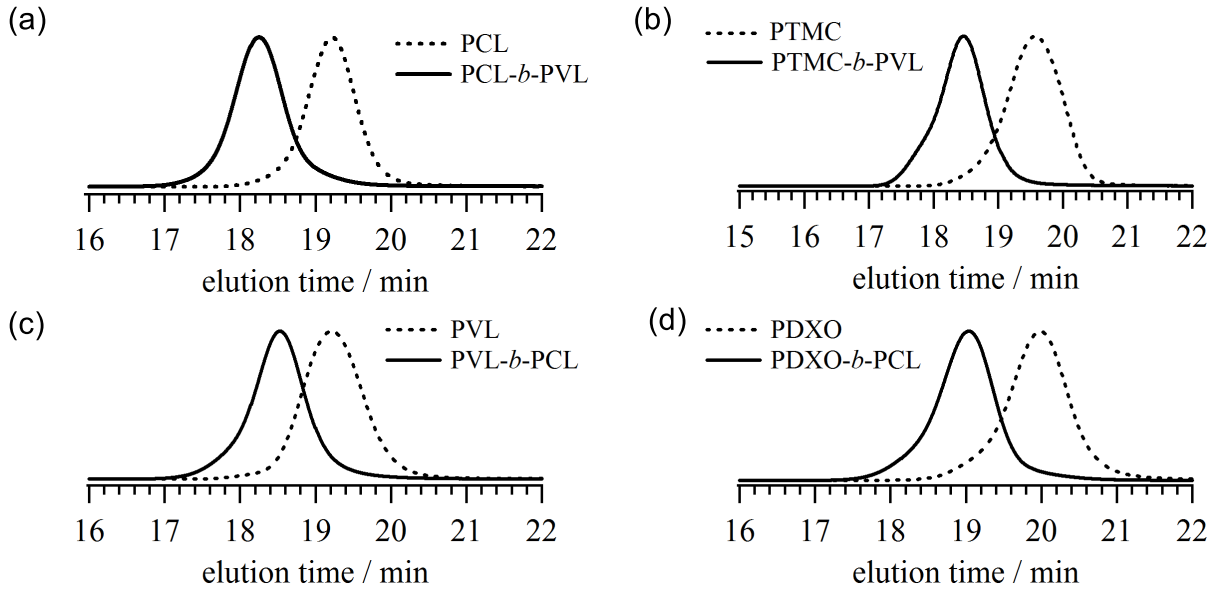

Figure 2.11. SEC traces of the polymer obtained from 1st polymerization (dotted line) and 2nd polymerization (solid line) (eluent, $CHCl_3$; flow rate, 1.0 mL min^{-1}).

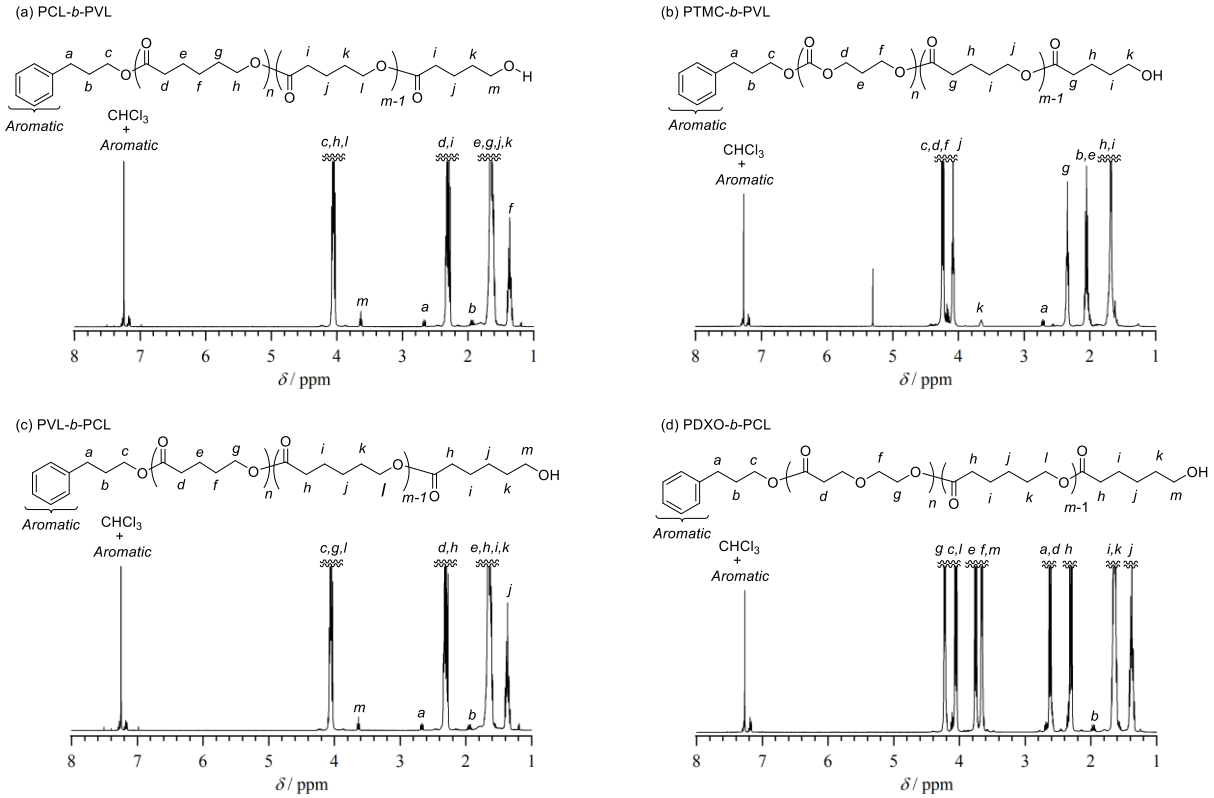

Figure 2.12. ^1H NMR spectra of the obtained block copolymer (solvent, $CDCl_3$).

2.2.4 Syntheses of Functional PCLs and PTMCs with Various Initiators

To further expand the synthetic utility of the present bulk polymerization procedure, the author attempted the synthesis of end-functionalized PCLs and PTMCs by combining functional alcohol initiators, such as 6-azido-1-hexanol (AHA), *N*-(2-hydroxyethyl)maleimide (HEMI), 1,3-propanediol, trimethylolpropane, and pentaerythritol, as shown in Scheme 2.2. AHA and HEMI possess highly reactive functional groups of azido and maleimide groups, respectively, which can be used to create various macromolecular architectures through the click reactions. The bulk polymerizations of CL at the $[CL]_0/[initiator]_0/[DPP]$ ratio of 50/1/0.05 using AHA and HEMI as the initiator proceeded in a well-controlled manner to afford the azido- and maleimide-functionalized PCLs (N_3-PCL and MI-PCL, respectively) and with relativity low *Đ*s (runs 22 and 23 in table 2.5, $Đ$ = 1.11 for N_3-PCL, 1.15 for MI-PCL). In a similar manner, the azido- and maleimide-functionalized PTMCs (N_3-PTMC and MI-PTMC) were obtained with *Đ* values less than 1.13. These results confirmed that a wide range of end-functionalized APE and APC can be produced by the present bulk polymerization procedure even at a higher reaction temperature.

Scheme 2.2. Synthesis of functionalized polyesters and polycarbonate using functional initiators

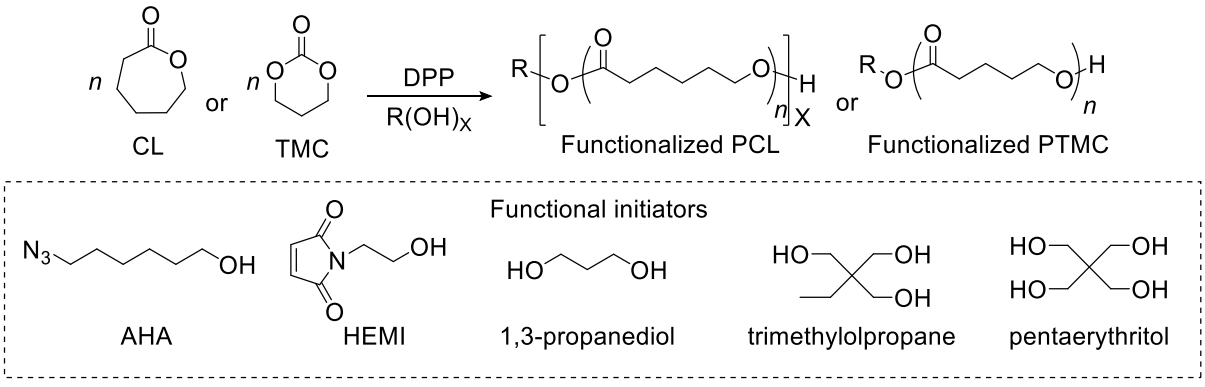

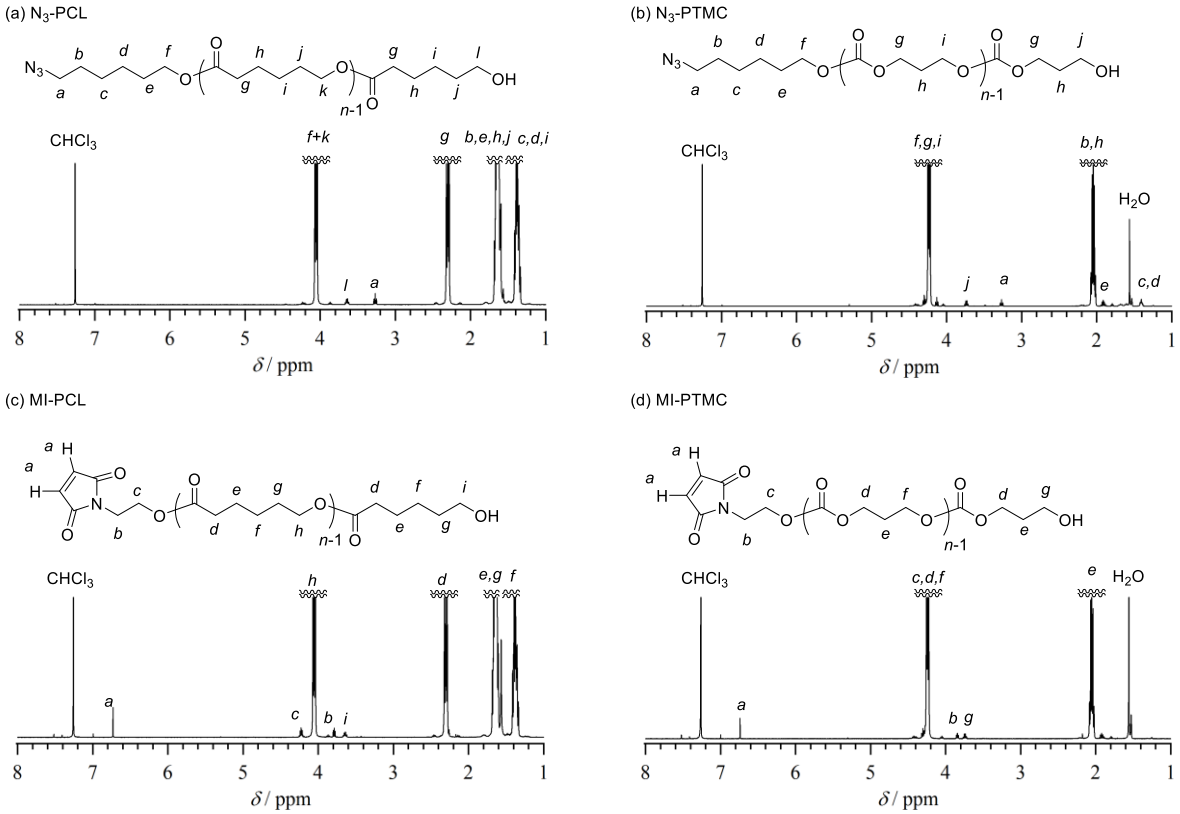

Figure 2.13. ^{1}H NMR spectra of the obtained end-functionalized PCLs and PTMCs (solvent, $CDCl_3$).

To elevate the DPP-catalyzed bulk ROP system to be more versatile, the syntheses of the PCL-polyols, which are industrially important raw materials for the polyurethane synthesis, were conducted using polyols, such as 1,3-propanediol, trimethylolpropane, and pentaerythritol, as an initiator to afford PCL-diol, PCL-triol, and PCL-tetraol, respectively. It is notable that the DPP-catalyzed ROPs of CL using trimethylolpropane and pentaerythritol were unsuccessful in solution because such polyol initiators are usually insoluble in organic solvents. In contrast, the reacting mixtures of the bulk polymerization using trimethylolpropane and pentaerythritol became homogeneous with the reaction time, though the polymerization heterogeneously initiated. The SEC traces of the obtained PCL-polyols exhibited a monodisperse elution peak with a low *Đ*s (*Đ* = 1.13 for PCL-diol, 1.07 for PCL-triol, and 1.04 for PCL-tetraol). The ^{1}H NMR spectra suggest that the polymerization proceeded from all the initiating sites of the

initiator (Figures 2.14). The integration ratios of the signal due to methylene protons adjacent to the ω-end hydroxyl group of PCL and the signal due to the methyl protons of the trimethylolpropane residue or methylene protons of the pentaerythritol residue were calculated and found to be reasonable values of 2:1 for the PCL-triol and 1:1 for the PCL tetraol. The $M_{n,NMR}$s of the obtained PCLs were in good agreement with the $M_{n,th.}$s, and the molecular weight values of the PCL-tetraols were controlled up to 16,100 along with low $Đ$s in the range of 1.04-1.08.

Table 2.5. Bulk ring-opening polymerization of CL or TMC with various initiators [a]

run	M	initiator	time (h)	conv. (%) [b]	$M_{n,th.}$ [c]	$M_{n,NMR}$ [b]	$M_{n,SEC}$ [d]	$Đ$ [d]
22	CL	AHA	7.0	90.3	5,300	5,500	12,700	1.11
23	CL	HEMI	7.5	90.8	5,300	5,500	13,400	1.15
24	TMC	AHA	19	85.6	4,500	4,500	5,600	1.09
25	TMC	HEMI	19	91.0	4,800	4,700	6,400	1.13
26	CL	1,3-propanediol	3.0	88.8	5,100	5,100	11,400	1.13
27	CL	trimethylolpropane	2.5	86.0	5,000	5,200	11,500	1.07
28	CL	pentaerythritol	2.0	95.5	5,600	5,600	11,900	1.04
29 [e]	CL	pentaerythritol	7.2	85.3	9,600	10,600	16,900	1.07
30 [f]	CL	pentaerythritol	21	64.1	14,800	16,100	28,000	1.08

[a] Polymerization conditions: atmosphere, Ar; temperature, 80 ˚C; $[M]_0/[initiator]_0/[DPP]$, 50/1/0.05. [b] Determined by ^1H NMR spectrum of the obtained polymer in $CDCl_3$. [c] Calculated from $[M]_0/[initiator]_0 \times$ conv. $\times$ (M.W. of M) + (M.W. of initiator). [d] Determined by SEC measurement of the obtained polymer in $CHCl_3$ using polystyrene standards. [e] Polymerization was conducted with $[M]_0/[initiator]_0/[DPP]$ = 100/1/0.05. [f] Polymerization was conducted with $[M]_0/[initiator]_0/[DPP]$ = 200/1/0.05.

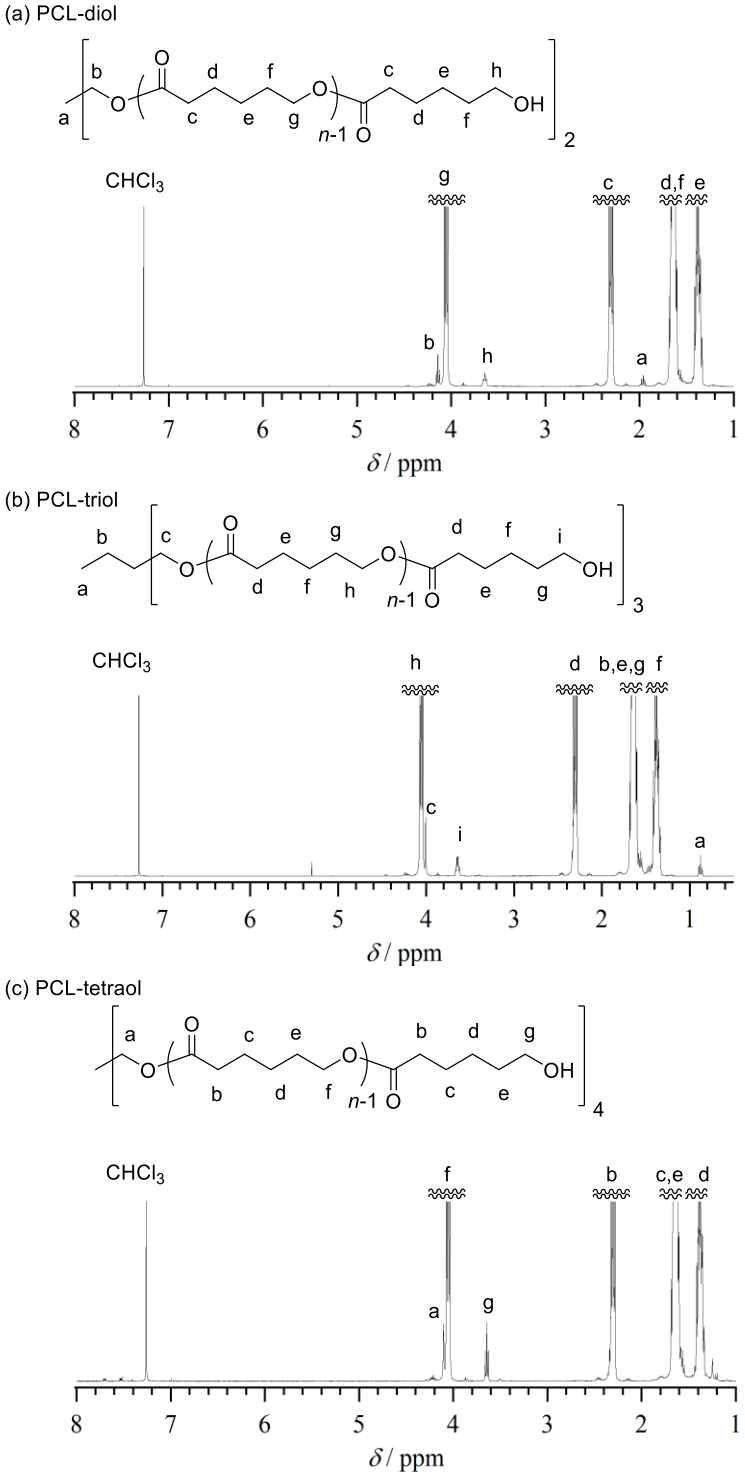

Figure 2.14. ^{1}H NMR spectra of the obtained PCL-polyols (solvent, $CDCl_3$).

2.2.5 One-pot Synthesis of PCL-based Polyurethane via Organophosphate-catalyzed Bulk ROP

Polyurethanes are industrially produced using organometallic catalysts represented by organotin compounds, which are difficult to remove from the product, therefore, an alternative metal-free route is required to achieve environmentally-benign and safe production. Recently, Hedrick *et al.* reported that organic acids efficiently promoted the polyurethane formation reaction.[38] Inspired by the report, the one-pot synthesis of polyurethane via the organophosphate-catalyzed bulk ROP was demonstrated as shown in Scheme 2.3. CL was first polymerized at the $[CL]_0/[1,3\text{-propanediol}]_0/[DPP]$ ratio of 25/1/0.05 to afford the PCL-diol, and an equimolar amount of 4,4'-diphenylmethane diisocyanate (MDI) with respect to 1,3-propanediol was then added to the reaction mixture while keeping the temperature at 80 ˚C. After the addition of MDI, the viscosity of the reacting mixture drastically increased, implying the production of a higher molecular weight product. The SEC measurement revealed that the PCL-diol was completely consumed to afford the PCL-based polyurethane (PCL-PU) within 16 h (Figure 2.15(a)). The ^{1}H NMR measurement provide further evidence of the polyurethane formation. The characteristic signals due to the urethane bond in addition to the signals due to the PCL and MDI residue were observed, while the triplet signal due to the methylene protons adjacent to the ω-end hydroxyl group of PCL had disappeared (Figure 2.15(b)). In addition, the FT-IR spectrum of the PCL-PU showed the characteristic absorptions at 1,532 cm^{-1} and 3,346 cm^{-1} due to the NH deformation and stretching vibrations, respectively (Figure 2.16). Although the polyurethane formation in the absence of DPP was observed, there was some remaining unreacted PCL-diol even after 16 h (Figure 2.15(c)). The result suggested that DPP plays important roles to promote not only the ROP of CL, but also the polyurethane formation reaction. Thus, the present bulk polymerization procedure coupled with DPP has the potential for the polyurethane synthesis without using any organometallic catalysts in all the processes.

Scheme 2.3. One-pot synthesis of PCL-based polyurethane using organophosphate-catalyzed bulk ROP system

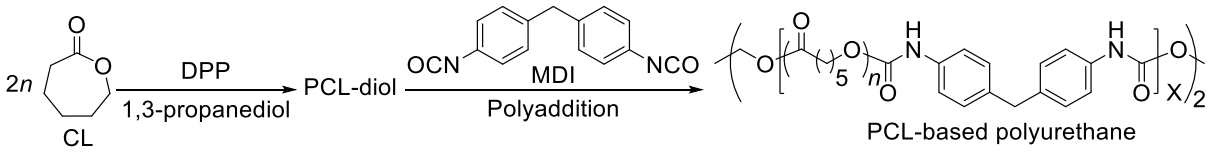

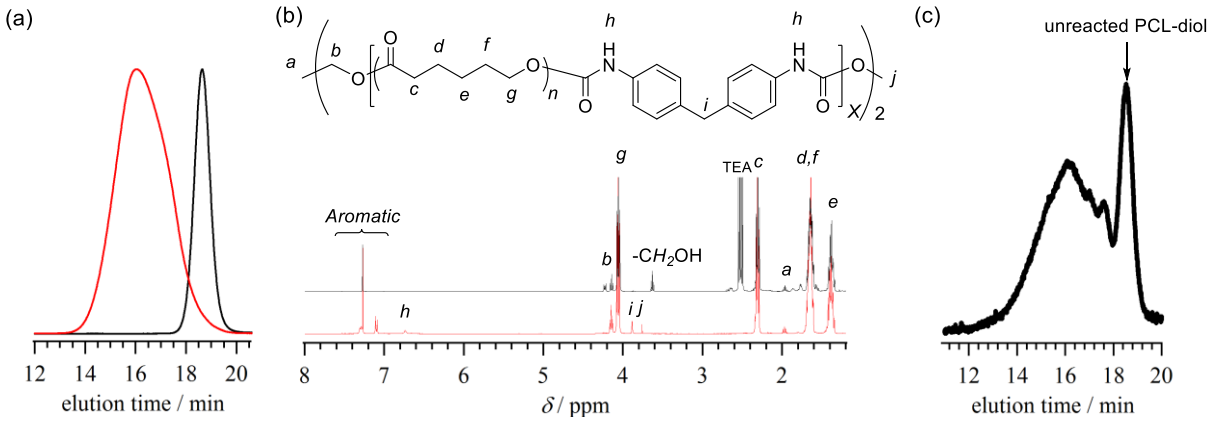

Figure 2.15. (a) SEC traces of the PCL-PU (red line) and corresponding PCL-diol obtained before adding MDI (conv. = 95.0%; black line), (b) ^{1}H NMR spectra in $CDCl_3$, and (c) SEC trace of the obtained PCL-PU in the in the absence of DPP (eluent, $CHCl_3$; flow rate, 1.0 mL min^{-1}).

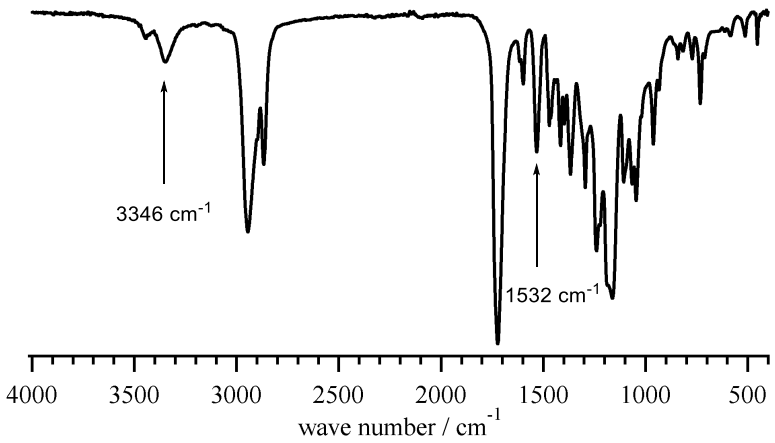

Figure 2.16. FT-IR spectrum of the obtained PCL-based polyurethane in the presence of DPP.

2.3 Conclusions

In this study, the environmentally-benign way to produce well-defined APE, APC, and APEE was established by using organophosphate as a catalyst under bulk conditions. The significant advantages of the present polymerization procedure were fully demonstrated regarding a shorter reaction time, remarkably lower catalyst loading, and wider scope of applicable monomers. The kinetic and block copolymerization studies revealed the controlled/living nature of the present polymerization system even under the bulk conditions, which enables the production of well-defined end-functionalized and multi-hydroxylated APEs. These demonstrations confirmed that the bulk conditions overcome the difficulties of the organophosphate-catalyzed ROP, such as the amount of loaded catalyst and the use of solvent. Furthermore, the high catalytic abilities of the organophosphate for both the ROP and urethane formation reaction enabled the production of a PCL-based polyurethane in one-pot through a metal-free route. Considering the low acidity, low toxicity, and high chemically stability of the organophosphates, the organophosphate-catalyzed bulk ROP is an attractive candidate for the environmentally-benign production of various polymers for both industrial and biomedical purposes.

2.4 Experimental Section

Materials. *ε*-Caprolactone (CL; >99%, Tokyo Kasei Kogyo Co., Ltd. (TCI)), *δ*-valerolactone (VL; >99%, Sigma Aldrich), 3-phenyl-1-propanol (PPA, TCI), and 1,3-propanediol were distilled over CaH_2 under reduced pressure. Di(2,6-xylyl)phosphate (DXP), 6-azido-1-hexanol (AHA), and *N*-(2-hydroxyethyl)maleimide (HEMI) were synthesized according to previous reports.[39-41] 1,5-Dioxepan-2-one (DXO; >98%, TCI), and trimethylene carbonate (TMC; >98%, TCI) were dried by azeotropic distillation. L-Lactide (L-LA; >98%, TCI) was purified by recrystallization from dry toluene (twice). Diphenylphosphate (DPP; >99%, TCI), bis(4-nitrophenyl)phosphate) (BNPP; >99%, TCI), pentaerythritol (>98%, TCI), 4,4',-diphenylmethane diisocyanate (>97%, TCI), trimethylolpropane (>98%, TCI), and Amberlyst® A21 (Organo Co., Ltd.) were used as received.

Instruments. The polymerization was carried out in an MBRAUN stainless steel glove box equipped with a gas purification system (molecular sieves and copper catalyst) in a dry argon atmosphere (H_2O, O_2 < 1 ppm). The moisture and oxygen contents in the glove box were monitored by an MB-MO-SE 1 and MB-OX-SE 1, respectively. The number-average molecular weight ($M_{n,NMR}$) was determined from the ^1H NMR spectra recorded using a JEOL JNM-A400II instrument. The size exclusion chromatography (SEC) was performed at 40 °C in $CHCl_3$ (1.0 mL min^{-1}) using a Shodex GPC-101 system equipped with a Shodex K-G guard column and a set of two Shodex K-805L columns (linear, 8 mm × 300 mm; bead size, 5 μm; exclusion limit, 4×10^6). The dispersity (*Đ*) of the polymers was calculated on the basis of a polystyrene calibration. Matrix-assisted laser desorption ionization time-of-flight mass spectrometry (MALDI-TOF MS) of the obtained polymers was performed using an Applied Biosystems Voyager-DE STR-H equipped with a 337-nm nitrogen laser (3 ns pulse width). Two hundred shots were accumulated for the spectra at a 20 kV acceleration voltage in the reflector mode and the obtained spectra were calibrated using polystyrene (average M_n = 3,600, Waters

Associates) as the standard. Samples for the MALDI-TOF MS were prepared by mixing the polymer (4.0 mg mL^{-1}, 0.5 μL) and a matrix (2,5-dihydroxybenzoic acid, 60 mg mL^{-1}, 0.5 μL) in THF. For the measurement, a sample plate, which was coated by a solution (1.0 μL) of NaI as the cationic agent in acetone (1.0 mmol L^{-1}), was used. The Fourier transform infrared spectroscopy (FT-IR) analysis was carried out using a Perkin-Elmer Frontier MIR spectrometer equipped with a Single Reflection Diamond Universal Attenuated Total Reflection (ATR) accessory. The turnover frequency (TOF) for the propagation reaction was evaluated using the following formula.

$$\text{TOF } (h^{-1}) = \frac{[M]_0 \times \text{conv.}}{[DPP] \times \text{polymerization time (h)}}$$

Bulk ring-opening polymerization of *ε*-caprolactone catalyzed by diphenyl phosphate.

A typical procedure for the polymerization is as follows (Procedure A): CL (1.120 mL, 10.0 mmol), PPA (27.2 μL, 200 μmol), and DPP (2.50 mg, 10.0 μmol) were placed in a reaction vessel, which was sealed under an argon atmosphere. The reaction mixture was stirred at 80 °C in an oil bath. After 250 min, we obtained a portion of the reaction mixture for determining the monomer conversion from the ^{1}H NMR measurements, and the polymerization was quenched by adding Amberlyst® A21. Before the addition of the Amberlyst® A21, we obtained a portion of the reaction mixture and then added a small amount of triethylamine for determining the monomer conversion from the ^{1}H NMR measurements. The reaction mixture was purified by reprecipitation from a CH_2Cl_2 solution into cold methanol/*n*-hexane (v/v = 9/1) to give PCL (713 mg) as a white solid. Yield, 66.6%. $M_{n,NMR}$ = 5,500; $M_{n,SEC}$ = 11,100, $Đ$ = 1.08. ^{1}H NMR ($CDCl_3$, 400 MHz): δ (ppm) 1.36 (m, 2H × *n*, (-$CH_2CH_2CH_2CH_2CH_2$-)$_n$), 1.61 (m, 2H × *n*, (-$CH_2CH_2CH_2O$-)$_n$), 1.63 (m, 2H × *n*, (-$COCH_2CH_2CH_2$-)$_n$), 1.94 (q, 2H, *J* = 6.3 Hz, Ar$CH_2CH_2CH_2$-), 2.29 (t, 2H × *n*, *J* = 7.6 Hz, (-$OCOCH_2CH_2$-)$_n$), 2.67 (t, 2H, *J* = 8.0 Hz,

ArCH_2CH$_2$-), 3.63 (t, 2H, J = 6.4 Hz, -CH$_2$CH_2OH) 4.04 (t, 2H ×(n-1), J = 6.6 Hz, (-CH$_2$CH_2O-)$_{n-1}$), 4.08 (m, 2H, ArCH$_2$CH$_2$CH_2O-), 7.15-7.30 (m, 5H, aromatic).

Bulk ring-opening polymerization of δ-varelolactone catalyzed by diphenyl phosphate.

Procedure A was used for the ROP of VL (0.905 mL, 10.0 mmol) in the presence of PPA (27.2 μL, 200 μmol) and DPP (2.50 mg, 10.0 μmol) for 40 min to give PVL (719 mg) as a white solid. Yield, 79.5%. $M_{n,NMR}$ = 5,000; $M_{n,SEC}$ = 9,400, $Đ$ = 1.08. ^{1}H NMR (CDCl$_3$, 400 MHz): δ (ppm) 1.66 (m, 2H × n, (-CH$_2$CH_2CH$_2$O-)$_n$), 1.69 (m, 2H × n, (-COCH$_2$CH_2CH$_2$-)$_n$), 1.93 (quin, 2H, J = 7.2 Hz, ArCH$_2$CH_2CH$_2$-), 2.32 (m, 2H × n, (-OCOCH_2CH$_2$-)$_n$), 2.66 (t, 2H, J = 7.8 Hz, ArCH_2CH$_2$-), 3.63 (t, 2H, J = 6.4 Hz, -CH$_2$CH_2OH), 4.08 (t, 2H × (n-1), J = 6.0 Hz, (-CH$_2$CH_2O-)$_{n-1}$), 4.10 (m, 2H, ArCH$_2$CH$_2$CH_2O-), 7.15-7.34 (m, 5H, aromatic).

Bulk ring-opening polymerization of trimethylene carbonate catalyzed by diphenyl phosphate.

Procedure A was used for the ROP of TMC (510 mg, 5.00 mmol) in the presence of PPA (13.6 μL, 100 μmol) and DPP (1.2 mg, 0.50 μmol) for 17 h to give PTMC (389 mg) as a colorless waxy solid. Yield, 83.0%. $M_{n,NMR}$ = 4,700; $M_{n,SEC}$ = 6,800, $Đ$ = 1.07. ^{1}H NMR (CDCl$_3$, 400MHz): δ (ppm) 1.92 (m, 2H, -CH_2CH$_2$OH), 1.97-2.11 (m, 2H, ArCH$_2$CH_2-; 2H × (n-1), (-OCH$_2$CH_2-)$_{n-1}$), 2.70 (t, 2H, J = 7.8 Hz, ArCH_2-), 3.74 (q, 2H, J = 9.0 Hz, -CH_2OH), 4.13-4.32 (m, 2H, ArCH$_2$CH$_2$CH_2-, m, 4H × n-1, (-OCH_2CH$_2$CH_2O-)$_{n-1}$; 2H, -CH_2CH$_2$CH$_2$OH), 7.16-7.29 (m, 5H, aromatic).

Bulk ring-opening polymerization of 1,5-dioxepane-2-one catalyzed by diphenyl phosphate.

Procedure A was used for the ROP of DXO (580 mg, 5.00 mmol) in the presence of PPA (13.6 μL, 100 μmol) and DPP (1.2 mg, 0.50 μmol) for 450 min to give PDXO (470 mg) as a colorless waxy solid. Yield, 91.6%. $M_{n,NMR}$ = 5,300; $M_{n,SEC}$ = 4,400, $Đ$ = 1.13. ^{1}H NMR ($CDCl_3$, 400MHz): δ (ppm) 1.97 (m, 2H, $ArCH_2CH_2$-), 2.63 (t, 2H × *n-1*, *J* = 6.6 Hz, (-$COCH_2$-)$_{n-1}$), 2.76 (m, 2H, $ArCH_2$-), 3.67 (t, 2H × *n-1*, *J* = 5.0 Hz, (-CH_2CH_2OCO-)$_{n-1}$), 3.76 (t, 2H × *n-1*, *J* = 6.4 Hz, (-$COCH_2CH_2$-)$_{n-1}$), 4.09 (t, 2H, *J* = 6.6 Hz, $ArCH_2CH_2CH_2$-), 4.21 (t, 2H × *n-1*, *J* = 4.8 Hz, (-CH_2OCO-)$_{n-1}$), 7.15-7.29 (m, 5H, aromatic).

One-Pot Synthesis of PCL-based Polyurethane via Organophosphate-Catalyzed Bulk ROP.

CL (2.240 mL, 20.0 mmol), 1,3-propanediol (57.6 μL, 800 μmol) and DPP (5.00 mg, 40.0 μmol) were placed in a reaction vessel, which was sealed under an argon atmosphere. The reaction mixture was stirred at 80 °C in an oil bath. After 120 min, we obtained a portion of the reaction mixture for SEC measurement and ^{1}H NMR measurement, then MDI (200 mg, 800 μmol) was added to the reaction mixture. The polymerization was quenched by adding Amberlyst® A21. The reaction mixture was purified by reprecipitation from CH_2Cl_2 solution into cold methanol to give the PCL-based polyurethane (1.73 g) as a white solid. Yield, 69.8%. $M_{n,SEC}$ = 32,800, $Đ$ = 2.03. ^{1}H NMR ($CDCl_3$, 400 MHz): δ (ppm) 1.38 (m, 2H × *n*, (-$CH_2CH_2CH_2CH_2CH_2$-)$_n$), 1.61-1.72 (m, 2H × *n*, (-$CH_2CH_2CH_2O$-)$_n$; 2H × *n*, (-$COCH_2CH_2CH_2$-)$_n$), 1.97 (m, 2H, -$OCH_2CH_2CH_2O$-), 2.31 (t, 2H × *n*, *J* = 8.2 Hz, (-$OCOCH_2CH_2$-)$_n$), 3.88 (s, 2H × *X*, -$ArCH_2Ar$-), 4.06 (t, 2H × *n*, *J* = 6.6 Hz, (-CH_2CH_2O-)$_n$), 4.14 (t, 4H, *J* = 8.4 Hz, -$CH_2CH_2CH_2$-), 6.74 (s, 2H × *X*, N*H*), 7.08-7.31 (m, 8H × *X*, aromatic).

2.5 References

1. Kamber, N. E.; Jeong, W.; Waymouth, R. M.; Pratt, R. C.; Lohemeijer B. G. G.; Hedrick, J. L. *Chem. Rev.* **2007**, *107*, 5813−5840.
2. Kiesewetter, M. K. Shin, E. J.; Hedrick, J. L.; Waymouth, R. M. *Macromolecules* **2010**, *43*, 2093−2107.
3. Dove, A. P. *ACS Macro Lett.* **2012**, *1*, 1409−1412.
4. Thomas, C.; Bibal, B. *Green Chem*. **2014**, *16*, 1684−1699.
5. Ottou, W. N.; Sardon, H.; Mecerreyes, D.; Vignolle, J.; Taton, D. *Prog. Polym. Sci.* **2016**, *56*, 64−115.
6. Hu, S.; Zhao, J.; Zhang, G.; Schlaad, H. *Prog. Polym. Sci.* **2017**, *74*, 34−77.
7. Shibasaki, Y.; Sanada, H.; Yokoi, M.; Sanda, F.; Endo, T. *Macromolecules* **2000**, *33*, 4316–4320.
8. Gazeau-Bureau, S.; Delcroix, D.; Martín-Vaca, B.; Bourissou, D.; Navarro, C.; Magnet, S. *Macromolecules* **2008**, *41*, 3782–3784.
9. Makiguchi, K.; Satoh, T.; Kakuchi, T. *J. Polym. Sci., Part A: Polym. Chem.* **2011**, *49*, 3769–3777.
10. Jin, Y.; Ji, Y.; He, X.; Kan, S.; Xia, H.; Liang, B. Chen, J.; Wu, H.; Guo, K.; Li, Z. *Polym. Chem.* **2014**, *5*, 3098–3106.
11. Sanda, F.; Sanada, H.; Shibasaki, Y.; Endo, T. *Macromolecules* **2002**, *35*, 680–683.
12. Liu, J.; Liu, L. *Macromolecules* **2004**, *37*, 2674–2676.
13. Xu, J.; Song, J.; Pispas, S.; Zhang, G. *J. Polym. Sci., Part A: Polym. Chem.* **2014**, *52*, 1185–1192.
14. Makiguchi, K.; Satoh, T.; Kakuchi, T. *Macromolecules* **2011**, *44*, 1999–2005.
15. Makiguchi, K.; Saito, T.; Satoh, T.; Kakuchi, T. *J. Polym. Sci., Part A: Polym. Chem.* **2014**, *52*, 2032–2039.
16. Kan, S.; Jin, Y.; He, X.; Chen, J.; Wu, H.; Ouyang, P.; Guo, K.; Li, Z. *Polym. Chem.* **2013**, *4*, 5432–5439.
17. Delcroix, D.; Couffin, A.; Susperregui, N.; Navarro, C.; Maron, L.; Martin-Vaca, B.; Bourissou, D. *Polym. Chem.* **2011**, *2*, 2249–2256.
18. He, X.; Ji, Y.; Jin, Y.; Kan, S.; Xia, H.; Chen, J.; Liang, B.; Wu, H.; Guo, K.; Li, Z.; *J. Polym. Sci., Part A: Polym. Chem.* **2014**, *52*, 1009–1019.
19. Nederberg, F.; Connor, E. F.; Möller, M.; Glauser, T.; Hedrick, J. L. *Angew. Chem. Int.*

Ed. **2001**, *40*, 2712–2715.

20. Lohmeijer, B. G. G.; Pratt, R. C.; Leibfarth, F.; Logan, J. W.; Long, D. A.; Dove, A. P.; Nederberg, F.; Choi, J.; Wade, C.; Waymouth, R. M.; Hedrick, J. L. *Macromolecules* **2006**, *39*, 8574–8583.
21. Connor, E. F.; Nyce, G. W.; Myers, M.; Möck, A.; Hedrick, J. L. *J. Am. Chem. Soc.* **2002**, *124*, 914–915.
22. Pratt, R. C.; Lohmeijer, B. G. G.; Long, D. A.; Waymouth, R. M.; Hedrick, J. L. *J. Am. Chem. Soc.* **2006**, *128*, 4556–4557.
23. Zhang, L.; Pratt, R. C.; Nederberg, F.; Horn, H. W.; Rice, J. E.; Waymouth, R. M.; Wade, C. G.; Hedrick, J. L. *Macromolecules* **2010**, *43*, 1660–1664.
24. Shin, E. J.; Jones, A. E.; Waymouth, R. M. *Macromolecules* **2012**, *45*, 595–598.
25. Dove, A. P.; Pratt, R. C.; Lohmeijer, B. G. G.; Waymouth, R. M.; Hedrick, J. L. *J. Am. Chem. Soc.* **2005**, *127*, 13798–13799.
26. Pratt, R. C.; Lohmeijer, B. G. G.; Long, D. A.; Lundberg, P. N. P.; Dove, A. P.; Li, H. B.; Wade, C. G.; Waymouth, R. M.; Hedrick, J. L. *Macromolecules* **2006**, *39*, 7863–7871.
27. Miyake G. M.; Chen, E. Y. -X. *Macromolecules* **2011**, *44*, 4116–4124.
28. Coady, D. J.; Engler, A. C.; Horn, H. W.; Bajjuri, K. M.; Fukushima, K.; Jones, G. O.; Nelson, A.; Rice, J. E.; Hedrick, J. L. *ACS Macro Lett.* **2012**, *1*, 19–22.
29. Kadota, J.; Pavlović, D.; Desvergne, J.-P.; Bibal, B.; Peruch, F.; Deffieux, A. *Macromolecules* **2010**, *43*, 8874–8879.
30. Koeller, S.; Kadota, J.; Peruch, F.; Deffieux, A.; Pinaud, N.; Pianet, I.; Massip, S.; L*é*ger, J.-M.; Desvergne, J.-P.; Bibal, B. *Chem. Eur. J.* **2010**, *16*, 4196–4205.
31. Alba, A.; Schopp, A.; De Souza Delgado, A.-P.; Cherif-Cheikh, R.; Mertín-Vaca, B.; Bourissou, D. *J. Polym. Sci., Part A, Polym. Chem.* **2010**, *48*, 959–965.
32. Thomas, C.; Peruch, F.; Deffieux, A.; Milet, A.; Desvergne, J.-P.; Bibal, B. *Adv. Synth. Catal.* **2011**, *353*, 1049–1054.
33. Thomas, C.; Peruch, F.; Bibal, B. RSC Adv. **2012**, ***2***, 12851–12856.
34. Makiguchi, K.; Kikuchi, S.; Yanai, K.; Ogasawara, Y.; Sato, S.-i.; Satoh, T.; Kakuchi, T. *J. Polym. Sci., Part A, Polym. Chem.* **2014**, *52*, 1047–1054.
35. Kadota, J.; Pavlović, D.; Hirano, H.; Okada, A.; Agari, Y.; Bibal, B.; Deffieux, A.; Peruch, F. *RSC Adv*. **2014**, *4*, 14725–14732.
36. Makiguchi, K.; Ogasawara, Y.; Kikuchi, S.; Satoh, T.; Kakuchi, T. *Macromolecules* **2013**,

46, 1772–1782.

37. Krasovec, F.; Jan, J. *Croat. Chem. Acta* **1963**, *35*, 183–193.
38. Sardon, H.; Engler, A. C.; Chan, J. M. W.; García, J. M.; Coady, D. J.; Pascual, A.; Mecerreyes, D.; Jones, G. O.; Rice, J. E.; Horn, H. W.; Hedrick, J. L. *J. Am. Chem. Soc.* **2013**, *135*, 16235–11624.
39. Speers, A. E.; Adam, G. C.; Cravatt, B. F. *J. Am. Chem. Soc.* **2003**, *125*, 4686–4687.
40. Health, W. H.; Palmieri, F.; Adams, J. R.; Long, B. K.; Holcombe, T. W.; Zieren, S.; Truitt, M. J.; White, J. L.; Willson, C. G. *Macromolecules* **2008**, *41*, 719–726.
41. Nifant'ev, I. E.; Tavtorkin, A. N.; Korchagina, S. A.; Gavrilenko, I. F.; Glebova, N. N.; Kostitsyna, N. N.; Yakovlev, V. A.; Bondarenko, G. N.; Filatova, M. P. *Appl. Catal., A* **2014**, *478*, 219–227.

Chapter 3

Trimethyl Glycine as Environmentally-benign and Biocompatible Catalyst for Ring-opening Polymerization

3.1 Introduction

Since Hedrick et al. reported the ROP of lactide using 4-dimethylaminopyridine as an organocatalyst in 2001, the organocatalytic ring-opening polymerization (ROP) has been assumed to be an ideal process to achieve the truly environmentally-benign production of aliphatic polyesters (APEs). To date, many organocatalytic ROP systems have been established to achieve the metal-free synthesis of APE. However, industrial issues, such as production costs and operability, have been ignored. In chapter 2, the author established the bulk ROP system of cyclic esters using an organophosphate catalyst to make the conventional solution ROP procedure to be a more practical approach. By applying the bulk polymerization conditions, the organophosphate-catalyzed ROP overcame the drawbacks of the conventional polymerization procedure, such as the use of a solvent and the amount of loaded catalyst, which leads to decreasing production costs. Furthermore, the shorter reaction time, wider scope of applicable monomers, and high selectivity for the propagating reaction of the bulk ROP system are great advantages on both the academic and industrial stages. The organophosphate-catalyzed bulk ROP system is now employed for the laboratory-scale synthesis of advanced APE materials.[1-4]

On the other hand, there are still many problems in order to achieve a practical organocatalytic ROP system. Organocatalysts used for the ROP including organophosphates are still expensive when compared to the conventional metal-based catalysts and sometime require a multistep reaction synthesis from commercially-available reagents, which leads to higher production costs. For example, the commercial price of diphenyl phosphate (DPP) is twenty times more expensive than that of $Sn(Oct)_2$, which has been widely used in industrial APE production. Therefore, the availability of the catalyst and economic cost are indispensable factors for realizing the industrial application. Apart from the economic viewpoint, the risk in using organocatalysts needs to be considered, because the catalyst residue in an industrial-scale production is sometimes not removed. In fact, Blankert and Mespouille et al. found a significant

cytotoxicity in the functionalized thioureas, while they were employed as an environmentally-benign hydrogen bond donor for the ROP of cyclic esters.[5] Kiesewetter et al. reported triclocarban (TCC), which was industrially used as an antibacterial compound, as a readily available hydrogen bond donor agent for the ROP. [6] The bifunctional catalytic systems using TCC with hydrogen bond acceptors, such as *N*-methyl-1,5,7-triazabicyclo[4,4,0]dec-5-ene (MTBD) and 2-*tert*-butylimino-2-diethylamino-1,3-dimethylperhydro-1,3,2-diazaphosphorine (BEMP), efficiently promote the ROP of ε-caprolactone (CL), and δ-valerolactone (VL). However, the Food and Drug Administration (FDA) recently banned the use of TCC in consumer soaps.[7] Therefore, an "organocatalyst" does not necessarily mean that the catalyst is non-toxic. Therefore, the author turned his attention to the development of a new class of organocatalysts satisfying the good availability and non-toxicity.

To this end, the author focused on naturally-occurring compounds, such as amino acids, taurine, and their derivatives, because their good availability and safety suit industrial use. Based on a screening, the author found trimethyl glycine (TMG), which is a zwitterionic compound found in plants as well as in humans,[8,9] as an appropriate bifunctional catalyst candidate for the ROP to achieve an environmentally-benign and practical ROP method. TMG possesses a quaternary ammonium cation and carboxylate anion, which are both used for the ROP of cyclic esters to activate the monomer and initiating/propagating chain end, respectively.[10,11] This indicates the potential of TMG to exhibit a bi-activation ability. Indeed, the catalytic ability of TMG was already revealed in organic reactions, such as the hydrosilylation of carbon dioxide with an amine,[12,13] which motivated us to apply TMG to the polymer synthesis. In addition to its attractive chemical structure, TMG is safe and environmentally-benign. Humans intake TMG on a daily basis from food, and it is also generated in humans as a metabolite of nutrient choline.[8] Additionally, the European Food Safety Authority Panel reported that 6 mg/kg/day of TMG is acceptable for adults in addition

to the daily ingestion from TMG- and choline-containing food,[9] supporting the biomedical application of TMG-synthesized polymeric materials. Furthermore, TMG is commercially available and it is inexpensive. In addition, the major source of TMG is beets, which ensures the sustainable characteristic of TMG. Therefore, TMG has a significant potential as an environmentally-benign organocatalyst satisfying the good availability and non-toxicity to achieve an environmentally-benign and practical APE production.

In this chapter, the author describes the efficient catalytic ability of naturally-occurring TMG for the bulk ROP of cyclic carbonates (Scheme 3.1), leading to aliphatic polycarbonates (APCs), a kind of APE used as prepolymers for polyurethane synthesis. [14,15] APCs also possess the characteristics of biodegradability and biocompatibility, and furthermore, they do not form acidic compounds in their decomposition process. Thus, APC materials are gaining attention for biomedical applications. [16-22] The bulk ROP of trimethylene carbonate (TMC) using TMG proceeds in a controlled manner to give well-defined poly(trimethylene carbonate) (PTMC) possessing a targeted molecular weight and narrow dispersity. The screening of TMG analogues for the catalyst of the ROP revealed that the combination of the carboxylate anion and quaternary ammonium cation in TMG is an essential structural requirement. The FT-IR measurement of TMC and alcohol initiator in the presence/absence of TMG revealed the bi-activation property of the TMG. The end-functionalized APCs were successfully obtained using alcohol initiators bearing clickable functionalities, such as azido and ethynyl group. Furthermore, the author successfully demonstrated the synthesis of the APC-diol and -triol using cyclic carbonate monomers, which can be used as a prepolymer for the APC-based polyurethane (APC-PU).

Scheme 3.1. Trimethyl glycine-catalyzed ring-opening polymerization of cyclic carbonates

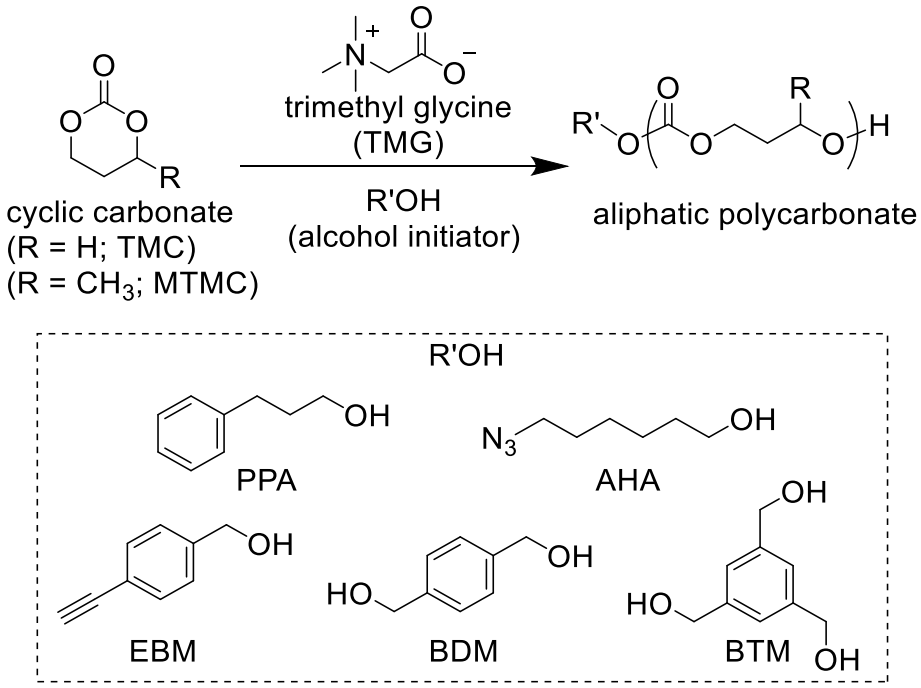

3.2 Results and Discussion

3.2.1 Ring-opening Polymerization of Cyclic Esters and Cyclic Carbonate Using Trimethyl Glycine as a Catalyst

To evaluate the catalytic activity of TMG for the ROP of cyclic esters and cyclic carbonate, the author first examined the ROP of L-lactide (L-LA), CL and TMC using TMG as a catalyst and 3-phenyl-1-propanol (PPA) as an initiator in bulk (runs 1-3 in Table 3.1). The ROP of L-LA with a $[\text{L-LA}]_0/[\text{PPA}]_0/[\text{TMG}]$ ratio 50/1/1 at 100 °C proceeded to reach a conversion rate of 70% in 50 h (run 1 in Table 3.1), while the reaction mixture gradually turned brown during the ROP. The size exclusion column chromatography (SEC) trace of the obtained poly(L-lactide) (PLLA) is monomodal and the molecular weight ($M_{n,SEC}$) and dispersity ($Đ$) are 6,000 and 1.09, respectively. Therefore, TMG possesses the catalytic activity toward the ROP of L-LA, albeit the resultant PLLA was brown in color. The ROP of ε-CL was also examined at a $[\varepsilon\text{-CL}]_0/[\text{PPA}]_0/[\text{TMG}]$ ratio 50/1/1 at 100 °C (run 2 in Table 3.1), however, the monomer conversion rate did not increase even after 48 h. Surprisingly, the ROP of TMC smoothly proceeded at 70 ºC in bulk and the monomer conversion reached 75% within 30 min (run 3 in Table 3.1), indicating that TMG efficiently promoted the ROP of TMC. In the ^{1}H NMR spectrum of the obtained PTMC, the signals due to the main chain of PTMC along with minor signals due to 3-phenyl-1-propoxy group are observed (Figure 3.1 (a)), implying that TMG and PPA worked as a catalyst and an initiator, respectively, in the present ROP system. In addition, the peak area for the signal due to the methylene group at benzyl position of the 3-phenyl-1-propanyl group (*a* in Figure 3.1(a)) is comparable to that of the methylene group adjacent to the ω-chain end hydroxyl group (*g* in Figure 3.1(a)), indicating a good end-group fidelity. It is noteworthy that the ether linkage formation through the decarboxylation, which is a major side reaction in the ROP of cyclic carbonates, is not observed in the ^{1}H NMR spectrum. The molecular weight determined from the ^{1}H NMR measurement ($M_{n,NMR}$) was 4,000, which is in

good agreement with the theoretical value of 4,000 calculated from the initial $[TMC]_0/[PPA]_0$ ratio and the monomer conversion ($M_{n,th.}$). The SEC trace of the obtained PTMC is monomodal and the $M_{n,SEC}$ and $Đ$ values are 6,600 and 1.12, respectively (Figure 3.1(b)). These results confirm that TMG has a catalytic ability for the bulk polymerization of TMC with good control over the molecular weight and dispersity.

Table 3.1. Bulk ring-opening polymerization of cyclic esters and cyclic carbonate using TMG as a catalyst [a]

run	M	$[M]_0/[PPA]_0$ /[TMG]	time (h)	conv. (%) [b]	$M_{n,th.}$ [c]	$M_{n,NMR.}$ [b]	$M_{n,SEC}$ [d]	$Đ$ [d]
1	L-LA	50/1/1.0	50	70	5,100	6,000	6,000	1.09
2	CL	50/1/1.0	24	<1	-	-	-	-
3 [e]	TMC	50/1/0.1	0.5	75	4,000	4,000	6,600	1.12

[a] Polymerization conditions: atmosphere, Ar; temp., 100 °C. [b] Determined by ^{1}H NMR spectrum in $CDCl_3$. [c] Calculated from $[M]_0/[PPA]_0$ × conv. × (M.W. of M) + (M.W. of PPA). [d] Determined by SEC measurement of the obtained polymer in THF using PSt standards. [e] Polymerization was conducted at 70 °C.

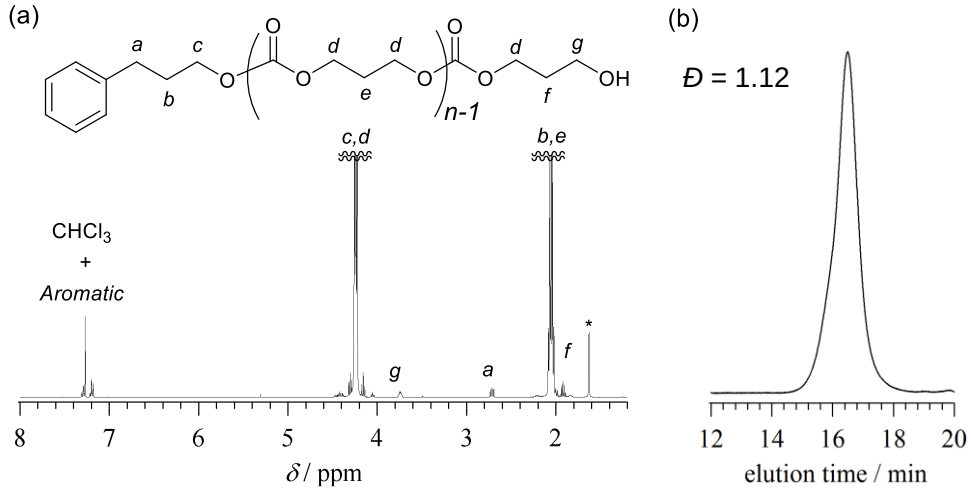

Figure 3.1 (a) ^{1}H NMR spectrum (in $CDCl_3$; the asterisk indicates the water) and (b) SEC trace (eluent, THF; flow rate, 1.0 mL min^{-1}) of the PTMC obtained from run 3 in Table 3.1.

To access the detailed structural information of the obtained PTMC, a matrix-assisted laser desorption/ionization time-of flight mass spectral (MALDI-TOF MS) analysis was conducted on the PTMC obtained from run 3. In the MALDI-TOF MS spectrum (Figure 3.2), a series of repeated peaks with ca. 102 Da intervals is observed in the range of <5000 Da, which once again confirms that the present ROP proceeded to give PTMC without decarboxylation. The peak appearing at *m*/*z* of 3015.97 can be closely matched with the calculated molecular weight of 28-mer of PTMC possessing a 3-phenyl-1-propoxy group and a hydroxyl group at the α and ω chain ends, respectively ($[M+Na]^+$ = 3016.97 Da), suggesting that the initiation reaction from PPA. Furthermore, there are no evidence of intra molecular transesterification that could lead to cyclic oligomer formation. Therefore, the ROP proceeded with high selectivity for the initiation/propagation reaction to give well-defined PTMC with a high degree of chain end fidelity.

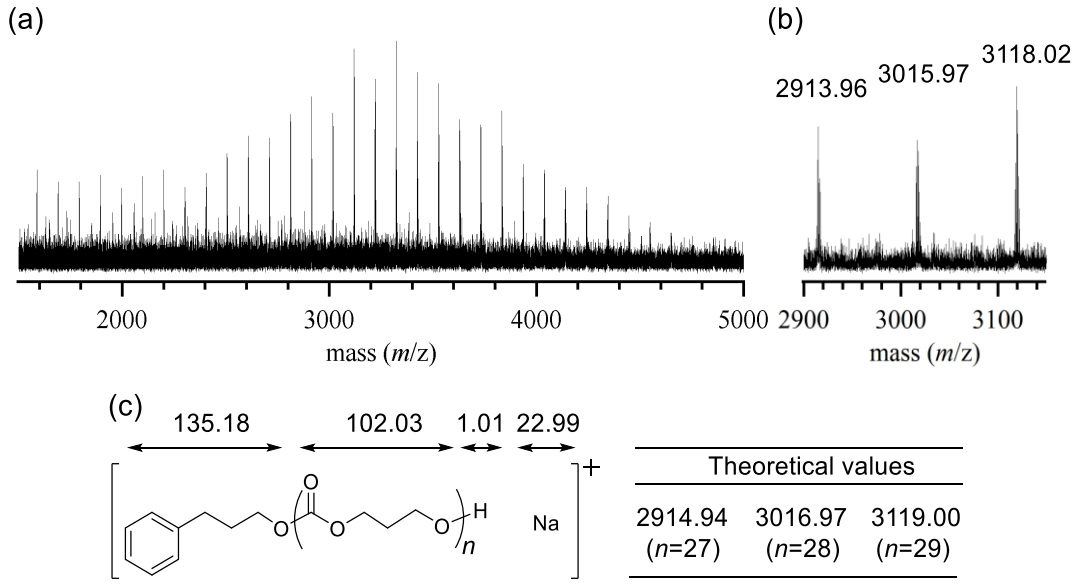

Figure 3.2. (a) MALDI-TOF MS spectrum of the PTMC obtained from run 3 in Table 3.1, (b) expanded spectrum ranging from 2900 to 3150, and (c) theoretical molecular weights.

Next the author conducted the ROP of TMC by varying the initial monomer-to-initiator ratio to control the molecular weight of the resulting PTMC. Here, the low molecular weight PTMC was targeted because the APC is mostly used as a raw material for polyurethane synthesis, where low molecular weight APC (ca. ~5,000) is required as the soft segment.[18-21] The ROP of TMC at a $[TMC]_0/[PPA]_0/[TMG]$ ratio of 25/1/0.1 gave a PTMC with an $M_{n,NMR}$ of 2,100 within 20 min (run 4 in Table 3.2). The monomodal SEC trace of the obtained PTMC appears in the low molecular weight region compared with that of run 3 (Figure 3.3), and the $M_{n,SEC}$ and $Đ$ values are determined as 3,200 and 1.13, respectively. In addition, a lower molecular weight PTMC ($M_{n,NMR}$ = 1,300, $M_{n,SEC}$ = 1,800, and $Đ$ = 1.22) was obtained from the ROP of TMC at a $[TMC]_0/[PPA]_0/[TMG]$ ratio of 15/1/0.1 (run 5 in Table 3.2). Thus, the author controlling the molecular weight of PTMC while maintaining its low dispersity.

Table 3.2. Ring-opening polymerization of TMC using TMG as a catalyst [a]

run	$[TMC]_0/[PPA]_0$ /[TMG]	time (min)	conv. (%) [b]	$M_{n,th.}$ [c]	$M_{n,NMR}$ [b]	$M_{n,SEC}$ [d]	$Đ$ [d]
3	50/1/0.1	30	75	4,000	4,000	6,600	1.12
4	25/1/0.1	20	78	2.100	2.100	3.200	1.13
5	15/1/0.1	15	70	1,200	1,300	1,800	1.22

[a] Polymerization conditions: atmosphere, Ar; temp., 70 °C. [b] Determined by ^{1}H NMR spectrum in $CDCl_3$. [c] Calculated from $[TMC]_0/[PPA]_0$ × conv. × (M.W. of TMC) + (M.W. of PPA). [d] Determined by SEC measurement of the obtained polymer in THF using PSt standards.

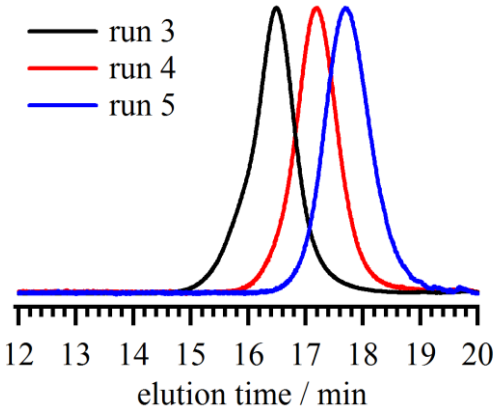

Figure 3.3. SEC traces of the PTMC obtained from run 3 (black line), run 4 (red line), and run 5 (blue line) in Table 3.2 (eluent, THF; flow rate, 1.0 mL min^{-1}).

3.2.2 Controlled/living Nature of the Present ROP System

To investigate the polymerization behavior of the present ROP system, the author next analyzed the molecular weight and dispersity of the resulting PTMC as a function of the monomer conversion. As shown in Figure 3.4(a), $M_{n,NMR}$s (○) linearly increases with the increase in monomer conversion, which is in good agreement with $M_{n,th.}$ (dashed line). More importantly, the $Đ$ value remains largely constant narrow (<1.3) throughout the polymerization. In addition, the SEC trace shifted to the higher molecular weight region with increasing the monomer conversion while keeping the monomodal distribution (Figure3.4 (b)). A shoulder peak in the higher molecular weight region appears in the SEC trace when the monomer conversion is > 98% (Figure 3.5). This suggests that side reactions, such as inter molecular transesterification, occur more pronounced when the monomer conversion is high. To avoid such a side reaction and to obtain narrowly dispersed PTMC, the polymerization should be terminated when the monomer conversion rate is in the range of 70–80%.

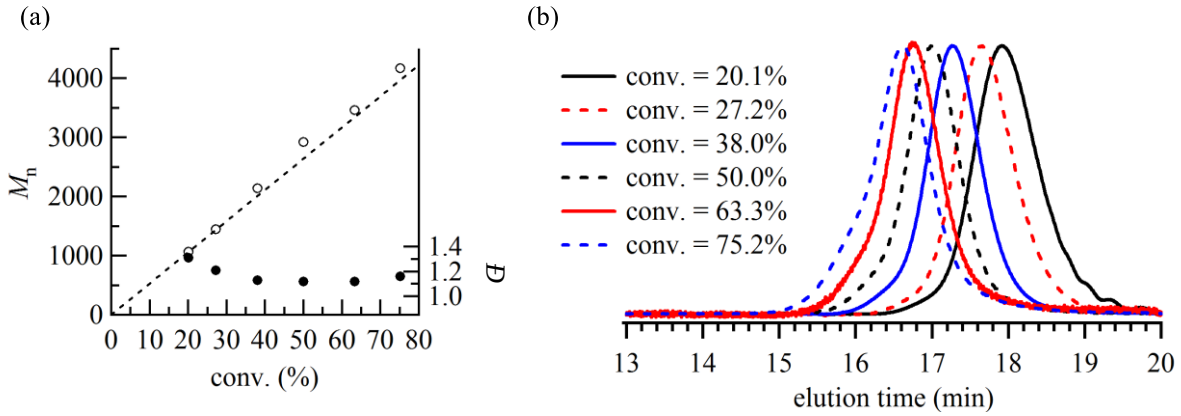

Figure 3.4 Kinetic analysis of the TMG-catalyzed ROP of TMC at a $[TMC]_0/[PPA]_0/[TMG]$ ratio of 50/1/0.1 in the bulk: (a) Plot of $M_{n,NMR}$ (○), $M_{n,th.}$ (dashed line), and $Đ$ (●) versus monomer conversion, and (b) SEC traces of the resulting PTMC obtained at each stage of polymerization.

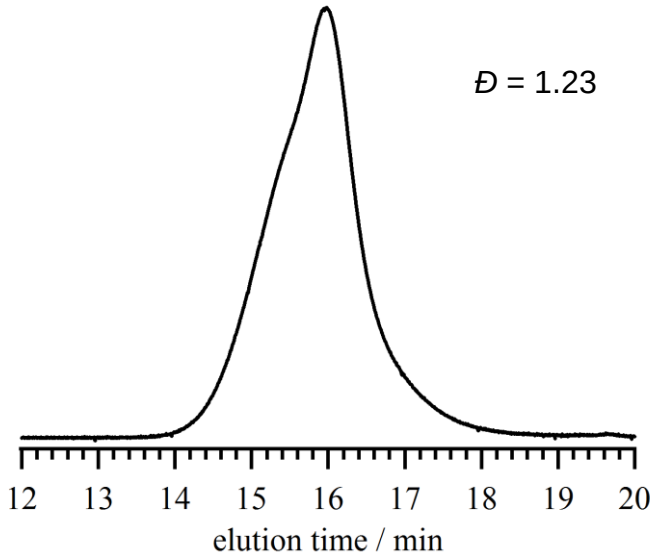

Figure 3.5. SEC trace of the PTMC obtained at >98% monomer conversion (eluent; THF, flow rate, 1.0 mL min^{-1}). Polymerization was conducted at the $[TMC]_0/[PPA]_0/[TMG]$ ratio of 50/1/0.1 at 70 ºC in the bulk.

To confirm the living characteristic of the propagating chain end, a chain extension experiment was then carried out. The first polymerization of TMC was conducted at a $[TMC]_0/[PPA]_0/[TMG]$ ratio of 25/1/0.1 at 70 °C in the bulk. After the monomer conversion reached 83%, 25 eq. of TMC with respect to the initiator was added to the reacting mixture to start the second polymerization. After the second addition of TMC, the total monomer conversion reached 73%. The SEC trace of the final product shifts to a higher molecular weight region compared with that of the PTMC obtained from the first polymerization (Figure S4), clearly demonstrating that the second polymerization was initiated from the hydroxyl group of the PTMC propagating chain end. This strongly suggests that the propagating chain end retains the living characteristic during the polymerization.

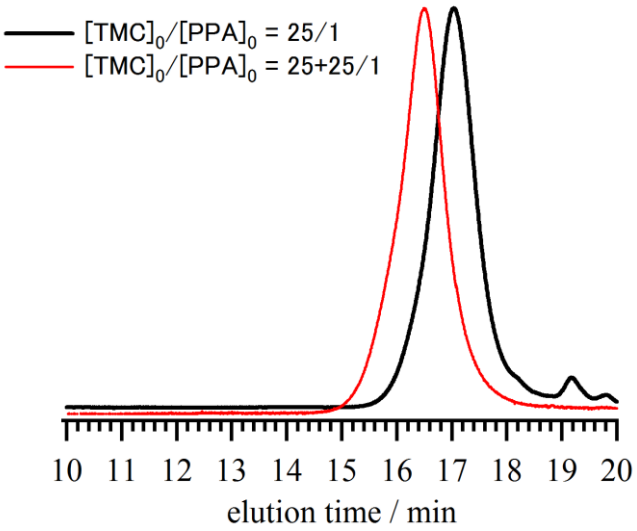

Figure 3.6. SEC traces of the PTMC obtained from first polymerization (black line; $M_{n,SEC}$ = 4,200, $Đ$ = 1.11) and second polymerization (red line; $M_{n,SEC}$ = 6,100, $Đ$ = 1.12). Polymerization was conducted at 70 ºC in the bulk.

3.2.3 Structure-Activity Relationship of TMG Analogues

The author next examined the catalytic ability of TMG analogues, such as tetramethylammonium acetate (TMAA), trimethyl glycine hydrochloride (TMG-HCl), and *N*,*N*-dimethyl glycine (DMG), to gain insight into the correlation between the catalyst structure and ability. The polymerizations with TMG analogues were conducted under the same reaction condition as in the run 3 listed in Table 3.3. The TMG analogues were found to catalyze the ROP of TMC to give PTMC within 6 h (runs 6-8 in Table 3.3) with good control over the molecular weight and dispersity. The SEC traces of the obtained PTMCs exhibit monodispersity and the their *Đ* values remain largely constant narrow (1.13 for the PTMC obtained from run 6, and 1.12 for run 7 and 8, respectively). In addition, the ROP did not proceed in the absence of catalyst, demonstrating that all the TMG analogues promoted the ROP of the TMC (run 9 in Table 3.3). As for the reaction rate, the ROP using TMAA shows the highest turnover frequency (TOF; 4,400 h^{-1}), with the monomer conversion rate reaching 75% in 5 min. On the other hand, the ROP using TMG-HCl and DMG proceeded slowly, exhibiting lower TOF values than that of TMMA and TMG (TOF = 115 h^{-1} for TMG-HCl and 62.5 h^{-1} for DMG). This shows that the combination of carboxylate anions and quaternary ammonium cations is essential to attain a good catalytic performance.

Table 3.3. Bulk ROP of cyclic carbonate using TMG and TMG analogues [a]

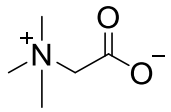
TMG

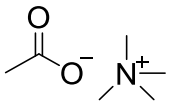
TMAA

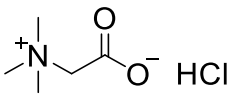
TMG-HCl

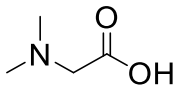
DMG

run	cat.	$[M]_0/[PPA]_0$ /[cat.]	time (min)	conv. (%) [b]	$M_{n,th.}$ [c]	$M_{n,NMR.}$ [b]	$M_{n,SEC}$ [d]	$Đ$ [d]	TOF (h^{-1})
3	TMG	50/1/0.1	30	75	4,000	4,000	6,600	1.12	750
6	TMAA	50/1/0.1	5	74	3,900	4,300	6,200	1.13	4,400
7	TMG-HCl	50/1/0.1	180	69	3,700	3,800	5,300	1.12	115
8	DMG	50/1/0.1	360	75	4,000	4,200	5,700	1.12	62.5
9	none	50/1/ -	1,440	<1	-	-	-	-	-

[a] Polymerization conditions: atmosphere, Ar; temp., 70 °C. [b] Determined by ^{1}H NMR spectrum in $CDCl_3$. [c] Calculated from $[TMC]_0/[PPA]_0$ × conv. × (M.W. of TMC) + (M.W. of PPA). [d] Determined by SEC measurement of the obtained polymer in THF using PSt standards.

3.2.4 Polymerization Mechanism

To reveal the catalytic mechanism of the present ROP system, Fourier-transform infrared spectroscopy (FT-IR) measurements were conducted on TMC and PPA in the presence of an equimolar amount of TMG at 70 °C (Figure 3.7). In the FT-IR spectrum of the mixture of TMC and TMG, the absorption peak due to C=O stretching vibration shifts to a lower wavenumber region compared with that of TMG alone (Figure 3.7 (a)), indicating the activation of carbonyl group on TMC by TMG. Similarly, the FT-IR analysis of the mixture of PPA and TMG shows that TMG efficiently activated the hydroxyl group of the initiator and propagating chain end, as evidenced by the broadening of the absorption peak due to the OH stretching vibration toward the lower wavenumber region after the addition of TMG (Figure 3.7(b)).[23] Therefore, TMG catalyzed the ROP of TMC by activating both the monomer and initiator/propagating chain end, as shown Figure 3.7(c),[23,24] which is responsible for the outstanding catalytic ability of TMG even under relatively low catalyst loading. Additionally, a similar experiment was performed using DMG, which has lower TOF than TMG. As expected, only minor peak shifts are observed in the OH and C=O stretching vibrations upon the addition of DMG to PPA and TMC, respectively (Figure 3.8), which again confirms that TMG is an efficient catalyst for the ROP of TMC via a bi-activation mechanism

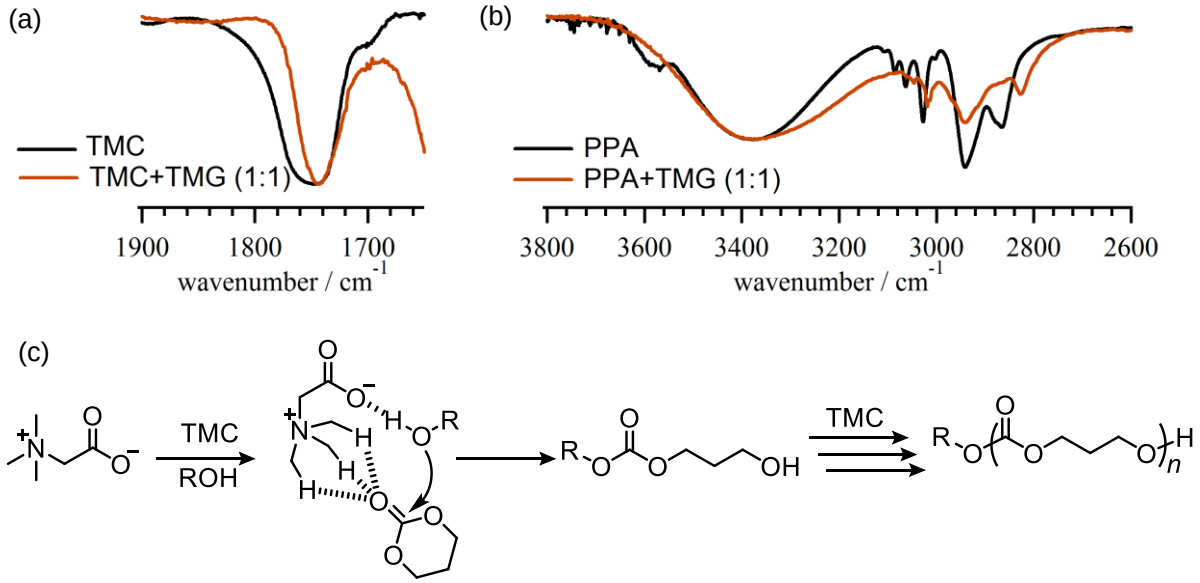

Figure 3.7. FT-IR analysis of TMG/TMC and TMG/PPA mixtures: (a) Expanded FT-IR spectra for the C=O stretching vibration band of TMC in the absence (black line) and presence of TMG (red line), (b) Expanded FT-IR spectra for the O-H stretching vibration band of PPA in the absence (black line) and presence of TMG (red line). The FT-IR spectra were acquired at 70 °C and normalized at the peaks due to the stretching vibration of C=O for TMC and O-H for PPA, and (c) Proposed reaction mechanism of the TMG-catalyzed ROP based on the FT-IR analysis.[24]

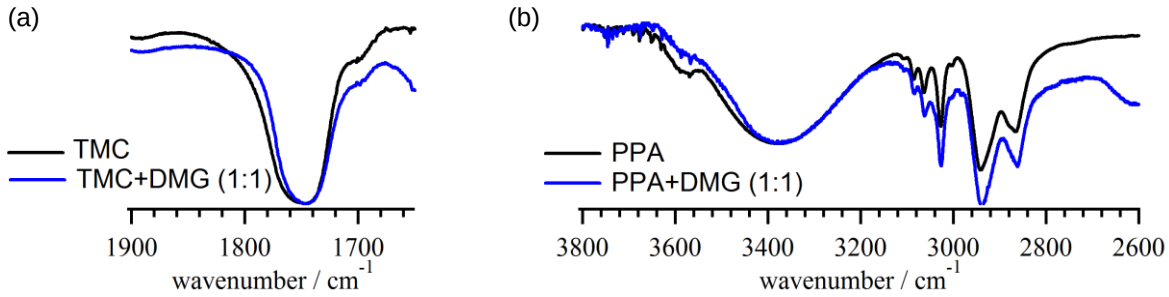

Figure 3.8. FT-IR analysis of DMG/TMC and DMG/PPA mixtures: (a) Expanded FT-IR spectra for the C=O stretching vibration band of TMC in the absence (black line) and presence of DMG (blue line), (b) Expanded FT-IR spectra for the O-H stretching vibration band of PPA in the absence (black line) and presence of DMG (blue line). The FT-IR spectra were acquired at 70 °C and normalized at the peaks due to the stretching vibration of C=O for TMC and O-H for PPA.

3.2.5 Synthesis of Functionalized APCs Using Functional Initiator

To extend the possible applications of the present ROP system, the synthesis of end-functionalized APCs was then examined using functional initiators (Scheme 3.2 and runs 10 and 11 in Table 3.4). The author first employed 6-azide-1-hexanol (AHA) as an initiator to produce APC having clickable azido group at the chain end; this can be used for the synthesis of block copolymers as well as macromolecular architectures. The ROPs using AHA was conducted at a $[TMC]_0/[AHA]_0/[TMG]$ ratio of 50/1/0.1 proceeded to reach a monomer conversion rate of 74% (run 10 in Table 3.4). The ^{1}H NMR spectrum of the obtained PTMC show minor signals due to the initiator residue (Figure 3.9), and $M_{n,NMR}$ (3,900) is in good agreement with the theoretical value (4,100). In the FT-IR spectrum, the characteristic absorption peak due to the azido group is observed at 2,100 cm^{-1} (Figure 3.10), strongly suggesting that the azido group is retained during the polymerization to give a PTMC having a clickable chain end group. Similarly, a PTMC having an ethynyl group, which is clickable group used for azide-alkyne and thiol-yne click reactions, was obtained using 4-ethynyl-benzenemethanol (EBM) as a functional initiator (run 11 in Table 3.4 and Figure 3.11). These demonstrations suggest the wide range application of the present ROP system for the preparation of APC-based advanced materials.[27,28]

Scheme 3.2. Synthesis of end-functionalized APCs and APC-polyols using TMG as a catalyst

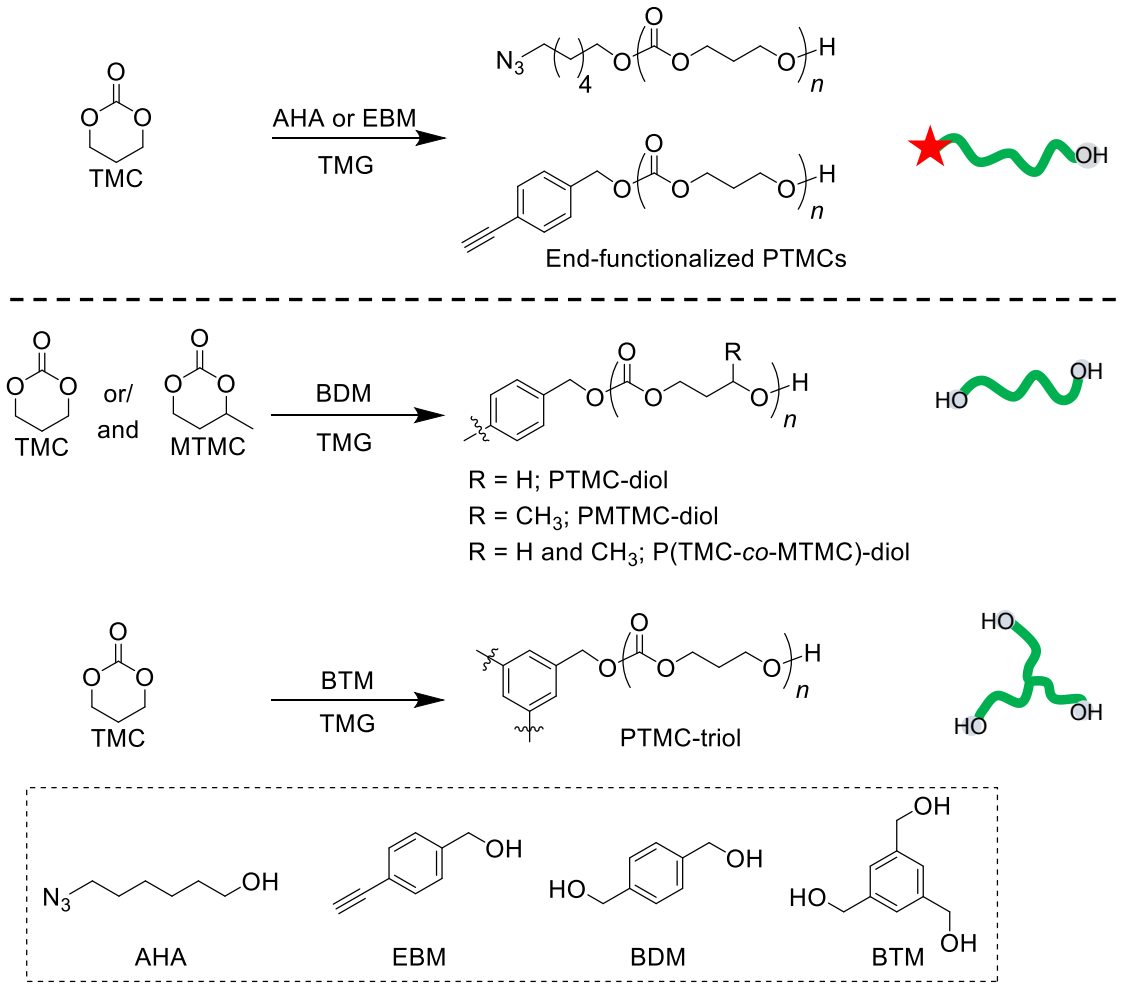

Table 3.4. TMG-catalyzed bulk ring-opening polymerization of TMC using functional initiators [a]

run	monomer	ini.	$[M]_0/[ini.]_0$ /[TMG]	time (min)	conv. (%) [b]	$M_{n,th.}$ [c]	$M_{n,NMR.}$ [b]	$M_{n,SEC}$ [d]	$Đ$ [d]
10	TMC	AHA	50/1/0.1	30	74	3,900	4,100	6,400	1.13
11	TMC	EBM	50/1/0.1	30	75	4,000	4,100	7,300	1.15
12	TMC	BDM	25/1/0.1	20	89	2,400	2,200	4,200	1.14
13	TMC	BTM	37.5/1/0.1	25	83	3,300	2,700	6,500	1.23
14	MTMC	BDM	25/1/0.1	540	78	2.400	2.200	4,000	1.17
15	TMC MTMC	BDM	12.5/12.5/1/0.1	120	93 63	2,200	2,200	3,500	1.13

[a] Polymerization conditions: atmosphere, Ar; temp., 70 °C. [b] Determined by ^{1}H NMR spectrum in $CDCl_3$. [c] Calculated from $[monomer]_0/[BDM]_0$ × conv. × (M.W. of monomer) + (M.W. of BDM). [d] Determined by SEC measurement of the obtained polymer in THF using PSt standards.

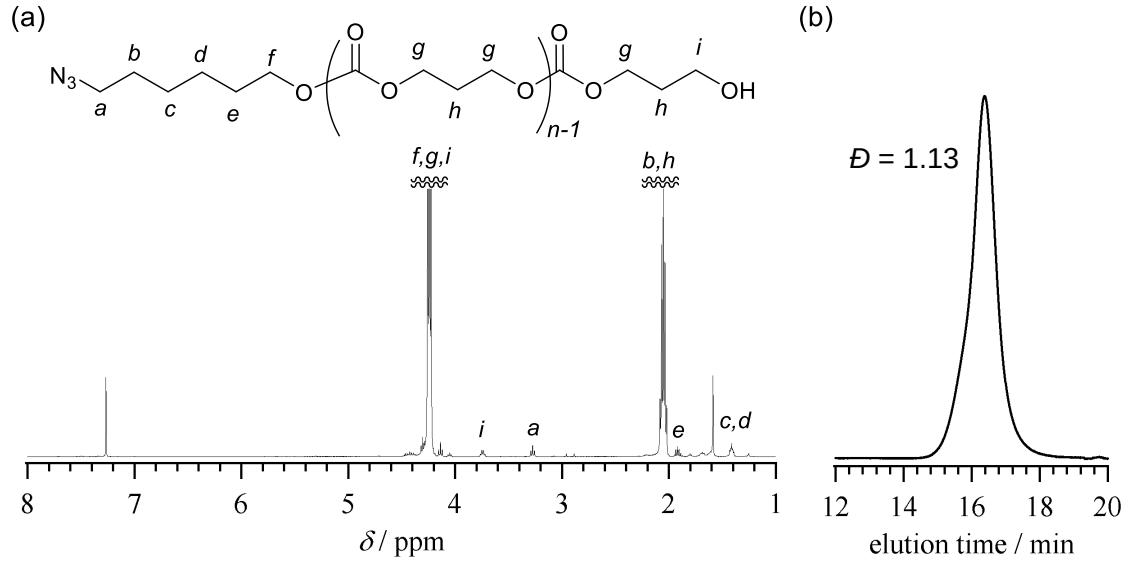

Figure 3.9. (a) ^{1}H NMR spectrum (* indicates the residual solvent) in $CDCl_3$, and (b) SEC trace (eluent, THF; flow rate, 1mL min^{-1}) of the PTMC obtained using AHA as an initiator.

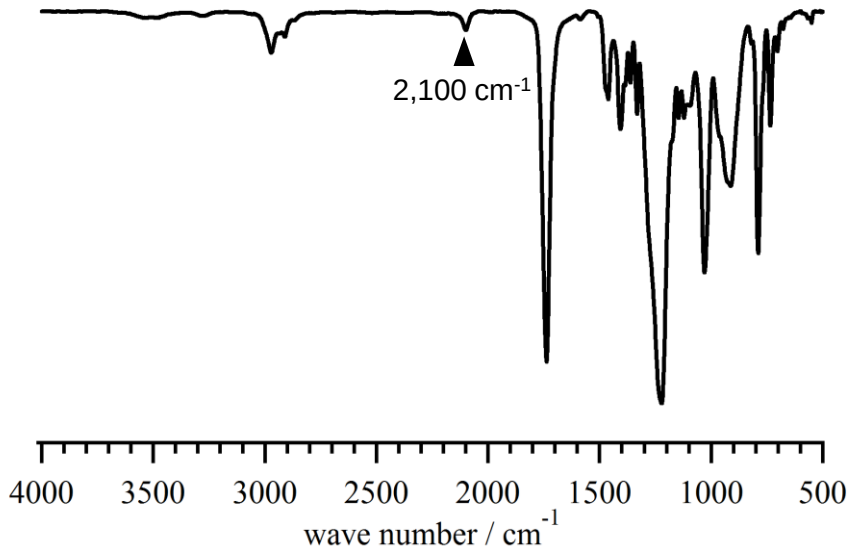

Figure 3.10. FT-IR spectrum of the PTMC obtained using AHA as an initiator.

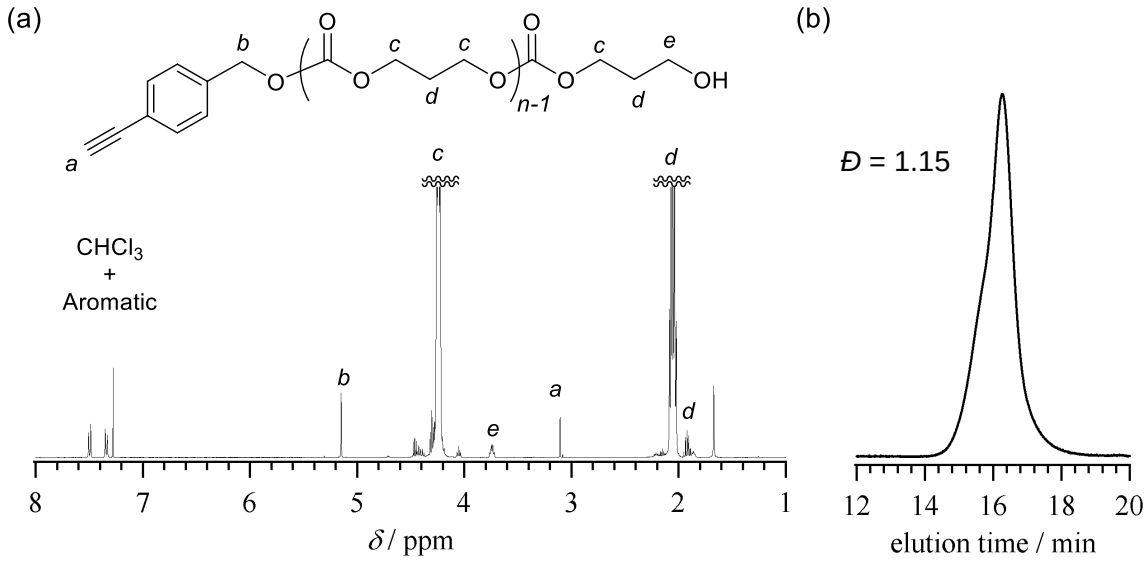

Figure 3.11. (a) ^{1}H NMR spectrum (* indicates the residual solvent) in $CDCl_3$, and (b) SEC trace (eluent, THF; flow rate, 1mL min^{-1}) of the PTMC obtained using EBM as an initiator.

The author next demonstrated the synthesis of APCs having multiple hydroxyl groups at the chain ends, which can be used for the polyurethane soft segments. Notably, APC-based polyurethane (APC-PU) has been investigated for biomedical and environmental applications. The ROP using 1,4-benzenedimethanol (BDM) as a difunctional initiator ($[TMC]_0/[BDM]_0/[TMG] = 25/1/0.1$) smoothly proceeded to give PTMC-diol (run 12 in Table 3.4 and Figure 3.12). The integration ratio of the signals due to the methylene protons adjacent to the ω-chain end hydroxyl group and BDIs aromatic proton is approximately estimated to 1:1, implying that the obtained PTMC has a hydroxyl group at each chain end. In addition, PTMC-triol was obtained using 1,3,5-benzenetrimethanol (BTM) as a multi-functional initiator (run 13 in Table 3.4 and Figure 3.13).

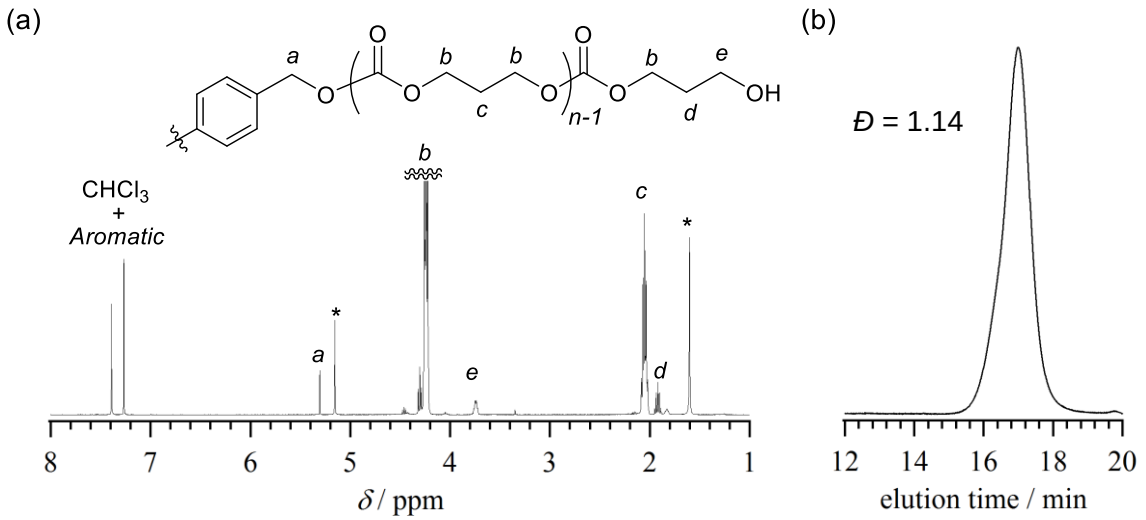

Figure 3.12. (a) ^{1}H NMR spectrum (* indicates the residual solvent) in $CDCl_3$ and (b) SEC trace (eluent, THF; flow rate, 1.0 mL min^{-1}) of the PTMC-diol obtained from run 12 in Table 3.4.

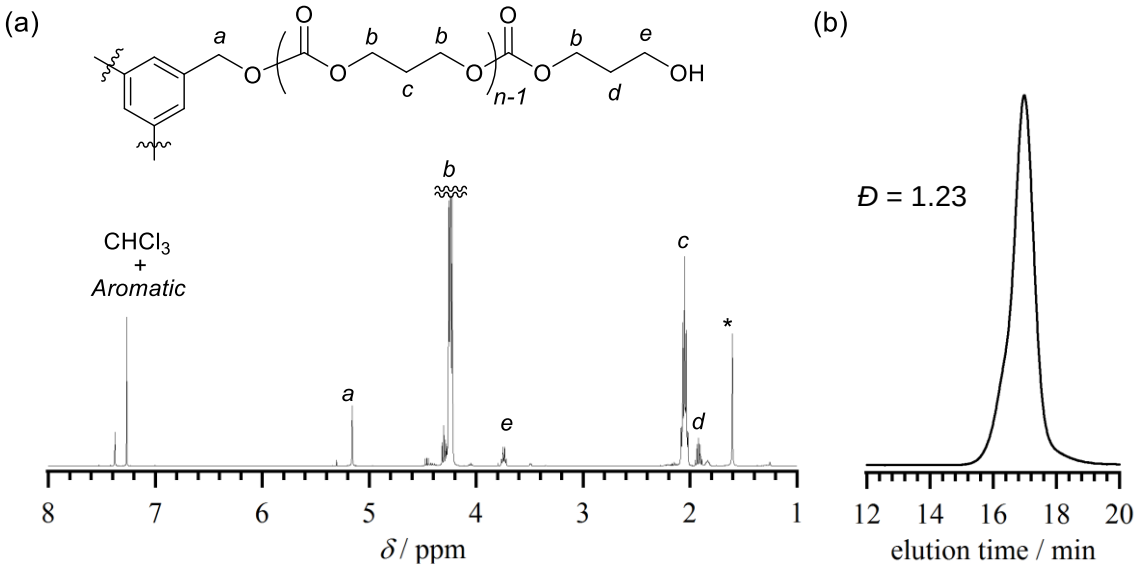

Figure 3.13. (a) ^{1}H NMR spectrum (* indicates the residual solvent) in $CDCl_3$, and (b) SEC trace (eluent, THF; flow rate, 1mL min^{-1}) of the PTMC-triol obtained from run 13 in Table 3.4.

The author attempted the ROP of α-methyl trimethylene carbonate (MTMC) with the present ROP system to expand the available APC structure. The ROP of MTMC proceeded under the same reaction condition as that of TMC (run 14 in Table 3.4 and Figure 14). The monomer conversion reached 78% in 9 h, indicating slower reaction rate than TMC. The possible reason is that the secondary hydroxyl group formation at the propagating chain end had lower reactivity toward the monomer due to the steric hindrance. The obtained poly(α-methyl trimethylene carbonate) (PMTMC) has the $M_{n,NMR}$ of 2,200, which well matches with the $M_{n,th.}$ of 2,400. Furthermore, the random copolymerization of TMC and MTMC was conducted using BDM at the initial $[TMC]_0/[MTMC]_0/[BDM]_0/[TMG]$ ratio of 12.5/12.5/1/0.1 to give P(TMC-*co*-MTMC)-diol (run 15 in Table 3.4). After the polymerization for 2 h, the monomer conversion of TMC and MTMC reached 93% and 63%, respectively. The ^{1}H NMR spectrum shows the signals due to both the PTMC and the PMTMC segments, indicating the statistical copolymerization proceeded to give P(TMC-*co*-MTMC) (Figure 3.15). The degree of polymerizations (DPs) for TMC and MTMC are estimated to be 12.5 and 6.3, respectively. The $M_{n,NMR}$ (2,200) well matches with the $M_{n,th.}$ (2,200) estimated from the monomer conversions of TMC and MTMC. The SEC trace is monomodal and the $Đ$ value is relatively low value of 1.13. These results supported that PTMC and PMTMC units were mutually introduced in a resulting polymer chain to obtain P(TMC-*co*-MTMC).

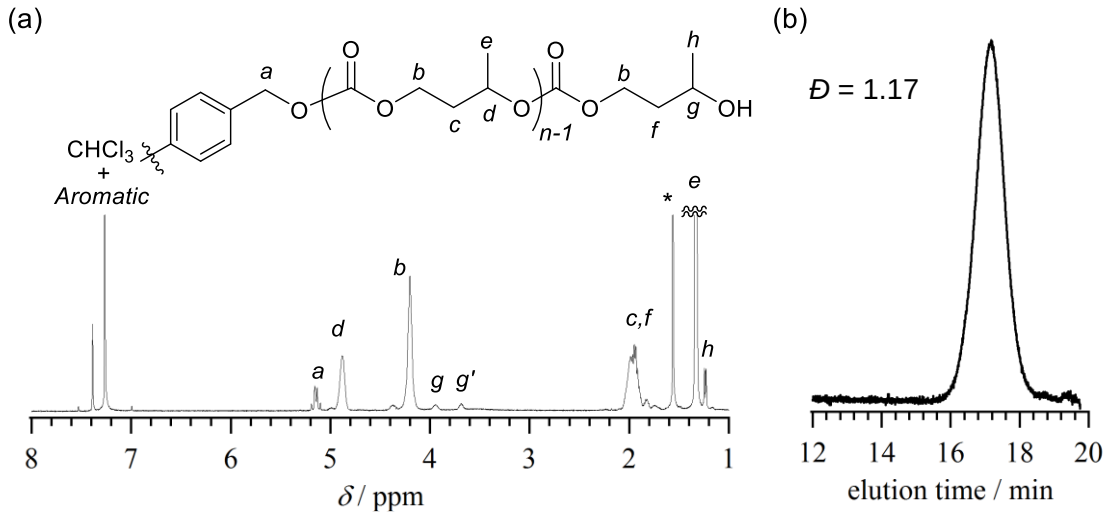

Figure 3.14 (a) ^{1}H NMR spectrum (* indicates the residual solvent) in $CDCl_3$, and (b) the SEC trace (eluent, THF; flow rate, 1mL min^{-1}) of the PMTMC obtained from run 14 in Table 3.4.

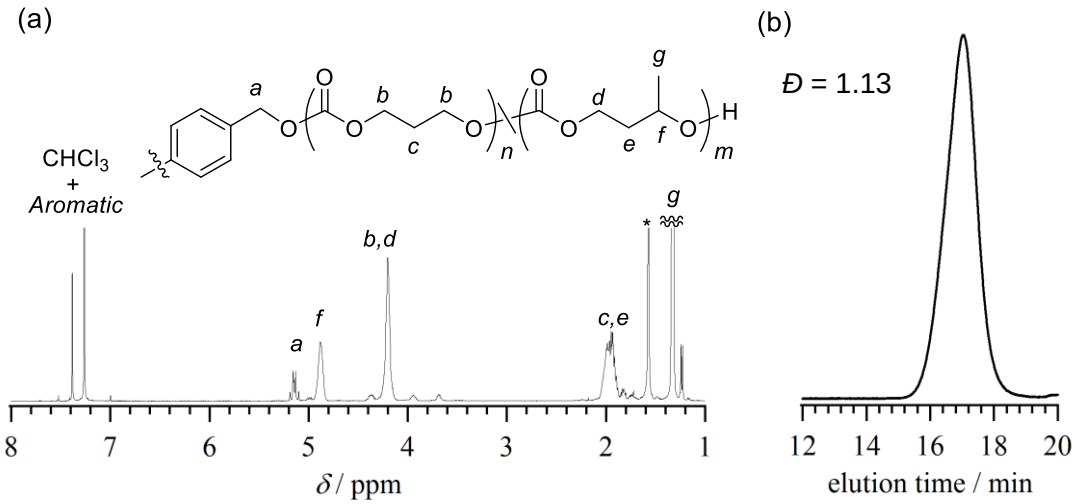

Figure 3.15. (a) ^{1}H NMR spectrum (* indicates the residual solvent) in $CDCl_3$, and (b) the SEC trace (eluent, THF; flow rate, 1mL min^{-1}) of the PTMC-*co*-PMTMC obtained from run 15 in Table 3.4.

Finally, the author applied the present ROP system to a one-pot synthesis of PTMC-PU (Scheme 3.3). The ROP of TMC was firstly conducted using 1,3-propanediol (PPD) as a bi-functional initiator at a $[TMC]_0/[PPD]_0/[TMG]$ ratio of 25/1/0.1 to produce a PTMC-diol. After the monomer conversion was >98%, 1 eq. of hexamethylene diisocyanate (HDI) with respect to PPD was added to the reaction mixture. The FT-IR and ^{1}H NMR analyses of the obtained polymer strongly support the formation of polyurethane. In the FT-IR spectrum, the characteristic absorptions of the urethane bond appear at 1530 and 3350 cm^{-1} (Figure 3.16), confirming the formation of the urethane bond. In the ^{1}H NMR spectrum of the soluble part of the final product, a peak due to N−*H* proton of the urethane bond is observed at 4.76 ppm along with peaks due to the PTMC main chain; peaks due to methylene proton resulting from the HDI residue are also seen (Figure 3.17). Therefore, the APC-diol obtained from the proposed ROP system can be used for APC-PU production, enabling the industrial application of the proposed ROP system.

Scheme 3.3. One-pot synthesis of PTMC-PU

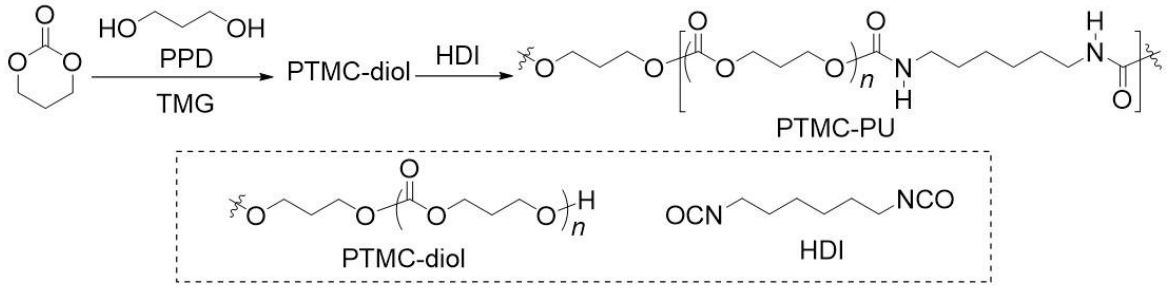

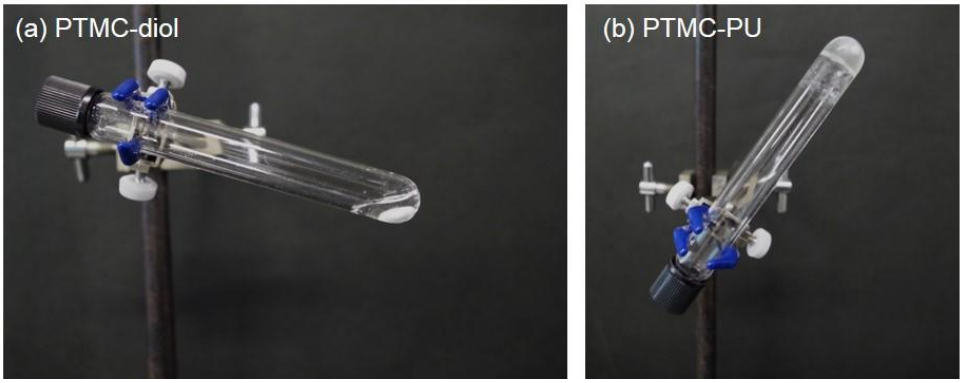

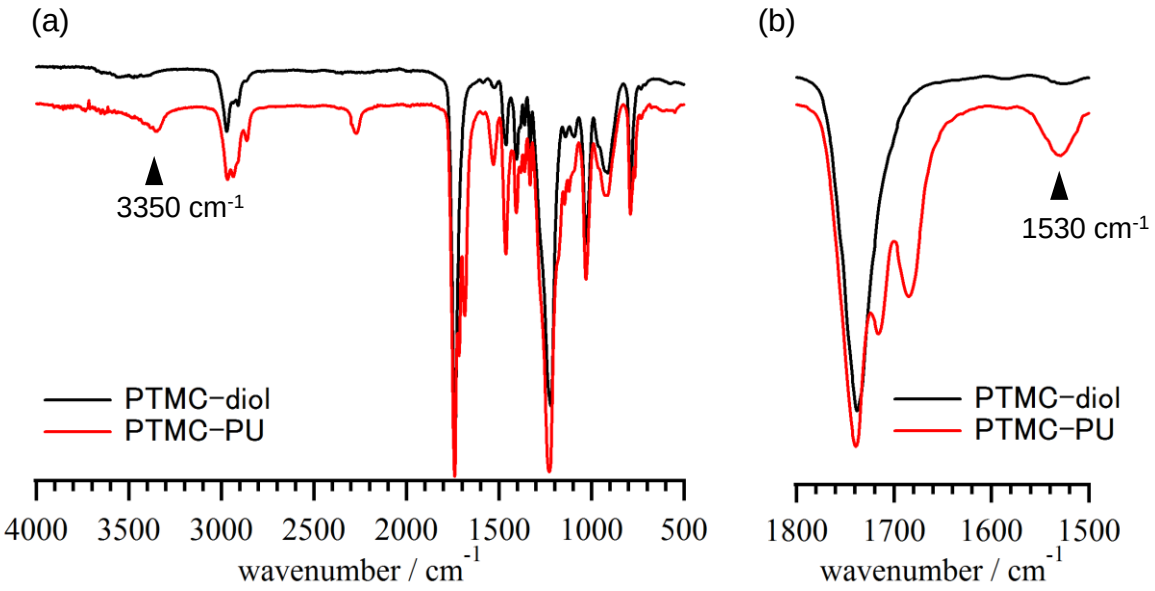

Figure 3.16. (a) is the FT-IR spectra of PTMC-diol synthesized using PPD (black line) and obtained PTMC-PU (insoluble part, red line), and (b) is expanded spectra ranging 1500 cm^{-1} to 1800 cm^{-1}.

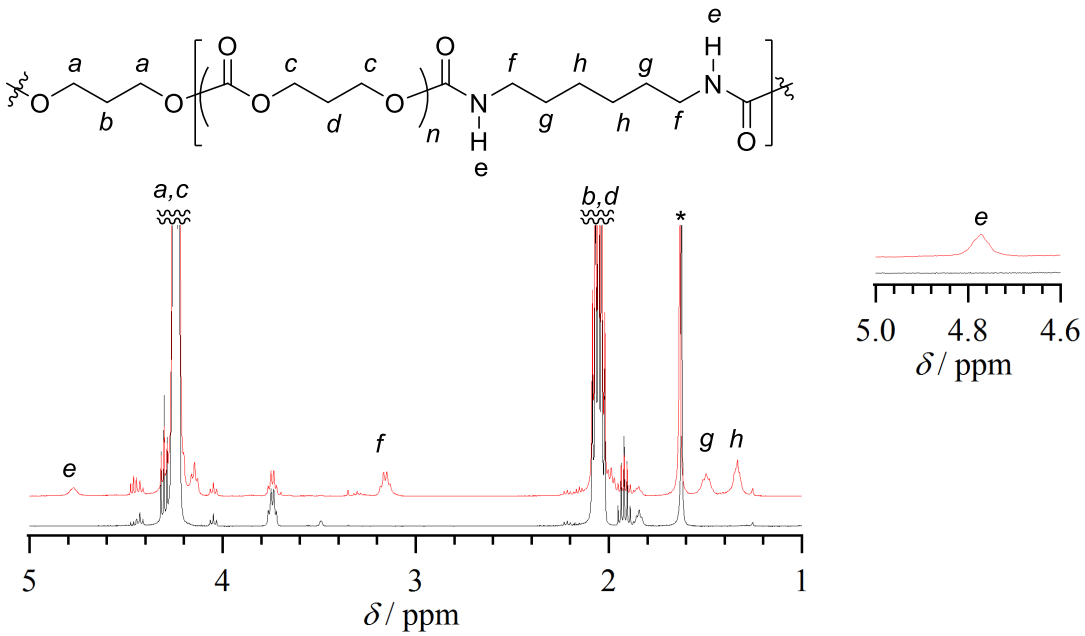

Figure 3.17. ^{1}H NMR spectra of the obtained PTMC-PU (red line) and PCL-diol synthesized by using PPD as a difunctional initiator (black line) in $CDCl_3$.

3.3 Conclusions

In summary, the author confirmed the excellent catalytic activity of the TMG toward the ROP of cyclic carbonates. The bulk ROP of TMC using the TMG catalyst proceeded in a controlled manner, with suppressed intra-/inter-molecular transesterification and decarboxylation even under the bulk polymerization condition. The obtained PTMC exhibited well-defined structure and low dispersity with a high degree of chain-end fidelity. The catalyst screening of TMG analogues and the FT-IR analyses of TMC and PPA in the presence/absence of TMG revealed that the zwitterionic structure containing carboxylate anions and quaternary ammonium cations in TMG helps efficiently produce APC materials via a bi-activation mechanism. In addition, the author prepared end-clickable APC for advanced materials as well as industry important APC-polyols by attempting the functional initiators. The ROP system established in this work can be implemented in bulk processes using a readily available, non-toxic catalyst. The system is suitable for manufacturing APCs for both conventional and future biomedical purposes. The author believes that the proposed ROP system is an environmentally-benign, sustainable, and practical strategy for producing biodegradable and biocompatible APCs.

3.4 Experimental Section

Materials. Trimethylene carbonate (TMC; >98%, Tokyo Kasei Kogyo Co., Ltd. (TCI)) was dried by azeotropic distillation. 3-Phenyl-1-propanol (PPA; >98%, TCI), ε-Caprolactone (CL; >99%, TCI), 1,6-hexamethylene diisocyanate (HDI; >98%, TCI), and 1,3-propanediol (PPD; >98%, TCI) were distilled over CaH_2 under reduced pressure. L-Lactide (L-LA; >98%, TCI) was purified by recrystallization from dry toluene. Trimethyl glycine anhydride (TMG; >97%, TCI), dimethyl glycine (DMG; >98%, TCI), trimethyl glycine hydrochloride (TMG-HCl; >98%, TCI), and tetramethylammonium acetate (TMAA; >98%, TCI) were dried under high vacuum at least 72 h prior to use. 1,4-Benzenedimethanol (BDM, >99%, TCI) and 1,3,5-benzenetrimethanol (BTM, >95%, TCI) were used as received.

Instruments. The polymerization was carried out in an MBRAUN stainless steel glove box with a gas purification system (molecular sieves and copper catalyst) in a dry argon atmosphere (H_2O, O_2 < 0.1 ppm). The moisture and oxygen contents in the glove box were monitored by an MB-MO-SE 1 and an MB-OX-SE 1, respectively. The ^{1}H NMR spectra were obtained using a JEOL JNM-A400II instrument. The size exclusion chromatography (SEC) was performed at 40 °C in THF (1.0 mL/min) using a Shodex GPC-101 system equipped with a shodex K-G guard column and a set of two Shodex KF-804L columns (linear, 8 mm × 300 mm; bead size, 5 μm; exclusion limit, 4 × 10^6). The molecular weight ($M_{n,SEC}$) and dispersity ($Đ$) of the polymers were estimated based on the polystyrene standard curve ranging from 1,200 to 1,320,000. Matrix-assisted laser desorption ionization time-of-flight mass spectrometry (MALDI-TOF MS) of the obtained polymers was performed using an AB SCIEX TOF/TOF 5800 system equipped with a 349-nm Nd: YAG laser. Samples for the MALDI-TOF MS were prepared by mixing the polymer (4.0 mg·mL^{-1}, 0.5 μL) and a matrix (2,5-dihydroxybenzoic acid, 60 mg·mL^{-1}, 0.5 μL) in THF. For the measurement, a sample plate, which was coated by

a solution (1.0 μL) of NaI as the cationic agent in acetone (1.0 mmol·L^{-1}), was used.

Typical procedure for Ring-opening polymerization of TMC using TMG as a catalyst.

Typical procedure of the ROP of TMC is as follows: In an argon-filled glove box, TMC (510 mg, 5.0 mmol), TMG (1,2 mg, 1.0 μmol), and PPA (13.6 μL, 100.0 μmol) were put into a reaction vessel. The reaction mixture was stirred at 70 °C under an argon atmosphere in an oil bath. After 30 min, the reaction mixture was purified by reprecipitation from a CH_2Cl_2 solution into cold methanol to give a PTMC (310 mg) as a colorless viscous liquid.

Yield, 60.7%. $M_{n,NMR}$ = 4000 g·mol^{-1}; $M_{n,SEC}$ = 6000 g·mol^{-1}; $Đ$ = 1.12. ^{1}H NMR ($CDCl_3$, 400MHz): δ (ppm) 1.92 (m, 2H, -C*H*$_2$CH$_2$OH), 1.97-2.11 (m, 2H, ArCH$_2$C*H*$_2$-; 2H × (*n-1*), (-OCH$_2$C*H*$_2$-)$_{n-1}$), 2.70 (t, 2H, J = 7.8 Hz, ArC*H*$_2$-), 3.74 (q, 2H, J = 9.0 Hz, -C*H*$_2$OH), 4.13-4.32 (m, 2H, ArCH$_2$CH$_2$C*H*$_2$-, m, 4H × *n-1*, (-OC*H*$_2$CH$_2$C*H*$_2$O-)$_{n-1}$, m, 2H, -C*H*$_2$CH$_2$CH$_2$OH), 7.16-7.32 (m, 5H, aromatic).

One pot synthesis of PTMC-PU

Procedure of the one-pot synthesis the PTMC-based polyurethane is as follows: TMC (1020 mg, 10.0 mmol), 1,3-propanediol (28.8 μL, 400.0 μmol), TMG (4.8 mg, 40.0 μmol) was put into the reaction vessel filled with Ar. The reaction mixture was stirred at 70 °C in an oil bath. After 30 min, HDI (63.6 μL, 400 μmol) was added to the reaction mixture to keep stirring at 70 °C. After 24 h, the reaction mixture was purified by reprecipitation from a CH_2Cl_2 solution into cold methanol to give PTMC-based polyurethane

3.5 References

1. Mato, Y.; Honda, K.; Tajima, K.; Yamamoto, T.; Isono, T.; Satoh, T. *Chem. Sci.* **2019**, DOI: 10.1039/C8SC04006K
2. Uyar, Z.; Oncel, A. *J. Polym. Res.* **2018**, *20*, 1–14.
3. Schneiderman, D. K.; Hillmyer, M. A. *Macromolecules* **2016**, *49*, 2419–2418.
4. Neitzel, A. E.; Haversang, E.; Thomas, J.; Hillmyer, M. A. *Ind. Eng. Chem. Res.* **2016**, *55*, 11747–11755.
5. Nachtergael, A.; Coulembier, O.; Dubois, P.; Helvenstein, M.; Duez, P.; Blankert, B.; Mespouille, L. *Biomacromolecules* **2015**, *16*, 507–514.
6. Dhamaratne, N. U.; Pothupitiya, J. U.; Bannin, T. J.; Kazakov, O. I.; Liesewetter, M. K. *ACS Macro Lett.* **2017**, *6*, 421–425.
7. Erickson, B. E. *Chem. Eng. News* **2016**, *94*, 16.
8. Day, C. R.; Kempson, S. A. *Biochem. Biophys. Acta* **2016**, *1860*, 1098–1106.
9. European Food Safety Authority *EFSA J.* **2017**, 15, 5057.
10. Thomas, C.; Milet, A.; Peruch, F.; Bibal, B. *Polym. Chem.* **2013**, *6*, 3491–3498.
11. Coady, D. J.; Fukushima, K.; Horn, H. W.; Rice, J. E.; Hedrick, J. L. *Chem. Commun.* **2011**, *47*, 3105–3107.
12. Kojio, K.; Nonaka, Y.; Masubuchi, T. *J. Polym. Sci., Part B: Polym. Phys.* **2004**, *42*, 4448–4458.
13. Xie, C.; Song, J.; Wu, H.; Zhou, B.; Congyi, W.; Han, B. *ACS Sustainable Chem. Eng.* **2017**, *5*, 7086−7092.
14. Liu, X.-F.; Li, X.-Y.; Qiao, C.; Fu, H.-F. *Angew. Chem. Int. Ed.* **2017**, *56*, 7425–7429.
15. Zhu, L.; Xue, W.; Zeng, Z. *New J. Chem*. **2018**, *42*, 15997–16004.
16. Brannigan, R. P.; Dove, A. P. *Biomater. Sci.* **2017**, *5*, 9–21.
17. Mespouille, L.; Coulembier, O.; Kawalec, M.; Dove, A.P.; Dubois, P. *Prog. Polym. Sci.* **2014**, *39*, 1144−1164.
18. Sobczak, M.; Dębek, C.; Olędzka, E.; Nałęcz-Jawecki, G.; Kołodziejski, W. L.; Rajkiewicz, M. *J. Polym. Sci., Part A: Polym. Chem.* **2012**, *50*, 3904–3913.
19. Fukushima, K.; Honda, K.; Inoue, Y.; Tanaka, M. *Eur. Polym. J.* **2017**, *95*, 728–736.
20. Asplund, J. O. B.; Bowden, T.; Mathisen T.; Hilborn, J. *Biomacromolecules* **2007**, *8*, 905–911.
21. Ma, Z.; Hong, Y.; Nelson, D. M.; Pichamuthu, J. E.; Leeson, C. E.; Wagner, W. R.

Biomacromolecules **2011**, *12*, 3265–3274.

22. Dai, Y.; Zhang, X. *Polym. Chem.* **2017**, *8*, 7429–7437.
23. Makiguchi, K.; Yamanaka, T.; Kakuchi, T.; Terada, M.; Satoh, T. *Chem. Commun.* **2014**, *50*, 2883−2885.
24. *α*-H Moieties of quaternary ammonium cation act as hydrogen bond donor in transesterification reaction as well as ROP of cyclic ester. See the references 10, 11, and 25.
25. Hatano M.; Tabata, Y.; Yoshida, Y.; Toh, K.; Yamashita, K.; Ogura, Y; Ishihara, K. *Green Chem.* **2018**, *20*, 1193−1198.
26. Binder, W. H.; Sachsenhofer, R. *Macromol. Rapid Commun.* **2008**, *29*, 952−981.
27. Kempe, K; Krieg, A.; Becer, C. R.; Schubert, U. S. *Chem. Soc. Rev.* **2012**, *41*, 176−191.
28. Fukushima, K. *Biomater. Sci*. **2016**, *4*, 9−24.

Chapter 4

Alkali Metal Carboxylate-catalyzed

Ring-opening Polymerization of Cyclic Esters

4.1 Introduction

The development of synthetic methods brings about progress in chemistry and sometimes produces unexpected innovations that create new paradigms in the fields of chemistry.[1-3] In polymer chemistry, establishment of a novel polymerization method is a significant event at both the academic and industrial stages, enabling the creation of a wide array of advanced polymeric materials, as well as their implementation into ideal commercial processes.[4,5] Regarding the ring-opening polymerization (ROP) of cyclic esters, leading biodegradable and biocompatible aliphatic polyesters, the emergence of organocatalytic ROP was one of the important turning points. Since first organocatalytic ROP was reported by Hedrick et al.,[6] considerable effort has been devoted to develop controlled/living organocatalytic ROP systems as an environmentally-benign approach in order to break away from conventional methods that rely on metal-based catalysts.[7-9] To date, several classes of organocatalysts including Brønsted/Lewis acids[10-14] or bases[6, 15-17] and bifunctional catalytic systems[18-21] have proven effective for the ROP of cyclic esters to produce well-defined aliphatic polyesters (APEs) with predictable molecular weights and narrow dispersities (*Đ*s). However, organocatalysts have not replaced metal-based catalysts in the industrial production of APEs yet because of the unavoidable difficulties of organocatalytic ROP, including high production costs, extremely strong acidity/basicity, and/or low activity.

The aim of this study is to establish an innovative ROP system that allows for the environmentally-benign and practical production of valuable APEs. In chapter 3, the author describes the bulk ring-opening polymerization (ROP) system of cyclic carbonate using trimethyl glycine (TMG) as an efficient bio-derived organocatalyst. The good availability and non-toxicity of the TMG are attractive characteristics for the biodegradable and biocompatible aliphatic polycarbonate (APC) synthesis for both the academic and industrial stages. However, the TMG-catalyzed ROP system is ineffective for cyclic esters, therefore, the remaining task is

the establishment of a novel polymerization system covering a wide scope of monomers and maintaining good availability and non-toxicity of the catalyst.

In the TMG-catalyzed ROP system, TMG exhibits a good catalytic activity due to its bi-activation property derived from the combination of the carboxylate anion and quaternary ammonium cation. Based on the hypothesis that other cationic species also activate the carbonyl group of cyclic monomers, the author turned his attention to a series of alkali metal carboxylates as a potential bifunctional catalytic system to establish a novel polymerization method. Sodium acetate, a representative example of an alkali metal carboxylate, is readily available and widely used as a food additive. Therefore, alkali metal carboxylates can successfully meet the industrial requirements of low cost, easy handling, and low toxicity. As catalysts, alkali metal carboxylates are of interest because their basic/acidic properties can be tuned by the choice of the carboxylate moieties and counter cations. Such a tunability would provide a general strategy for the controlled/living ROP of cyclic esters.

In this chapter, the author describes the alkali metal carboxylate-catalyzed ROP of cyclic esters as an unprecedented catalytic system substituting for conventional procedures using metal-based catalysts and organocatalysts (Scheme 4.1). In this study, the efficient catalytic ability of the alkali metal carboxylate was revealed for the ROP of cyclic esters. The bulk ROP of L-LA using sodium acetate proceeded in a controlled manner to give the well-defined poly(L-lactide) (PLLA). A matrix-assisted laser desorption/ionization time-of flight mass spectral (MALDI-TOF MS) analysis revealed that the role of the alkali metal carboxylate is totally different from the conventional living polymerization system of β-lactone using an alkali metal carboxylate. [22-24] The wide scope of application of the alkali metal carboxylate-catalyzed ROP system was verified regarding the available polymer structure as well as the applicable monomer. The ROP using functional initiators produced PLLAs possessing a clickable group and multi-hydroxyl groups and furthermore, the block copolymer consisting of

PLLA and poly(ethylene glycol) (PEG) segment was successfully prepared by using a PEG possessing a hydroxyl group at the chain end as a macroinitiator. As for the scope of the applicable monomer, sodium acetate efficiently catalyzed the ROP of the racemic DL-lactide (DL-LA) and trimethylene carbonate (TMC). Furthermore, the tunability of the alkali metal carboxylate enabled the ROP of *ε*-caprolactone (CL) and *δ*-valerolactone (VL) by the appropriate choice of the alkyl moiety and counter cation. Finally, the bi-activation property of the alkali metal carboxylate was confirmed by an FT-IR measurement.

Scheme 4.1. Alkali metal carboxylate-catalyzed ROP system used in this study

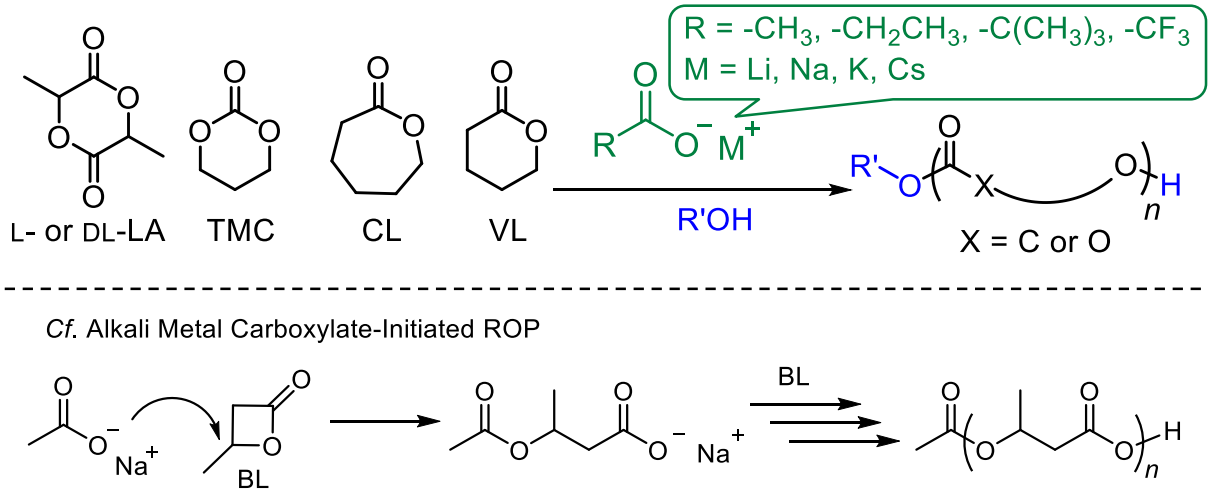

4.2 Results and Discussion

4.2.1 Ring-opening Polymerization of Cyclic Esters Using Alkali Metal Carboxylate as a Catalyst

The initial experiment included the ROP of L-lactide (L-LA) in the bulk using sodium acetate as a catalyst and 3-phenyl-1-propanol (PPA) as an initiator at an [L-LA]$_0$/[PPA]$_0$/[CH_3COONa] ratio of 50/1/0.5 at 130 ºC (run 1 in Table 4.1). After 4 h of polymerization, a NMR analysis indicated that the monomer conversion had reached 83.9% to produce a poly(L-lactide) (PLLA), implying that sodium acetate indeed promoted the ROP. The size exclusion chromatography (SEC) analysis revealed a rather narrow *Đ* value of 1.17, albeit with a small shoulder peak in the higher molecular weight region (Figure 4.1(a), dotted line). These observations encouraged us to further optimize the polymerization conditions to establish a well-controlled ROP system. After a thorough screening of the polymerization conditions, lowering the polymerization temperature to 100 °C (run 2 in Table 4.1) was found to be effective at minimizing the side reactions; the SEC trace of the obtained PLLA showed a monomodal elution peak without any shoulder peak (Figure 4.1(a), solid line), indicating the suppression of the intra- and intermolecular transesterifications. The ^{1}H NMR spectrum of the obtained PLLA showed minor signals due to the 3-phenyl-1-propoxy group, along with major signals due to the PLLA main chain (Figure 4.1(b)), and the NMR-based molecular weight ($M_{n,NMR}$) was found to be close to the theoretical value ($M_{n,NMR}$ = 6,600 and $M_{n,th.}$ = 6,200). It is worthy to note that the epimerization was also well-suppressed by lowering the polymerization temperature (Figure 4.1(c) and (d)), which was confirmed from the ^{1}H NMR spectrum of the PLLA obtained from run 2 with selective decoupling of the PLLA methyl resonance. The methine peak area derived from the syndiotactic sequence (*sis*, *sii*, *iis*, *isi*) became smaller when compared to the product from run 1, indicating isotactic-enriched PLLA production.

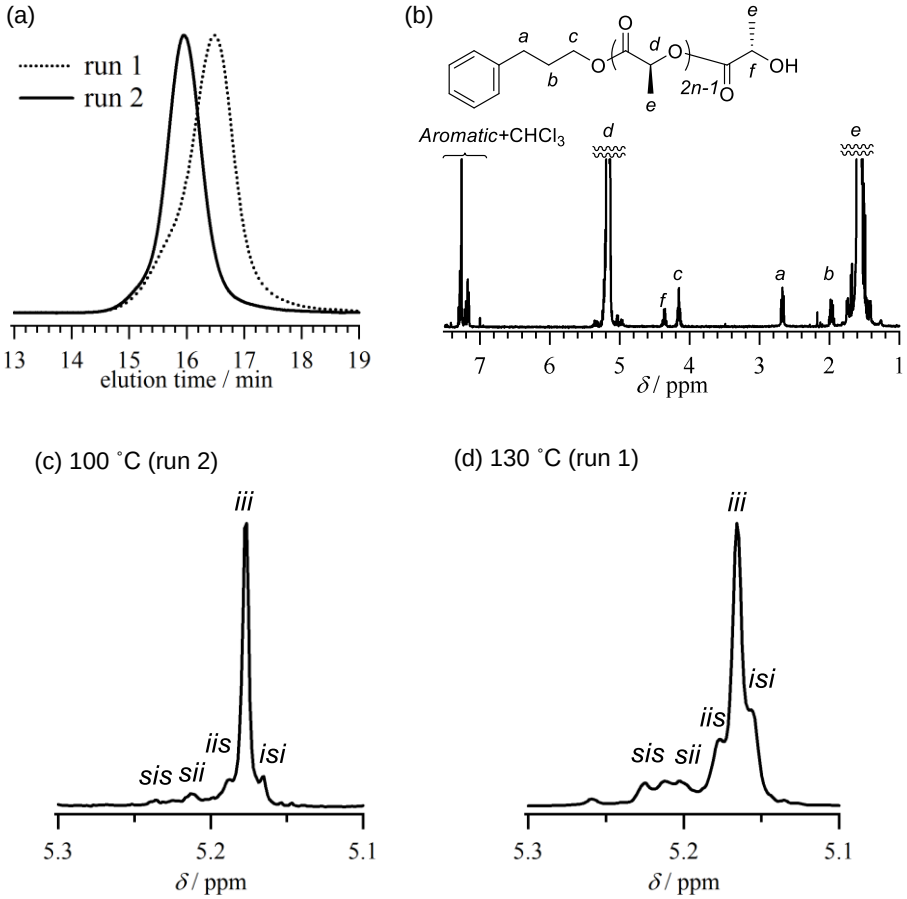

Figure 4.1. (a) SEC traces of PLLAs obtained from run 1 and run 2 in Table 4.1, (b) ^{1}H NMR spectrum of the PLLA (run 2), and methine resonances of PLLAs obtained from (c) run 2 and (d) run 1 with selective decoupling of PLLA methyl resonances (ranging from 5.1 to 5.3 ppm; solvent, $CDCl_3$; 400 MHz).

To obtain further structure information of the resultant PLLA, the MALDI-TOF MS analysis was conducted (Figure 4.2). In the spectrum of the PLLA obtained from run 2, three series of repeated peaks were observed, which are all assignable to the PLLA possessing a 3-phenyl-1-propoxy group at the α-chain end and a hydroxyl group at the ω-chain end. Therefore, the ROP proceeded through repeated *O*-acyl cleavage of L-LA (Case 1 in Scheme 4.2), attacked by the hydroxy group of PPA (initiation reaction) and the propagating chain end (propagation reaction), and there was no initiation from the sodium acetate via *O*-alkyl cleavage of L-LA (Case 2 in Scheme 4.2).[24] Additionally, the peak derived from the inter molecular transesterification (the peak assigned ■ in Figure 4.2) was insignificant and the peak

corresponding to the cyclic byproduct derived from the intra molecular transesterification was not detected, which again confirmed the controlled nature of the present ROP system.

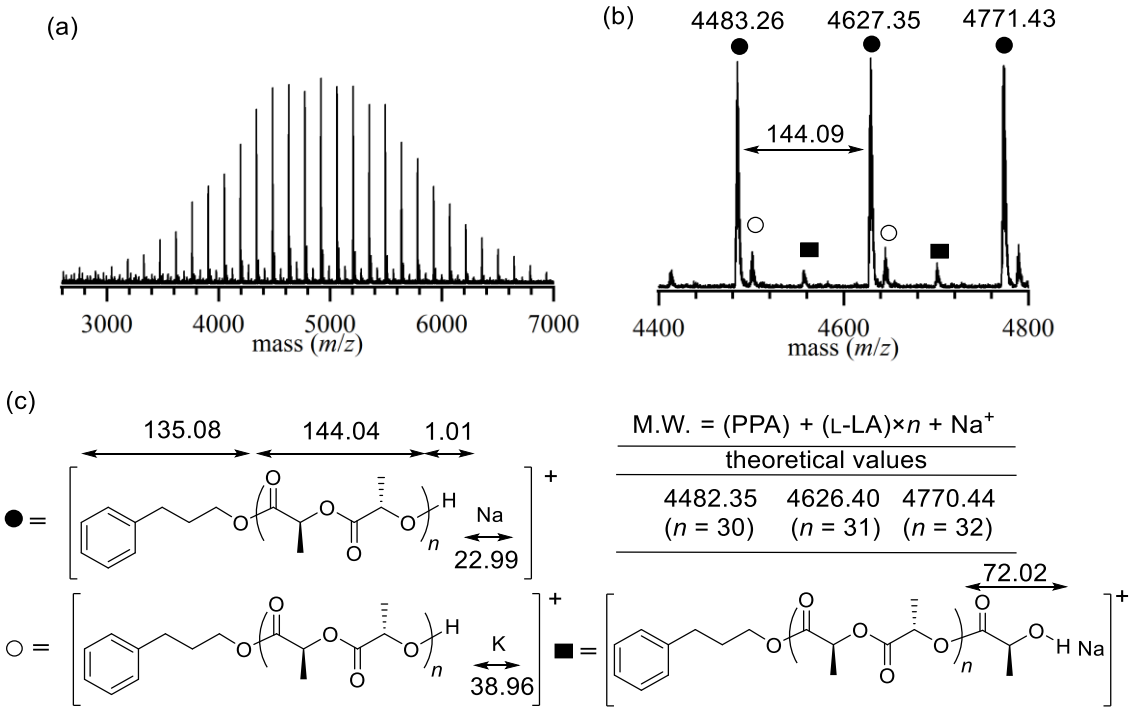

Figure 4.2. (a) MALDI TOF-MS spectrum of the PLLA obtained from run 2 in Table 4.1, (b) expanded spectrum ranging from 4,400 to 4,800, and (c) expected structure and theoretical molecular weight of the PLLA possessing 3-phenyl-1-propoxy group at the α-chain end and hydroxyl group at the ω-chain end.

Scheme 4.2. Possible ring-opening pathway of the present ROP system

Case 1. *O*-Acyl cleavage

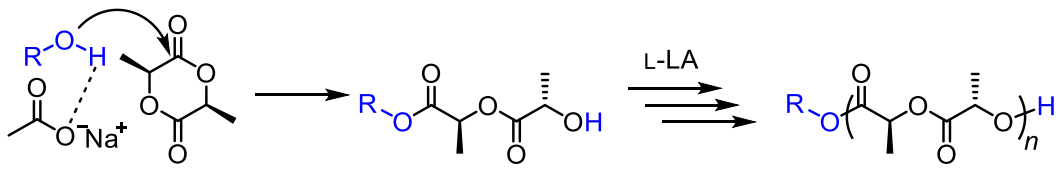

Case 2. *O*-Alkyl cleavage; Not observed

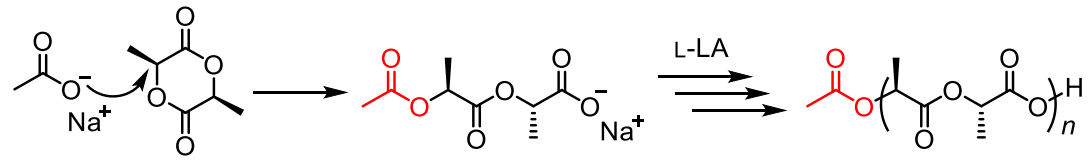

In the conventional ROP of *β*-lactone using alkali metal carboxylates, the carboxylate anion works as an initiator and the ROP proceeds through the *O*-alkyl cleavage. Indeed, the ROP of *β*-butyrolactone (BL) with sodium acetate proceeded in an *O*-alkyl cleavage manner even in the presence of PPA, and the poly(*β*-butyrolactone) (PBL) possessing a 3-phenyl-1-propoxy group at the *α*-chain end was not observed in the MALDI-TOF MS spectrum (Figure 4.3). Therefore, the present alkali metal carboxylate/alcohol initiator system is not effective for the ROP of *β*-lactone. Additionally, the ROP of L-LA in the presence of sodium acetate without adding an alcohol initiator proceeded, albeit in an uncontrolled manner. The MALDI-TOF MS analysis revealed that the product consisted of low molecular weight linear and cyclic oligomers, which were probably initiated from a small amount of water, and there was no evidence of the initiation reaction from the acetate anion even in the absence of an alcohol initiator (Figure 4.4). These results confirmed that sodium acetate acted as a catalyst in the present ROP system for L-LA, as opposed to the case of the conventional ROP of *β*-lactone.

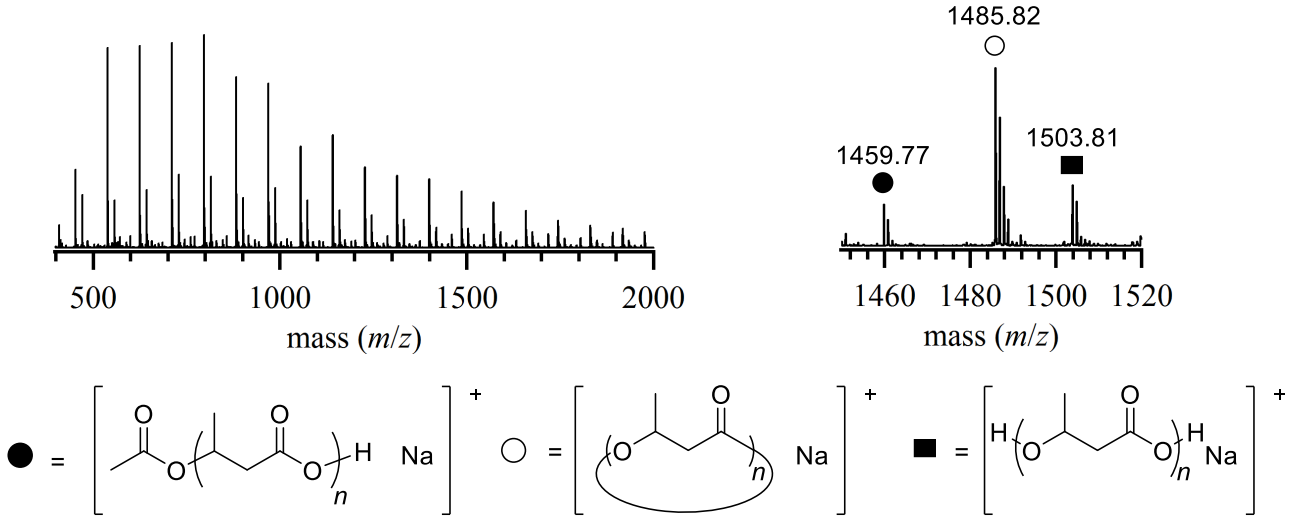

Figure 4.3. MALDI-TOF MS spectrum of the obtained PBL from the ROP of BL using sodium acetate in the presence of PPA at 80 °C in the bulk

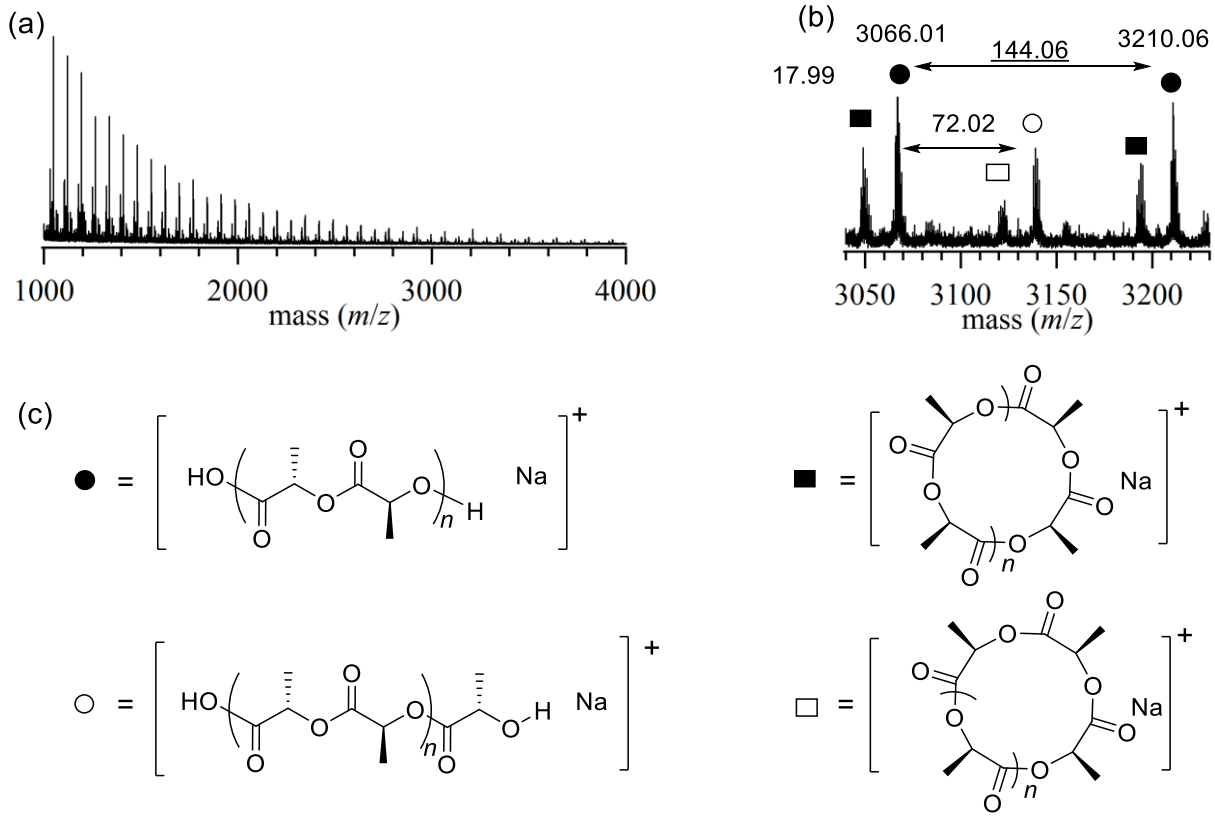

Figure 4.4. MALDI-TOF MS spectrum of the PLLA obtained from the ROP of L-LA using sodium acetate in the absence of PPA ([L-LA]$_0$/[CH_3COONa] = 100/1; temp., 100 °C; time, 24 h; conv. = 12.8%) in the bulk.

To further study the polymerization properties of the present catalytic system, a kinetic experiment with the [L-LA]$_0$/[PPA]$_0$/[CH_3COONa] ratio of 50/1/0.5 was performed at 100 °C. As shown in Figure 4.5(a), the $M_{n,NMR}$ value of the resulting PLLA linearly increased with increasing monomer conversion according to the theoretical line, which implied the good suppression of the termination and chain transfer reactions. In addition, the kinetic plot depicted in Figure 4.5(b) indicated that the ROP proceeded in the first-order kinetic manner. These results strongly indicated that the present polymerization proceeded in a controlled/living fashion.

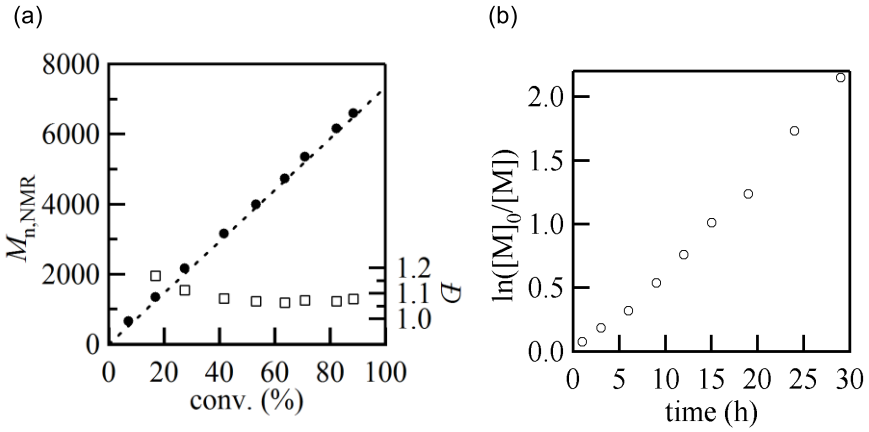

Figure 4.5. (a) Dependence of $M_{n,NMR}$ (●), $Đ$ (□), and $M_{n,th.}$ (dotted line) on the monomer conversion. (b) First-order kinetic plot for the ROP of L-LA at the [L-LA]$_0$/[PPA]$_0$/[CH_3COONa]$_0$ ratio of 50/1/0.5 at 100 ºC in the bulk.

The present polymerization system successfully produced PLLAs with the $M_{n,NMR}$ ranging from 3,500 to 22,600 while retaining a relatively narrow $Đ$ by adjusting the initial monomer-to-initiator ratio (runs 3–6 in Table 4.1). For the ROP of L-LA at the [L-LA]$_0$/[PPA]$_0$ ratio of 25/1, the monomer conversion reached 87.2% in 19 h to give a PLLA with the $M_{n,NMR}$ and $Đ$ values of 3,500 and 1.10, respectively. In a similar manner, a higher molecular weight PLLA was obtained by the ROP at the [L-LA]$_0$/[PPA]$_0$ ratio of 100/1. In the case of the ROPs at the [L-LA]$_0$/[PPA]$_0$ ratios of 150/1 and 200/1, the reaction was conducted in the presence of a small portion of toluene (L-LA/toluene = 25 mmol/1 mL) to reduce the viscosity of the reacting mixture. As the results, PLLAs with the $M_{n,NMR}$ of up to 22,600 were obtained with the relatively narrow $Đ$ value of 1.20. The SEC elution peak maximum shifted to the higher molar weight region by increasing the [L-LA]$_0$/[PPA]$_0$ ratio while keeping the relatively narrow $Đ$ value ranging from 1.07 to 1.20 (Figure 4.6). These controlled manners of the present ROP system for molecular weight, dispersity, and end structure of the attained PLLA are very comparable to the conventional controlled/living ROP using organometallic catalysts as well as organocatalysts.[7, 12]

Table 4.1. Ring-opening polymerization of L-LA using sodium acetate as a catalyst [a]

run	[L-LA]$_0$/[PPA]$_0$ /[CH_3COONa]	temp. (ºC)	time (h)	conv. (%) [b]	$M_{n,th.}$ [c]	$M_{n,NMR}$ [b]	$M_{n,SEC}$ [d]	$Đ$ [d]
1	50/1/0.5	130	4	83.9	6,200	6,000	7,200	1.17
2	50/1/0.5	100	24	84.1	6,200	6,600	9,700	1.07
3	25/1/0.25	100	19	87.2	3,300	3,500	6,100	1.10
4	100/1/1.0	100	31	84.4	12,300	11,300	13,700	1.13
5 [e]	150/1/1.5	100	89	80.2	17,500	18,200	18,400	1.18
6 [e]	200/1/2.0	100	116	79.9	23,200	22,600	22,000	1.20

[a] Polymerization conditions: [L-LA]/[CH_3COONa] = 50/0.5; Ar atmosphere; PPA as initiator. [b] Determined by ^{1}H NMR in $CDCl_3$. [c]Calculated from ([L-LA]$_0$/[PPA]$_0$) × conv. × (M.W. of L-LA) + (M.W. of PPA). [d]Determined by SEC measurement of the obtained polymer in THF. [e] Polymerization was conducted in the presence of a portion of toluene (L-LA/toluene =25 mmol/1 mL).

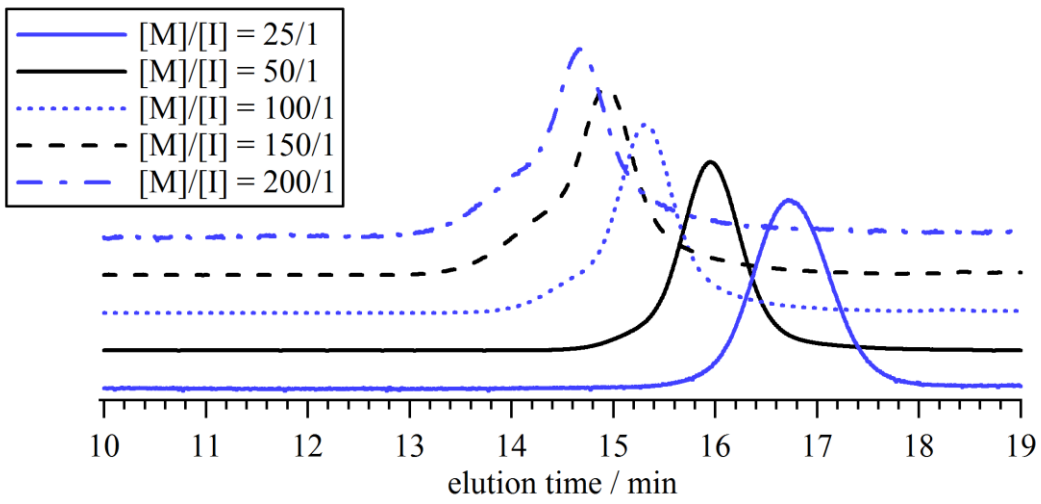

Figure 4.6. SEC traces of the obtained PLLA with various molar mass (runs 2-6 in Table 4.1) (eluent, THF; flow rate, 1 mL min^{-1}).

Additionally, the author examined the ROP of L-LA with decreasing the amount of loaded catalyst (Table 4.2). As the results, the ROP proceeded even at the [L-LA]$_0$/[PPA]$_0$/[CH_3COONa] of 50/1/0.05 to reach 82.5% monomer conversion within 90 h. The $M_{n,NMR}$ of the obtained PLLA was in good agreement with the $M_{n,th.}$ and the $Đ$ value was relatively narrow value of 1.10, suggesting that the controlled nature of the ROP was maintained even at the lower catalyst loading. Notably, the turn over frequency (TOF) value was increased with decreasing the amount of loaded catalyst, while longer reaction time was required to reach high conversion. Therefore, we could adjust the balance manufacturing time and catalyst cost by changing the amount of loaded catalyst, which is good advantage in industrial production.

Table 4.2. Polymerization of L-LA catalyzed by sodium acetate varying amount of catalyst [a]

run	[L-LA]$_0$/[PPA]$_0$ /[CH_3COONa]	time (h)	conv. (%) [b]	$M_{n,th.}$ [c]	$M_{n,NMR}$ [b]	$M_{n,SEC}$ [d]	$Đ$ [d]	TOF (h^{-1})
1	50/1/0.50	24	84.1	6,200	6,200	9,800	1.07	3.5
7	50/1/0.25	37	85.6	6,300	6,100	10,100	1.08	4.6
8	50/1/0.10	48	82.5	6,100	6,700	10,300	1.06	8.6
9	50/1/0.05	90	82.5	6,100	6,500	10,100	1.10	9.1

[a] Polymerization conditions: temp., 100˚C; atmosphere, Ar; initiator, PPA; cat., sodium acetate. [b] Determined by ^1H NMR in $CDCl_3$. [c] Calculated from ([L-LA]$_0$/[PPA]$_0$) × conv. × (M.W. of L-LA) + (M.W. of PPA). [d] Determined by SEC measurement of the obtained polymer in THF using PSt standards.

4.2.2 Syntheses of End-functionalized PLLA Using Functional Initiator

The present ROP system was further applied to the synthesis of various end-functionalized PLLAs and PLLA-polyols with the aid of functional initiators, such as 6-azide-1-hexanol, propargyl alcohol, 1,3-propanediol, trimethylolpropane, and pentaerythritol (runs 10-15 in Table 4.3). Based on the ^{1}H NMR spectra of the obtained products, the signals derived from the corresponding initiator residue were observed along with the signals due to the PLLA main chain and the SEC traces were monomodal, strongly suggesting that the ROP successfully proceeded to obtain end-functionalized PLLAs (Figure 4.7) and PLLA-polyols (Figure 4.8). It is worth noting that the molecular weight of the four-armed PLLA was controlled up to 80,000 with the narrow $Đ$ value of 1.08 in the ROP with $[\text{L-LA}]_0/[\text{pentaerythritol}]_0 = 800/1$ (run 15 in Table 4.3). Furthermore, the present ROP system is also useful for the synthesis of the PLLA-containing block copolymer. By using the poly(ethylene glycol) monomethyl ether (PEG-OH; $M_n = 2{,}000$, $Đ = 1.04$) as a macroinitiator, a PEG-*b*-PLLA with a very narrow $Đ$ value of 1.03 was successfully obtained in one-pot (run 16 in Table 4.3). The ^{1}H NMR and SEC analyses clearly demonstrated that a PLLA chain was grown from the PEG macroinitiator (Figure 4.9). These demonstrations suggested that the present ROP system is suitable for a wide range of applications to produce not only regular PLLAs, but also other advanced PLLA materials.

Scheme 4.3. Syntheses of end-functionalized PLLA using functional alcohol initiator

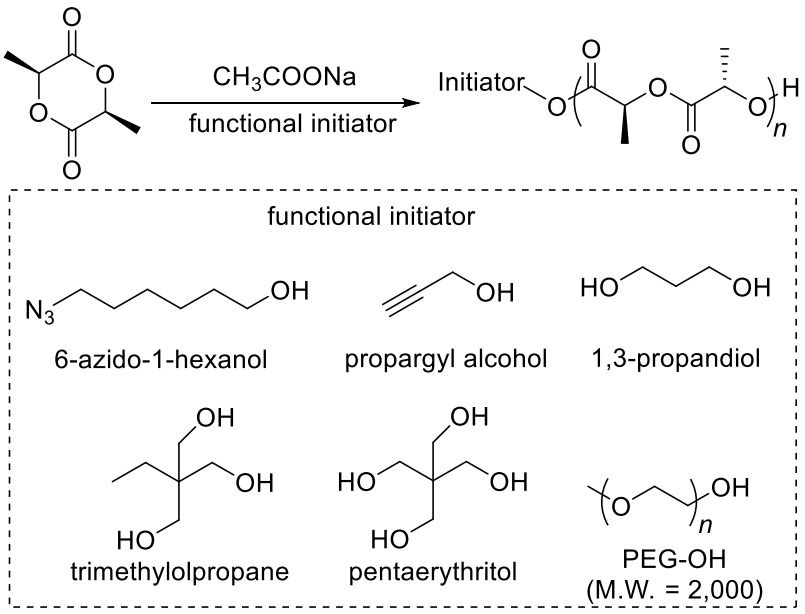

Table 4.3. Ring-opening polymerization of L-LA using functional initiators[a]

run	initiator	time (h)	conv. (%) [b]	$M_{n,th.}$ [c]	$M_{n,NMR}$ [b]	$M_{n,SEC}$ [d]	$Đ$ [d]
10	6-azido-1-hexanol	22	72.7	5,400	5,300	8,600	1.06
11	propargyl alcohol	22	73.6	5,400	4,500	7,500	1.05
12	1,3-propanediol	12	83.5	6,200	6,500	9,600	1.06
13	trimethylol propane	8	83.0	6,100	5,900	9,400	1.04
14	pentaerythritol	6	76.3	5,600	5,600	9,900	1.05
15 [e]	pentaerythritol	96	68.9	99,400	85,400	87,600	1.08 [f]
16	polyethylene glycol	22	84.8	8,100	9,100	9,700	1.08

[a] Polymerization conditions: [L-LA]/[ini.]/[cat.] = 50/1/0.5; temp., 100 ˚C; atmosphere, Ar; cat., CH_3COONa. [b] Determined by ^1H NMR in $CDCl_3$. [c] Calculated from ($[L\text{-LA}]_0/[ini.]_0$) × conv. × (M.W. of L-LA) + (M.W. of ini.). [d] Determined by SEC measurement of the obtained polymer in THF using polystylene standard. [e] Polymerization was conducted at [L-LA]/[ini.] = 800/1. [f] After purification by using preparative SEC to elucidate low molecular weight oligomer.

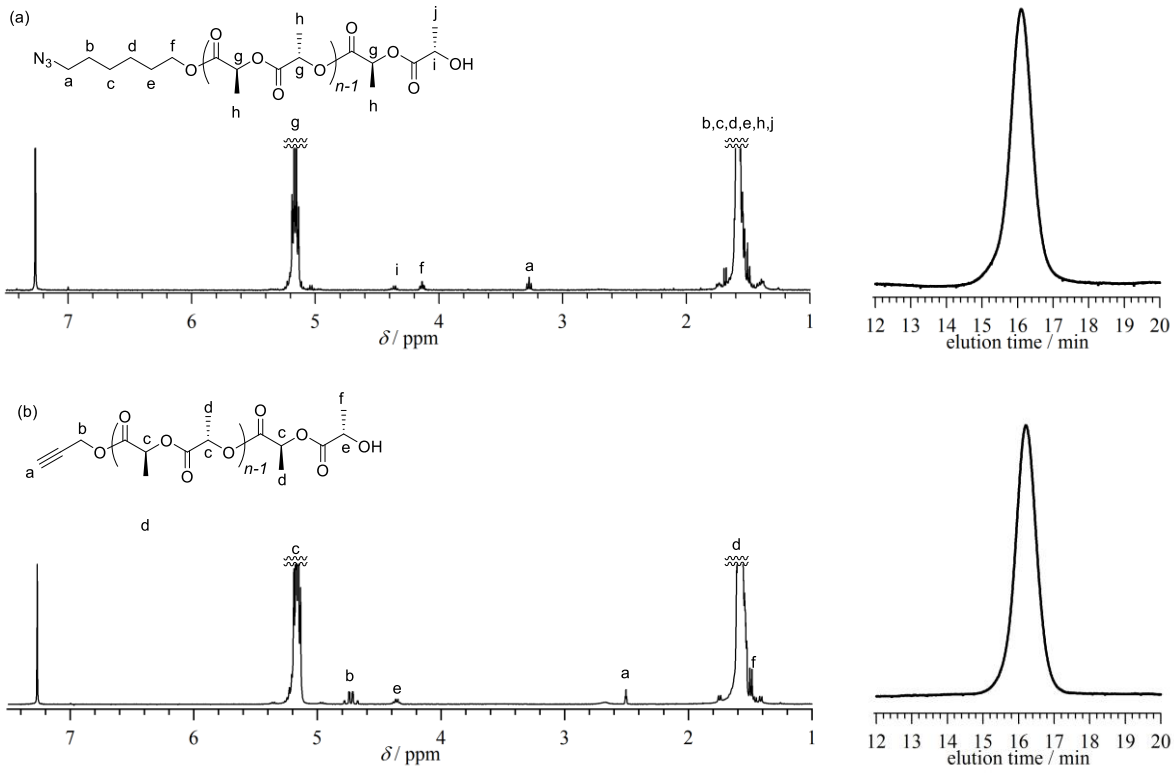

Figure 4.7. ^{1}H NMR spectra (in $CDCl_3$) and SEC traces (eluent, THF; flow rate, 1 mL min^{-1}) of the PLLA initiated from (a) 6-azido-1-hexanol and (b) propargyl alcohol.

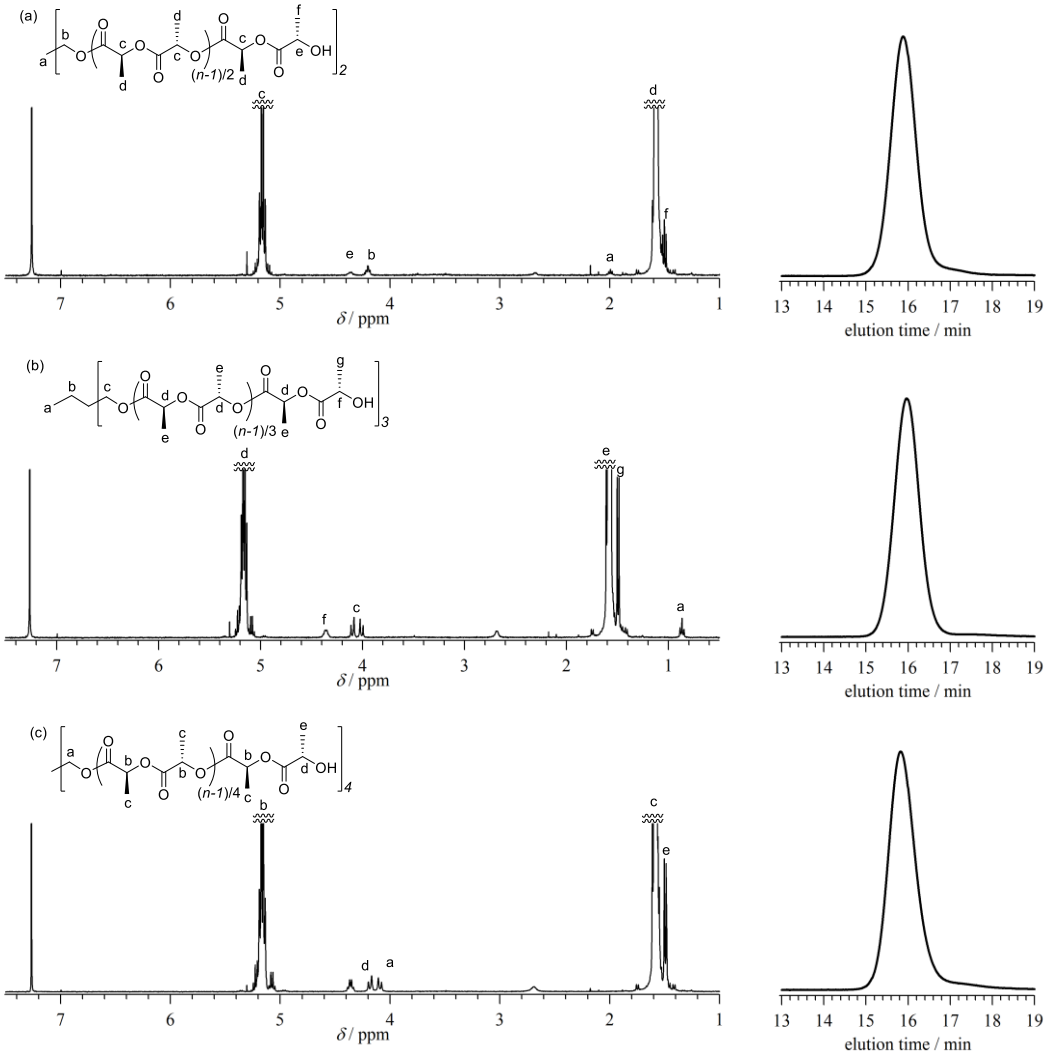

Figure 4.8. ^{1}H NMR spectra (in $CDCl_3$) and SEC traces (eluent, THF; flow rate, 1 mL min^{-1}) of the PLLA initiated from (a) 1,3-propanediol, (b) trimethylol propane, and (c) pentaerythritol.

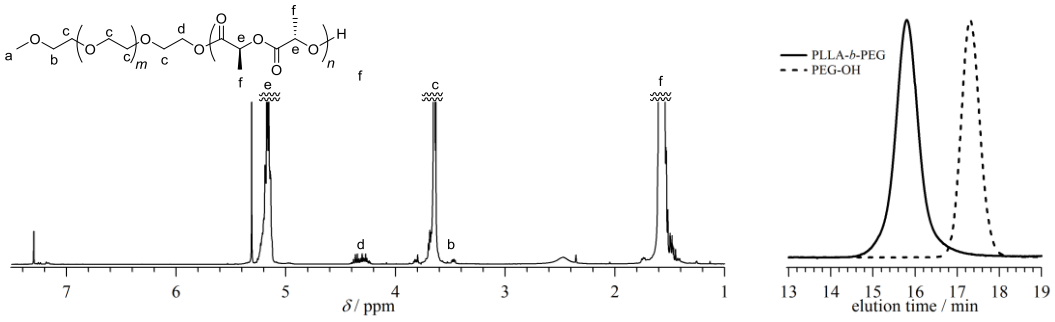

Figure 4.9. ^{1}H NMR spectrum of the obtained PEG-*b*-PLLA in $CDCl_3$ and SEC traces of PEG-OH and the obtained PEG-*b*-PLLA (eluent, THF; flow rate, 1 mL min^{-1}).

4.2.3 Tunable Nature of Alkali Metal Carboxylates for Controlling the ROP of L-LA

The author next examined the catalytic ability of a series of alkali metal carboxylates to correlate their structures with the catalytic performance (Table 4.4). The author first focused on sodium benzoate and potassium sorbate, which are also used as food additives. [25] The ROPs were conducted in the bulk at 100 °C with an $[\text{L-LA}]_0/[\text{PPA}]_0/[\text{cat.}]$ ratio of 50/1/0.5 to give PLLAs in a controlled manner (runs 17 and 18 in Table 4.4), which implied the unrevealed potential of alkali metal carboxylates to optimize the catalytic ability by the appropriate design of the catalyst structure. To gain insight into the effect of the catalyst design, the author next examined acetates with various countercations, such as Li, K, and Cs (runs 19-21 in Table 4.4). Although all the studied acetates promoted the ROP of L-LA in a controlled manner, the turnover frequency (TOF) value increased with the increasing cation size of the catalyst (Figure 4.10). For example, cesium acetate (pK_b = 6.04) exhibited the highest TOF value of 73.6 h^{-1}, while the lithium salt (pK_b = 6.87) had the lowest TOF value of 1.8 h^{-1}, implying that the polymerization rate depends on the pK_b value of the catalyst.[26] The effect of the alkyl substituent on the carboxylate moiety was also investigated using a series of sodium salts of acetate, propionate, pivalate, and trifluoroacetate (runs 22-25 in Table 4.4, acetic acid; pK_a = 4.76, propionic acid; pK_a = 4.87, pivalic acid; pK_a = 5.05, trifluoro acetic acid; pK_a = -0.26).[27] It was obvious that an electron-donating group on the alkyl moiety enhanced the catalytic activity, while an electron-withdrawing group reduced it. When sodium pivalate was used as the catalyst, the ROP reached an 87.6% conversion in 6 h, which was about four times faster than in the case of sodium acetate. This suggests that the polymerization properties could be easily tuned based on the choice of the alkyl group and counter cation of the catalyst. Based on these results, it can be reasonably expected that cesium pivalate should display a very high catalytic performance. Indeed, the ROP catalyzed by cesium pivalate reached a 74.2% monomer conversion in only 15 min, though tailing was observed in the SEC trace for the resulting PLLA, which was likely

due to backbiting caused by the exceedingly high catalytic activity. On the other hand, the ROP using sodium trifluoroacetate did not proceed, which again implied that basicity plays an important role in the present ROP system.

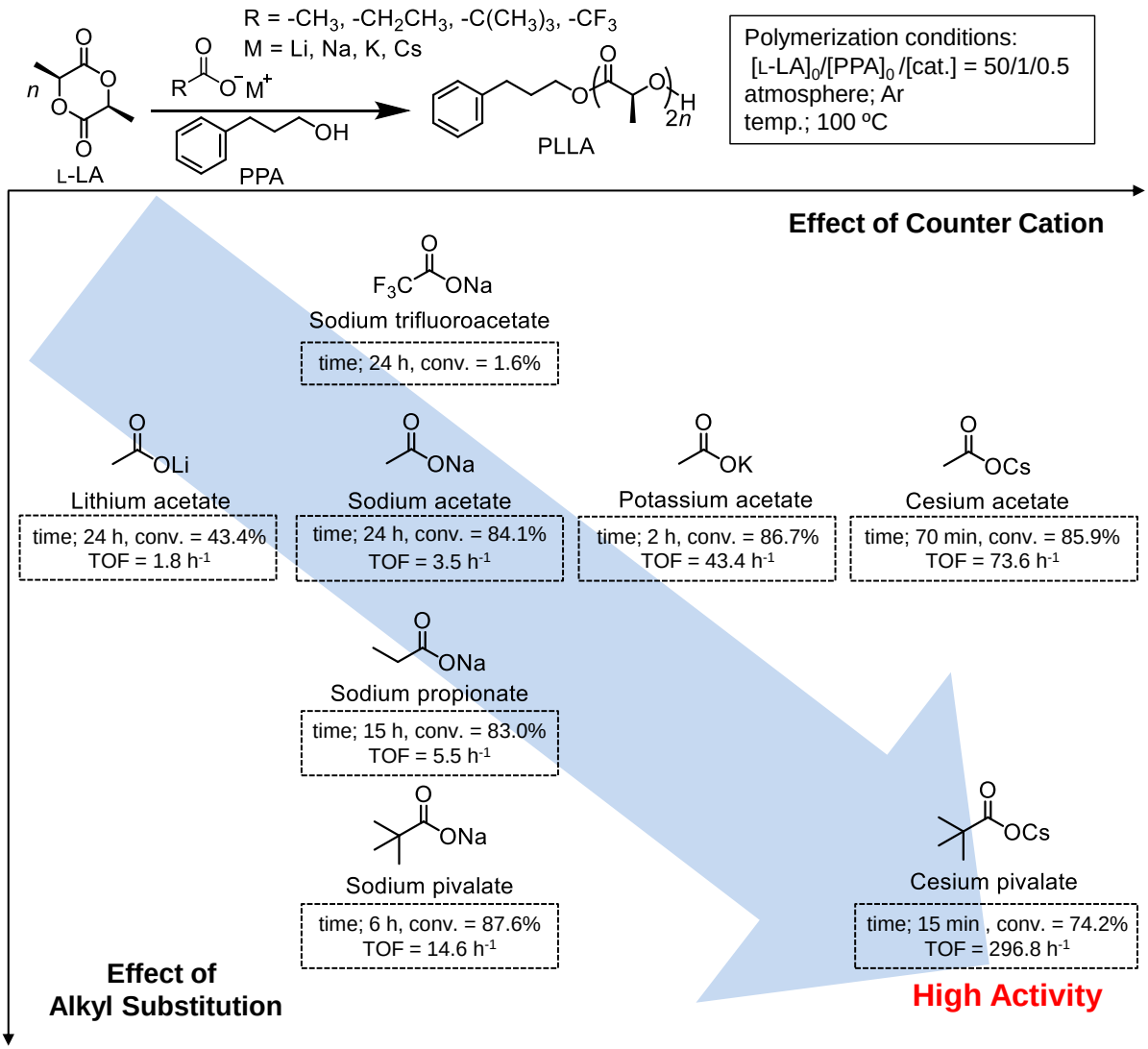

Figure 4.10. Catalytic performance of alkali metal carboxylate for the ROP of L-LA

Table 4.4. Ring-opening polymerization of L-LA using alkali metal carboxylates [a]

run	**R** [b]	**M** [b]	time (h)	conv. (%) [c]	$M_{n,th.}$ [d]	$M_{n,NMR}$ [c]	$M_{n,SEC}$ [e]	$Đ$ [e]	TOF (h^{-1})
17	C_6H_5	Na	44	71.1	5,300	5,000	8,100	1.07	1.4
18	C_5H_7 [f]	K	17	86.0	6,300	6,000	8,200	1.12	5.1
19	CH_3	Li	24	43.4	3,300	3,400	6,800	1.07	1.8
20	CH_3	K	2	86.7	6,400	6,800	9,400	1.10	43.4
21	CH_3	Cs	1.2	85.9	6,300	6,500	8,600	1.08	73.6
22	C_2H_5	Na	15	83.0	6,100	6,000	9,700	1.07	5.5
23	$(CH_3)_3C$	Na	6	87.6	6,500	6,300	9,800	1.09	14.6
24	$(CH_3)_3C$	Cs	0.25	74.2	5,500	5,400	7,000	1.19	296.8
25	CF_3	Na	24	1.6	n.d. [g]	n.d. [g]	n.d. [g]	n.d. [g]	n.d. [g]

[a] Polymerization conditions: $[\text{L-LA}]_0/[\text{PPA}]_0/[\text{cat.}] = 50/0.5$; Ar atmosphere; temp., 100 ºC; PPA as initiator. [b] **R** and **M** indicate the alkyl moiety and counter cation of the alkali metal carboxylate, respectively. [c] Determined by ^{1}H NMR in $CDCl_3$. [d] Calculated from ($[\text{L-LA}]_0/[\text{PPA}]_0$) × conv. × (M.W. of L-LA) + (M.W. of PPA). [e] Determined by SEC measurement of the obtained polymer in THF. [f] C_5H_7 indicates sorbate. [g] Not determined.

4.2.4 Scope of the Alkali Metal Carboxylate-catalyzed Ring-opening Polymerization

The author next turned our attention to the scope and limitations of the alkali metal carboxylate-catalyzed ROP system. Initially, the author conducted the ROP of the racemic DL-lactide (DL-LA) using sodium acetate as a catalyst (run 26 in Table 4.5). In this case, a portion of the toluene was added to the polymerization mixture (DL-LA/toluene = 50 mmol/1 mL) because the melting point of DL-LA is higher than that of L-LA. The ROP of DL-LA proceeded to reach a 91.2% monomer conversion within 22 h, affording a poly(DL-lactide) (PDLLA) with an expected molecular weight and narrow $Đ$ value (Figure 4.11). From the homonuclear decoupled ^{1}H NMR measurement, the probability of isotactic enchainment (P_i) of the resulting PDLLA was determined to be 0.57, implying that the ROP proceeded with no selectivity toward either an isotactic or syndiotactic stereosequence (Figure 4.11(b)). In addition, the one-pot synthesis of a PLLA-*b*-PDLLA-*b*-PLLA triblock copolymer was achieved by the polymerization of DL-LA using 1,3-propanediol as an initiator followed by the chain extension through the second polymerization of L-LA (Scheme 4.4 and Figure 4.12). The success of the sequential block copolymerization suggested that the propagating chain end is indeed living even at the last stage of the ROP, which is highly beneficial for the functional block copolymer synthesis.

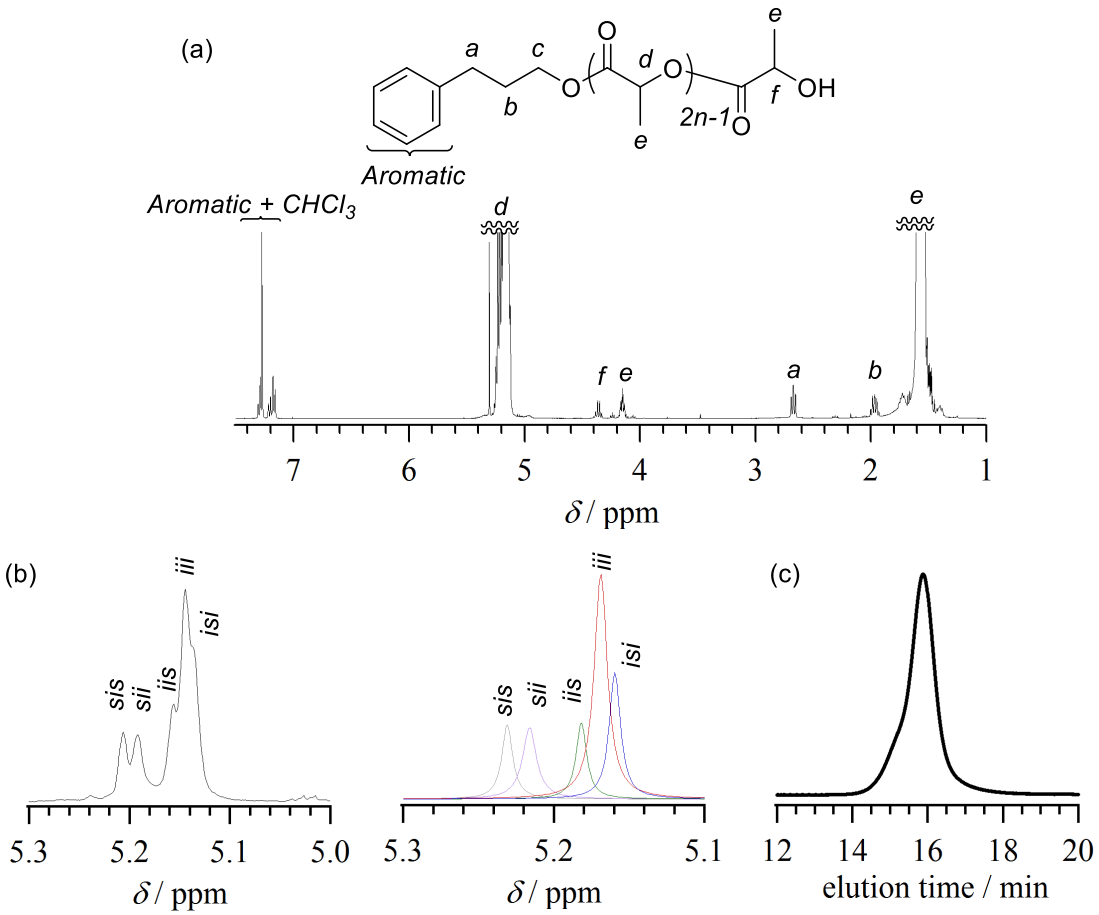

Figure 4.11. (a) ^{1}H NMR spectrum of the obtained PDLLA, (b) the spectrum of methine resonances with selective decoupling of PLA methyl resonances and the spectrum after wave separation for calculation of each tetrad area. Peak area: *sis*, 13.0%; *sii*, 12.4%; *iis*, 13.4%; *iii*, 39.1%; *isi*, 22.0% (in $CDCl_3$, 400 MHz). (c) the SEC trace of the obtained PDLLA (eluent, THF; flow rate, 1 mL min^{-1}).

Scheme 4.4 One-pot synthesis of PLLA-*b*-PDLLA-*b*-PLLA triblock copolymer

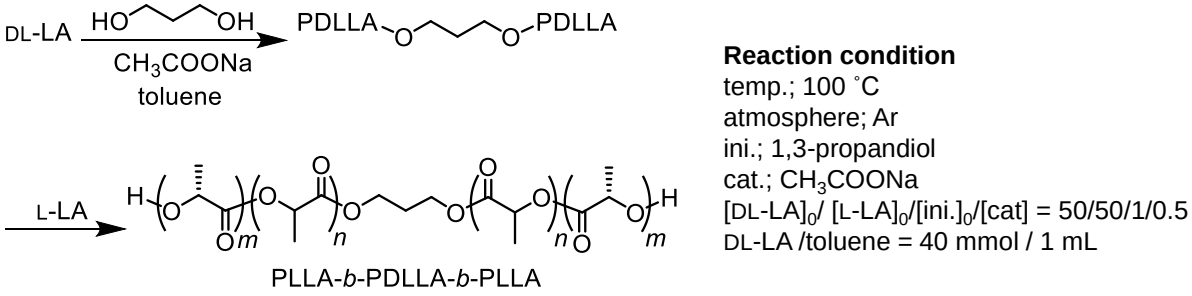

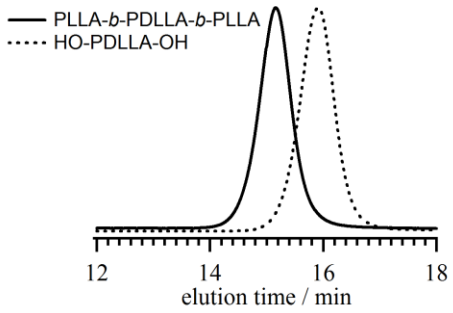

1st polymerization of DL-LA
time; 21h
conv.; 85.1%
$M_{n,th.}$ = 6,270
$M_{n,NMR}$ = 6,160
$M_{n,SEC}$ = 9,190
$Đ$ = 1.06

2nd polymerization of L-LA
time; 24h
conv.; 70.4%
$M_{n,th.}$ = 11,3400
$M_{n,NMR}$ = 10,500
$M_{n,SEC}$ = 15,400
$Đ$ = 1.06

Figure 4.12. SEC traces of PDLLA obtained from the 1st polymerization and PLLA-*b*-PDLLA-*b*-PLLA (eluent, THF; flow rate, 1.0 mL min^{-1}) and synthetic result of PLLA-*b*-PDLLA-*b*-PLLA.

Furthermore, other cyclic monomers including trimethylene carbonate (TMC), *ε*-caprolactone (CL), and *δ*-valerolactone (VL), were applied to the present catalyst system (runs 27-30 in Table 4.5). The ROP of TMC using sodium acetate coupled with PPA as the initiator smoothly proceeded and reached a 90.2% monomer conversion in 25 min to give poly(trimethylene carbonate) (PTMC) (run 27 in Table 4.5), while the ROP of CL did not proceed at 100 °C even after 96 h (run 28 in Table 4.5). Although the SEC trace of the obtained PTMC exhibited a shoulder peak, the $M_{n,NMR}$ value was very close to the $M_{n,th.}$ as shown in Figure 4.13(a). Importantly, no evidence of decarboxylation was observed in the ^{1}H NMR spectrum of the obtained PTMC. The absence of such a side reaction can be attributed to the mildly basic character of the catalyst. Interestingly, the ROPs of CL and VL successfully proceeded using sodium trifluoroacetate to give poly(*ε*-caprolactone) (PCL) and poly(*δ*-valerolactone) (PVL), respectively (runs 29 and 30 in Table 4.5 and Figures 4.13(b) and (c)), with narrow *Đ*s, whereas this catalyst did not promote the ROP of L-LA at all. This strongly suggests that the appropriate catalyst design can expand the applicable monomer scope. It should be emphasized that the ^{1}H NMR spectra of the obtained PTMC, PCL, and PVL confirmed that the resulting polymers contained the 3-phenyl-1-propoxy residue at the *α*-chain

end (Figure 4.13), which again confirmed that the alkali metal carboxylates acted as catalysts and not as initiators.

Table 4.5. Ring-opening polymerization of cyclic esters using alkali metal carboxylates [a]

run	monomer	cat.	temp. (°C)	time (h)	conv. (%) [b]	$M_{n,th.}$ [c]	$M_{n,NMR}$ [b]	$M_{n,SEC}$ [d]	$Đ$ [d]
26	DL-LA [e]	CH_3COONa	100	22	91.2	6,700	7,500	9,600	1.13
27	TMC	CH_3COONa	80	0.4	90.2	4,700	4,700	7,200	1.27
28	CL [f]	CH_3COONa	100	96	2.6	n.d.[g]	n.d.[g]	n.d.[g]	n.d.[g]
29	CL [f]	CF_3COONa	100	72	72.3	5,000	4,700	8,200	1.12
30	VL [f]	CF_3COONa	100	240	77.3	4,000	3,700	6,700	1.07

[a] Polymerization conditions: Ar atmosphere; PPA as initiator; $[monomer]_0/[PPA]_0/[cat.]_0$ = 50/1/0.5. [b] Determined by ^1H NMR in $CDCl_3$. [c] Calculated from $([monomer]_0/[PPA]_0) \times$ conv. × (M.W. of monomer) + (M.W. of PPA). [d] Determined by SEC measurement of the obtained polymer in THF. [e] DL-LA/toluene = 40 mmol/1 mL. [f] $[monomer]_0/[PPA]_0/[cat.]_0$ = 50/1/3.0. [g] Not determined.

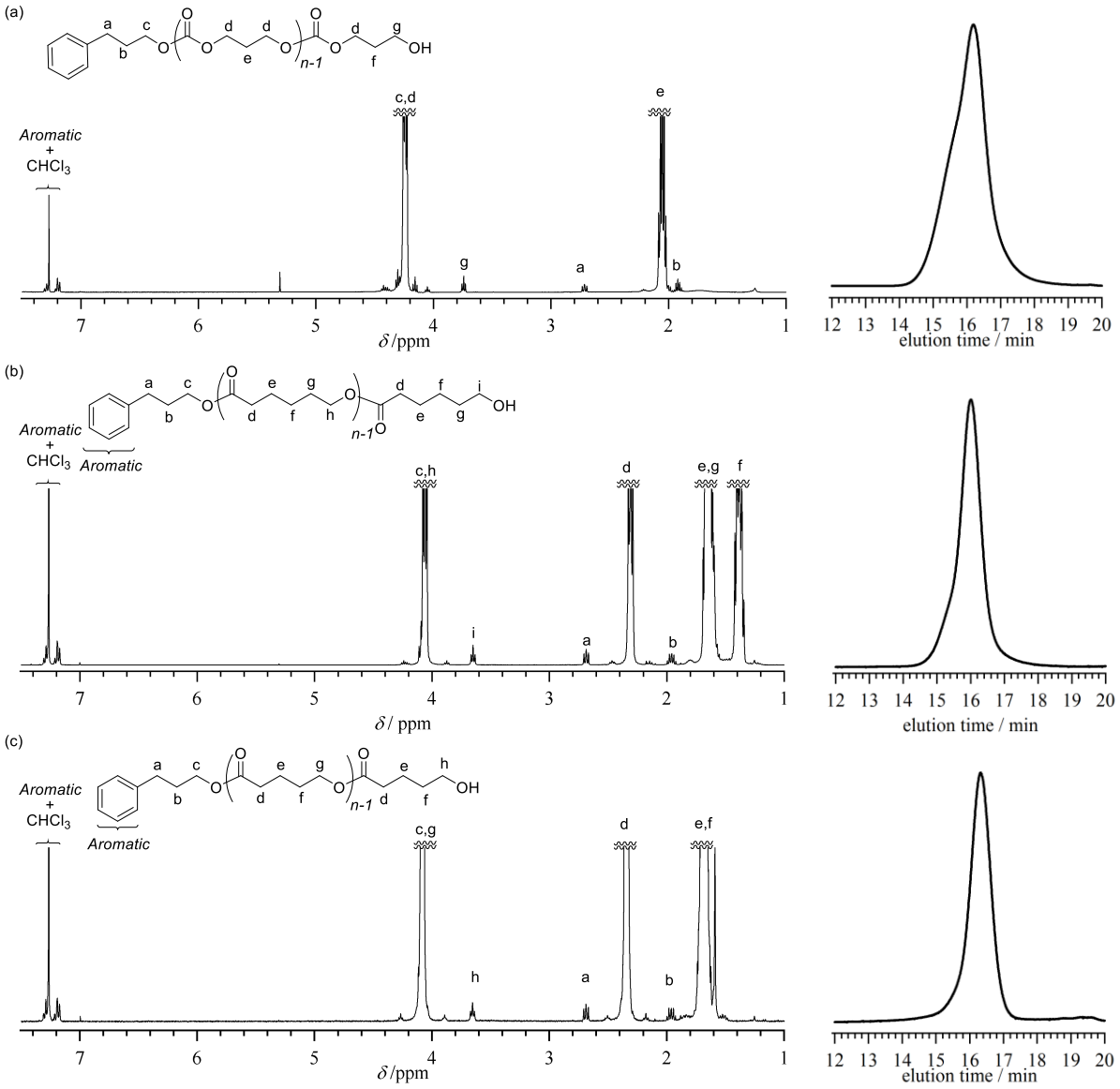

Figure 4.13. ^{1}H NMR spectra (in $CDCl_3$) and SEC traces (eluent, THF; flow rate, 1 mL min^{-1}) of the obtained (a) PTMC, (b) PCL, and (c) PVL (runs 27, 29 and 30 in Table 4.5).

4.2.5 Mechanistic Insight of the Alkali Metal Carboxylate-catalyzed Ring-opening Polymerization

To gain a mechanistic insight into the present catalyst system, FT-IR measurements were carried out on methyl L-lactate as a model compound of the PLLA propagating chain end in the presence/absence of alkali-metal carboxylates (Figure 4.14(a)). The FT-IR spectrum of the methyl L-lactate with an equimolar amount of sodium acetate displayed a broad absorption peak due to the OH stretching vibration of methyl L-lactate around 3200 cm^{-1}, while this peak appeared at ~3500 cm^{-1} in the absence of sodium acetate. This shift implied that sodium acetate efficiently activates the hydroxyl group of the propagating chain end/initiator. In addition, the peak shift became clearer as the catalytic activity increased by varying both the counter cation and the alkyl moiety, and only a slight shift was observed in the presence of sodium trifluoroacetate. The FT-IR measurements of L-LA in the presence/absence of sodium acetate also showed a slight shift in the absorption peak due to the C=O stretching vibration of L-LA to the lower wavenumber region (Figure 4.14(b)), implying an interaction between the L-LA and alkali metal carboxylates. Therefore, the author concluded that alkali metal carboxylates catalyzed the ROP via a bi-activation mechanism (Figure 4.14(c)),[28] in which the capability of activating the propagating chain end and monomer can be finely tuned by the choice of the alkyl chain and counter cation of the catalyst.

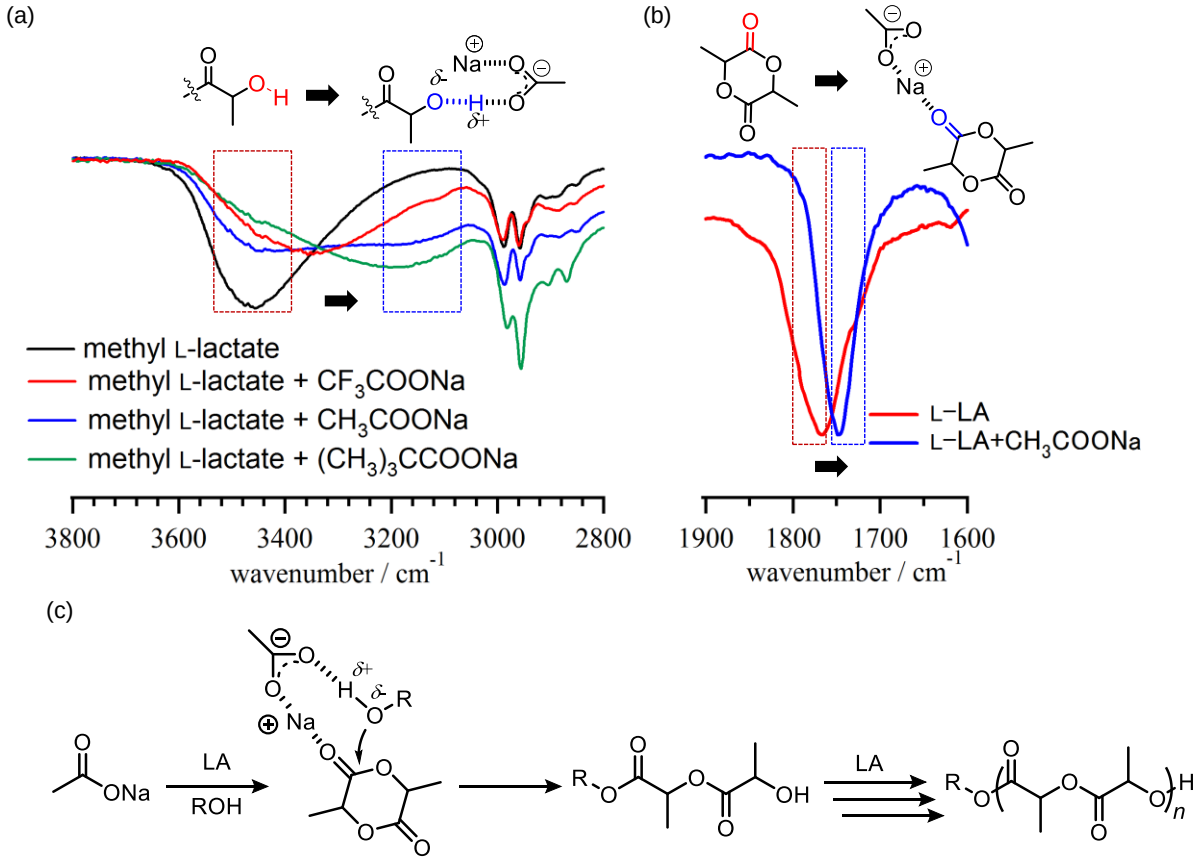

Figure 4.14. (a) FT-IR spectra of methyl L-lactate (black line) and 1:1 mixtures of methyl L-lactate + CF_3COONa (red line), methyl L-lactate + CH_3COONa (blue line), and methyl L-lactate + $(CH_3)_3CCOONa$ (green line) at room temperature (normalized at the C=O stretching vibration of methyl L-lactate). (b) FT-IR spectra of L-LA (red line) and 1:1 mixtures of L-LA + CH_3COONa (blue line) at 100 °C. (c) Proposed polymerization mechanism.

4.3. Conclusions

In this chapter, the author demonstrated the potential of alkali metal carboxylates as an environmentally-benign, biocompatible, and inexpensive catalyst system for the well-controlled ROP of cyclic esters. These small and simple molecules exhibited excellent performance, comparable to those of the metal-based catalysts and organocatalysts, to produce well-defined PLLA, PTMC, PCL and PVL with predictive molecular weights, narrow *Đ*s, and desired chain end structures. To the best of knowledge, this is the first report of the alkali-metal carboxylate-catalyzed ROP system of cyclic esters, in which alcohols act as the initiator. The present polymerization system is completely different in terms of the role of the carboxylate as well as the polymerization mechanism from the conventional ROP of *β*-lactone in which the alkali-metal carboxylate works as the initiator. This study defines a new paradigm for both the laboratory and industrial scale productions of valuable APEs for conventional use and future biomedical and environmental applications.

4.4 Experimental Section

Materials. L-Lactide (L-LA; >98%, Tokyo Kasei Kogyo Co., Ltd. (TCI)) and DL-lactide (DL-LA; >98%, Musashino Chemical Co., Ltd.) were purified by recrystallization from dry toluene. Trimethylene carbonate (TMC; >98%, TCI) was dried by azeotropic distillation. Sodium acetate (>99%, Sigma Aldrich), sodium benzoic acid (99.5%, Nacalai Tesque), sodium sorbate (>98.0%, TCI), potassium sorbate (>99.0%, TCI), sodium trifluoroacetate (>98.0%, TCI), sodium propionate (>98.0%, TCI), sodium hexanoate (>99.0%, TCI), sodium pivalate hydrate (>98.0%, TCI), lithium acetate (>98.0%, TCI), potassium acetate (>99.0%, Sigma Aldrich), cesium acetate (>98.0%, TCI), and cesium pivalate (>97.0%, TCI) were dried by heating at 100 °C under high vacuum for at least 72 h prior to use. ε-Caprolactone (CL; >99%, TCI), δ-valerolactone (VL; >99%, Sigma Aldrich), 3-phenyl-1-propanol (PPA; >98%, TCI), 1,3-propanediol (>98%, TCI), and propargyl alcohol (PGA; >99%, Sigma Aldrich) were distilled over CaH_2 under reduced pressure. Poly(ethylene glycol) monomethyl ether (PEG-OH; typical M_n = 2,000, $M_{n,SEC}$ = 3,380, $Đ$ =1.04, Sigma Aldrich) was dried by azeotropic distillation in benzene. Methyl L-lactate (>98%, TCI), trimethylolpropane (>98%, TCI), and pentaerythritol (>98%, TCI) were used as received. 6-Azide-1-hexanol (AHA) was synthesized according to a previous report and distilled over CaH_2 under reduced pressure. [29]

Instruments. The polymerization was carried out in an MBRAUN stainless steel glove box equipped with a gas purification system (molecular sieves and copper catalyst) in a dry argon atmosphere (H_2O, O_2 < 1 ppm). The moisture and oxygen contents in the glove box were monitored by an MB-MO-SE 1 and MB-OX-SE 1, respectively. The ^1H NMR spectra were obtained by a JEOL JNM-A400II instrument (400 MHz). The size exclusion chromatography (SEC) was performed at 40 °C in THF (1.0 mL min^{-1}) using a Shodex GPC-101 system equipped with a Shodex K-G guard column and a set of two Shodex K-805L columns (linear,

8 mm × 300 mm; bead size, 5 μm; exclusion limit, 4 × 106). The estimation of the molecular weight ($M_{n,SEC}$) and dispersity ($Đ$) of the polymers were based on the polystyrene standard curve ranging from 1,200 to 1,320,000. Matrix-assisted laser desorption ionization time-of-flight mass spectrometry (MALDI-TOF MS) of the polymers was performed using an Applied Biosystems ABSCIEX MALDI TOF/TOF 5800 in the reflector mode. The MALDI-TOF MS sample was prepared by depositing a mixture of the polymer (4.0 mg mL^{-1}, 0.5 μL) and a matrix (2,5-dihydroxybenzoic acid, 60 mg mL^{-1}, 0.5 μL) in THF on a sample plate that was coated by an acetone solution (1.0 mmol L^{-1}, 1.0 μL) of NaI as the cationic agent. Fourier transform infrared spectroscopy (FT-IR) analysis was carried out using a Perkin Elmer Frontier MIR spectrometer equipped with a single reflection diamond universal attenuated total reflection (ATR) accessory. The FT-IR experiments at elevated temperature were carried out in the transmission mode using a Perkin Elmer Frontier MIR spectrometer equipped with a Mettler Toledo HS82 hot stage system.

Typical procedure for ring-opening polymerization of L-LA using sodium acetate as the catalyst.

Typical procedure of the ROP of L-LA is as follows: In an argon-filled glove box, L-LA (580 mg, 4.00 mmol), sodium acetate (3.3 mg, 40.0 μmol), and PPA (10.9 μL, 80.0 μmol) were placed in a reaction vessel. The reaction mixture was stirred at 100 °C under an argon atmosphere in an oil bath. After 22 h, the polymerization was terminated by diluting the reaction mixture with CH_2Cl_2. The reaction mixture was purified by reprecipitation from a CH_2Cl_2 solution into cold methanol/*n*-hexane (v/v = 9/1) to give PLLA (320 mg) as a white powder. Yield: 66.0%. $M_{n,NMR}$ = 6,150; $M_{n,SEC}$ = 9,820; $Đ$ = 1.07. ^{1}H NMR ($CDCl_3$, 400 MHz): δ (ppm) 1.48, (m, 3H, -CH(CH_3)OH), 1.57, (m, 3H × *n*, (CH_3)$_{n-1}$), 1.95 (q, 2H, *J* = 7.2 Hz, ArCH$_2$CH_2-),

2.66(t, 2H, *J* = 7.6 Hz, ArC*H*$_2$-), 4.14 (m, 2H, ArCH$_2$CH$_2$C*H*$_2$-), 4.34 (q, 1H, *J* = 6.8 Hz, -C*H*(CH$_3$)OH), 5.10-5.25 (m, 1H × (*n*-1), (-C*H*(CH$_3$)O-)$_{n-1}$), 7.14-7.29 (m, 5H, *aromatic*)

4.5 References

1. Chen, X.; Engle, K. M.; Wang, D.-H.; Yu, J.-Q. *Angew. Chem. Int. Ed.* **2009**, *48*, 5094−5115.
2. Trnka, T. M.; Grubbs, R. H. *ACC. Chem. Rev.* **2001**, *34*, 18−29.
3. Doyle, A. G.; Jacobsen, E. N. *Chem. Rev.* **2007**, *107*, 5713−5743.
4. Braunecker, W. A.; Matyjaszewski, K. *Prog. Polym. Sci.* **2007**, *32*, 93−146.
5. Ouchi, M.; Terashima, T.; Sawamoto, M. *Chem. Rev.* **2009**, *109*, 4963−5050.
6. Nederberg, F.; Connor, E. F.; Möller, M.; Glauser, T.; Hedrick, J. L. *Angew. Chem. Int. Ed.* **2001**, *40*, 2712−2715.
7. Kamber, N. E.; Jeong, W.; Waymouth, R. M. Pratt, R. C.; Lohemeijer B. G. G.; Hedrick, J. L. *Chem. Rev.* **2007**, *107*, 5813−5840.
8. Kiesewetter, M. K. Shin, E. J.; Hedrick, J. L.; Waymouth, R. M. *Macromolecules* **2010**, *43*, 2093−2107.
9. Ottou, W. N.; Sardon, H.; Mecerreyes, D.; Vignolle, J.; Taton, D. *Prog. Polym. Sci*. **2016**, *56*, 64−115.
10. Shibasaki, Y.; Sanada, H.; Yokoi, M.; Sanda, F.; Endo, T. *Macromolecules* **2000**, *33*, 4316−4320.
11. Gazeau-Bureau, S.; Delcroix, D.; Martín-Vaca, B.; Bourissou, D.; Navarro, C.; Magnet, S. *Macromolecules* **2008**, *41*, 3782−3784.
12. Bourissou, D.; Martin-Vaca, B.; Dumitrescu, A.; Graullier, M.; Lacombe, F. *Macromolecules* **2005**, *38*, 9993–9998.
13. Makiguchi, K.; Satoh, T.; Kakuchi, T. *Macromolecules* **2011**, *44*, 1999−2005.
14. Xu, J.; Song, J.; Pispas, S.; Zhang, G. *Polym. Chem.* **2014**, *5*, 4726−4733.
15. Lohmeijer, B. G. G.; Pratt, R. C.; Leibfarth, F.; Logan, J. W.; Long, D. A.; Dove, A. P.; Nederberg, F.; Choi, J.; Wade, C.; Waymouth, R. M.; Hedrick, J. L. *Macromolecules* **2006**, *39*, 8574−8583.
16. Myers, M.; Connor, E. F.; Glauser, T.; Mock, A.; Nyce, G.; Hedrick, J. L. *J. Polym. Sci., Part A: Polym. Chem.* **2002**, *40*, 844−851.
17. Zhang, L.; Nederberg, F.; Pratt, R. C.; Waymouth, R. M.; Hedrick, J. L.; Wade, C. G. *Macromolecules* **2007**, *40*, 4154−4158.
18. Dove, A. P.; Pratt, R. C.; Lohmeijer, B. G. G.; Waymouth, R. M.; Hedrick, J. L. *J. Am. Chem. Soc.* **2005**, *127*, 13798−13799.
19. Miyake, G. M.; Chen, E. Y.-X. *Macromolecules* **2011**, *44*, 4116−4124.

20. Zhang, X.; Jones, G. O.; Hedrick, J. L.; Waymouth, R. M. *Nat. Chem.* **2016**, *8*, 1047−1053.
21. Lin B.; Waymouth, R. M. *J. Am. Chem. Soc.* **2017**, *139*, 1645−1652.
22. Coulembier, O.; Dubois P. In Handbook of Ring-Opening Polymerization, Dubois, P.; Coulembier, O.; Raquez, J.-M. Wiley-VCH, 2009, p. 232.
23. Juzwa, M.; Jedlinski, Z. *Macromolecules* **2006**, *39*, 4627−4630.
24. Liu, K. L.; Goh S. H.; Li, J. C *Polymer* **2008**, *49*, 732−741.
25. Zor, S. D.; Asci, B.; Donmez, O. A.; Kucukkaraca, D. Y. *J. Chromatogr. Sci.* **2016**, *54*, 952–957.
26. Tang, C. M.; McLean, J. A. *Inorg. Chem.* **1981**, *20*, 2652−2655.
27. Zeng, Y.; Chen, X.; Zhao, D.; Li, H.; Zhang, Y.; Xiao, X. *Fluid Ph. Equilibria* **2012**, *313*, 148−155.
28. Makiguchi, K.; Yamanaka, T.; Kakuchi, T.; Terada, M.: Satoh, T. *Chem. Commun.* **2014**, *50*. 2883−2885.
29. Speers, A. E.; Adam, G. C.; Cravatt, B. F. *J. Am. Chem. Soc.* **2003**, *125*, 4686–4687.

Chapter 5

Conclusions

In this thesis, the author described the environmentally-benign and practical synthesis of biodegradable and biocompatible aliphatic polyesters (APEs) and aliphatic polycarbonates (APCs) via a ring-opening polymerization (ROP) using organophosphates, trimethyl glycine, and alkali metal carboxylates as the catalysts. In chapter 2, the author established a facile, versatile, and environmentally-benign ROP process by applying the bulk polymerization condition to the conventional organophosphate-catalyzed ROP. Significant advantages of the bulk ROP condition regarding the amount of the loaded catalyst and solvent, reaction time, and wide scope of application were revealed, which are suitable for both the laboratory- and industry-scale APE productions. In chapters 3 and 4, the author tried to develop novel ROP catalysts from inexpensive, readily available, and non-toxic compounds. In chapter 3, naturally-occurring trimethyl glycine was demonstrated to be an efficient catalyst for the ROP of a cyclic carbonate leading to the well-defined APC. In chapter 4, the author established an alkali-metal carboxylate catalytic system as an innovative ROP system substituting for conventional procedures using metal-based catalysts as well as organocatalysts. Sodium acetate, a representative alkali metal carboxylate used as a food additive, showed a good catalytic ability for the ROP of L-lactide and trimethylene carbonate. It should be again noted that the ROP system described in this thesis can be operated without using toxic compounds as well as an organic solvent to achieve well-defined APE and APC syntheses. Furthermore, the ROP systems established in this thesis cover a wide scope of applications, such as block copolymer synthesis, end functionalized polymer synthesis as well as multi-hydroxylated polymer synthesis. These are great advantages for both the laboratory- and industry-scale production for conventional uses as well as advanced applications. Therefore, the author surely established versatile, practical, and environmentally-benign ROP systems beyond conventional systems using metal-based catalysts as well as organocatalysts.

A summary of this thesis is as follows:

In chapter 2, the organophosphate-catalyzed bulk ROP system was established as an environmentally-benign and practical synthesis method to give APEs, APCs, and aliphatic polyester-ether possessing controlled molecular weights and narrow dispersities. The polymerization proceeded in a controlled manner even under harsh bulk conditions to achieve well-defined polymer syntheses. The bulk condition overcame the difficulty of the conventional solution polymerization procedure, such as reduced catalyst loading and drastic reduction of reaction time. Furthermore, the author found the advantages of the bulk condition, which provide a wider scope of applications for the present bulk ROP system. Taking the advantage of the bulk conditions, poly(ε-caprolactone)s (PCLs) possessing multi-hydroxyl groups were easily obtained, which enable the one-pot synthesis of the PCL-based polyurethane.

In chapter 3, the author determined the catalytic ability of trimethyl glycine, a zwitterionic compound existing in plants as well as in humans, for the ROP of cyclic carbonates. The ROP of trimethylene carbonate (TMC) proceeded under a controlled manner using trimethyl glycine in the bulk to give the well-defined poly(trimethylene carbonate) (PTMC). The controlled/living nature of the present ROP system was confirmed by the chain extension experiment. The bi-activation property of trimethyl glycine was revealed by FT-IR measurement of TMC and alcohol initiator in the presence/absence of timethyl glycine. Furthermore, the syntheses of APC-diol and -triol, which are industrially important materials for the APC-based polyurethane, were successfully demonstrated by using functional initiators.

In chapter 4, the author established the alkali metal carboxylate-catalyzed ROP system of cyclic esters as an unprecedented catalytic system substituting for conventional procedures using metal-based catalysts and organocatalysts. This synthetic system was shown to be effective for the polymerization of a variety of cyclic monomers to produce the corresponding polymer with predictable molecular weights and narrow dispersities. Moreover, the catalytic ability was found to be tunable by modifying both the alkyl moiety and the counter cation of the catalyst, which allowed not only control of the polymerization behavior, but also to expand the scope of the applicable monomers. Alkali metal carboxylates catalyzed the ROP via a bi-activation mechanism, in which the alkali metal cation activates the monomer whereas the carboxylate activates the initiating/propagating chain end.

Overall, the author established the environmentally-benign and practical ROP systems of cyclic esters to produce APE and APC materials. Since 2001, the organocatalytic ROP of cyclic esters has been significantly developed to achieve the metal-free synthesis of biodegradable and biocompatible APEs. To date, many researchers have made considerable efforts to develop various organocatalysts to build the foundation of organocatalytic polymerization. The dawn of organocatalytic polymerization has already passed, and it is time to consider the industrial stage. In order to break the dependence on conventional metal-based catalysts, the author developed organocatalytic ROP according to the three concepts of (1) no use of toxic compounds, (2) low production cost, and (3) easy operation to achieve environmentally-benign and practical ROP systems. The author believes that his work has definitely made a progress to realize the environmentally-benign APE production on an industrial stage.